KINETICS AND MECHANISMS OF THE REDOX REACTIONS OF MALACHITE GREEN WITH SOME OXY-ANIONS IN AQUEOUS ACIDIC MEDIUM

BY

MADINA IMAM

DEPARTMENT OF CHEMISTRY
FACULTY OF SCIENCE
AHMADU BELLO UNIVERSITY,
ZARIA, NIGERIA

OCTOBER, 2016

KINETICS AND MECHANISMS OF THE REDOX REACTIONS OF MALACHITE GREEN WITH SOME OXY-ANIONS IN AQUEOUS ACIDIC MEDIUM

BY

MADINA IMAM, B.Sc Chemistry (ABU) 2010

MSc/SCIE/39033/2012-2013

A DISSERTATION SUBMITTED TO THE SCHOOL OF POSTGRADUATE STUDIES, AHMADU BELLO UNIVERSITY, ZARIA

IN PARTIAL FULFILLMENT OF THE REQUIREMENTS FOR THE AWARD OF A MASTER OF SCIENCE DEGREE IN INORGANIC CHEMISTRY

DEPARTMENT OF CHEMISTRY
FACULTY OF SCIENCE
AHMADU BELLO UNIVERSITY,
ZARIA, NIGERIA

OCTOBER, 2016

Declaration

I declare that the work in this dissertation entitled "Kinetics and mechanisms of the redox reactions of malachite green with some oxy-anions in aqueous acidic medium" has been carried out by me in the Department of Chemistry of Ahmadu Bello University, Zaria under the supervision of Professor S.O. Idris and Dr. A.D. Onu. To the best of my knowledge, no part of this work was previously presented for the award of another degree and/or diploma by me or anyone else at this or any other institution. All information obtained from literature has been duly acknowledged in the text and a list of references provided.

Madina IMAM _____ _____

Signature Date

Certification

This dissertation entitled: "KINETICS AND MECHANISMS OF THE REDOX REACTIONS OF MALACHITE GREEN WITH SOME OXY-ANIONS IN AQUEOUS ACIDIC MEDIUM" by Madina IMAM, meets the regulations governing the award of the degree of Master of Science in Inorganic Chemistry of Ahmadu Bello University Zaria, and is approved for its contribution to knowledge and literary presentation.

Professor S.O. Idris _____ _____
Chairman, Supervisory Committee Signature Date

Dr. A.D. Onu
Member, Supervisory Committee _____ _____
Signature Date

Professor A.O. Oyewale
Head of Department _____ _____
Signature Date

Professor Kabir Bala
Dean, School of Postgraduate Studies _____ _____
Signature Date

Dedication

This work is dedicated to my beloved parents and all those who contributed positively to my life.

Acknowledgment

All praises and gratitude are due to Almighty Allah, for making it possible for this work to be completed successfully.

My profound gratitude goes to Professor S.O. Idris and Dr. A.D. Onu, my able supervisors who deligently guided me from inception to the completion of this work.

I would like to thank the Head of Department, Professor V.O Ajibola and all the members of staff of the Department of Chemistry. My extreme gratitude goes to Prof. J.O. Amupitan for his invaluable guidance, motivation and support. I also want to acknowledge the encouragement of Mrs S.A. Hamza, Mrs S. Abdulsalam, Mal. M.A. Lawal, Mal. N. Tajudeen, Mal. N.S. Lawal and Mr B.I. Anweting. To all the postgraduate students of the Department, your cordial interaction and useful discussions is appreciated. Special mention is here made of Omotosho Kemi Margaret and Ismaila Ibrahim.

I sincerely and specially appreciate my lovely husband, Bashir Imam and my beautiful angels, Fareedah and Fawzeeyah not forgeting my wonderful maid Halima.

To the Lawals, I say thank you for your encouragement, love and care.

I am most grateful to my Parents for their moral and spiritual support. May you live long.

Abstract

The kinetics of the redox reactions of malachite green, MG^+ with these oxy-anions: Bromate (BrO_3^-), Metabisulphite ($S_2O_5^{2-}$), Sulphite (SO_3^{2-}) and Chlorite (ClO_2^-) in aqueous acidic medium were studied under the following experimental conditions:

i. $[H^+] = 1.0 \times 10^{-2}$ mol dm^{-3} (H_2SO_4), I = 0.5 mol dm^{-3} (Na_2SO_4) and T = 28 ± 1°C for MG^+ - BrO_3^- system.

ii. $[H^+] = 5.0 \times 10^{-3}$ mol dm^{-3} (HCl), I = 0.5 mol dm^{-3} (NaCl) and T = 28 ± 1°C for MG^+ - $S_2O_5^{2-}$ system

iii. $[H^+] = 5.0 \times 10^{-3}$ mol dm^{-3} (HCl), I = 0.1 mol dm^{-3} (NaCl) and T = 27 ± 1°C for MG^+ - SO_3^{2-} system

iv. $[H^+] = 1.0 \times 10^{-2}$ mol dm^{-3} (H_2SO_4), I = 0.3 mol dm^{-3} (Na_2SO_4) and T = 26 ± 1°C for MG^+ - ClO_2^- system

The stoichiometries of the reactions were found to be 2:1 for MG^+ - BrO_3^- system, 1:1 for MG^+ - $S_2O_5^{2-}$, MG^+ - SO_3^{2-} and MG^+ - ClO_2^- systems. The order of the reaction was one with respect to both oxidant and reductant in all the systems. Increase in reaction rate with increasing acid concentration $[H^+]$ was observed for MG^+ - BrO_3^- and MG^+ - ClO_2^- systems while a converse effect was observed for MG^+ - $S_2O_5^{2-}$ system and the rate of reaction for MG^+ - SO_3^{2-} system was independent on $[H^+]$. The influence of $[H^+]$ on the rates of reactions showed two parallel pathways for $S_2O_5^{2-}$ and ClO_2^- systems, one pathway for BrO_3^- system and no pathway was available for the SO_3^{2-} system.

The reactions conformed to the following rate equations:

$$\frac{-d[MG^+]}{dt} = (a\,[H^+]^2)[MG^+][BrO_3^-]$$

where $a = 3.32 \times 10^{-1}$ dm^9 mol^{-3} s^{-1}

$$\frac{-d[MG^+]}{dt} = (b + c\,[H^+]^{-1})[MG^+][S_2O_5^{2-}]$$

where $b = 9.80 \times 10^{-2}$ dm^3 mol^{-1} s^{-1} and $c = 1.38 \times 10^{-3}$ s^{-1}

$$\frac{-d[MG^+]}{dt} = [H^+]^0\,[MG^+][SO_3^{2-}] \text{ and}$$

$$\frac{-d[MG^+]}{dt} = (d + e\,[H^+])[MG^+][ClO_2^-]$$

where d = 0.11 $dm^3\ mol^{-1}\ s^{-1}$ and e = $8.40 \times 10^{-2}\ s^{-1}$

Increase in ionic strength increased the rate of reaction for all the systems except for the MG^+-ClO_2^- system where the reaction rate was not affected by changes in ionic strength of reaction medium. Added ions inhibited the rate of reactions for BrO_3^- and $S_2O_5^{2-}$ systems and had no effect on the rate of reaction for the ClO_2^- system. The rate of reaction for the SO_3^{2-} system was catalysed by added anions. Polymerisation test suggested the absence of free radicals in the ClO_2^- system only. Spectroscopic investigations and Michaelis-Menten plot showed no evidence of intermediate complex formation in all the reactions except for MG^+ - ClO_2^- an evidence of intermediate complex formation was noticed by a shift in λ_{max} from 620-600 nm. Outer-sphere mechanism is proposed for all the systems except MG^+ - ClO_2^- system where the reaction is believed to proceed via inner-sphere mechanism.

Table of Contents

	Page
Cover page	i
Fly Leaf	ii
Title page	iii
Declaration	iv
Certification	v
Dedication	vi
Acknowledgement	vii
Abstract	viii
Table of Contents	x
List of Figures	xiv
List of Tables	xviii
Abbreviations	xx
CHAPTER ONE	
1.0 INTRODUCTION	1
1.1 Electron Transfer Reactions	1
1.2 Types of Electron Transfer Reactions	2
1.3 Points of Mechanistic Interest in Electron Transfer Reactions	3
1.4 Mechanisms of Electron Transfer Reactions	4
1.4.1 Inner-sphere mechanism	4
1.4.2 Outer-sphere mechanism	4
1.5 Justification of the Research Work	5
1.6 Aim and Objectives of the Research Work	5

Page

CHAPTER TWO

2.0 LITERATURE REVIEW 6

2.1 Uses and Reactions of Malachite Green 6

2.2 Reactions of Bromate Ion 8

2.3 Reactions of Metabisulphite Ion 9

2.4 Reactions of Sulphite Ion 11

2.5 Reactions of Chlorite Ion 12

CHAPTER THREE

3.0 Materials and Methods 15

3.1 Materials 15

3.1.1 Preparation of malachite green solution 15

3.1.2 Preparation of potassium bromate solution 16

3.1.3 Preparation of sodium metabisulphite solution 16

3.1.4 Preparation of sodium sulphite solution 16

3.1.5 Preparation of sodium chlorite solution 16

3.1.6 Preparation of standard sulphuric acid solution 16

3.1.7 Preparation of standard hydrochloric acid solution 16

3.1.8 Preparation of sodium carbonate solution 17

3.1.9 Preparation of sodium sulphate solution 17

3.1.10 Preparation of sodium chlorite solution 17

3.1.11 Preparation of other salt solutions 17

3.2 Methods 17

3.2.1 Stoichiometric study 17

3.2.2 Kinetic measurements 18

Page

3.2.3 Effect of $[H^+]$ on the reaction rate 19

3.2.4 Effect of ionic strength and dielectric constant of the reaction medium on the reaction rate 20

3.2.5 Effect of added ions on the reaction rate 20

3.2.6 Test for intermediate complex formation 20

3.2.7 Test for the presence of free radicals 21

3.2.8 Product analysis 21

CHAPTER FOUR

4.0 RESULTS 22

4.1 Stoichiometry 22

4.2 Determination of Order of the Reactions with Respect to the Reactants 27

4.3 Effect of Hydrogen Ion Concentration on the Rates of the Reactions 40

4.4 Effect of Ionic Strength of the Reaction Medium on the Reaction Rate 47

4.5 Effect of Changes in Dielectric Constant of the Reaction Medium on the Reaction Rate 47

4.6 Effect of Added Ions on the Reaction Rate 55

4.7 Test for Intermediate Complex Formation 55

4.7.1 Test for the presence of free radicals 55

4.7.2 Michaelis-Menten plot 55

4.7.3 Spectrophotometric test 78

4.8.0 Products analysis 78

CHAPTER FIVE

5.0 DISCUSSION 83

5.1 Malachite Green - Bromate Ion System 83

5.2 Malachite Green - Metabisulphite Ion System 86

Page

5.3 Malachite Green - Sulphite Ion System 89

5.4 Malachite Green - Chlorite Ion System 91

CHAPTER SIX

6.0 SUMMARY, CONCLUSION AND RECOMMENDATION 94

6.0 Summary and Conclusion 94

6.1 Recommendation 95

REFERENCES 96

List of Figures **Page**

Figure 2.1: Structure of malachite green 6

Figure 4.1: Plot of absorbance versus mole ratio for the redox reaction of malachite green with bromate ions 23

Figure 4.2: Plot of absorbance versus mole ratio for the redox reaction of malachite green with metabisulphite ions 24

Figure 4.3: Plot of absorbance versus mole ratio for the redox reaction of malachite green with sulphite ions 25

Figure 4.4: Plot of absorbance versus mole ratio for the redox reaction of malachite green with chlorite ions 26

Figure 4.5: Typical pseudo-first order plot for the redox reaction of malachite green with bromate ions 28

Figure 4.6: Typical pseudo-first order plot for the redox reaction of malachite green with metabisulphite ions 29

Figure 4.7: Typical pseudo-first order plot for the redox reaction of malachite green with sulphite ions 30

Figure 4.8: Typical pseudo-first order plot for the redox reaction of malachite green with chlorite ions 31

Figure 4.9: Pseudo-first order plot of log k_1 versus log $[BrO_3^-]$ for the redox reaction of malachite green with bromate ions 36

Figure 4.10: Pseudo-first order plot of log k_1 versus log $[S_2O_5^{2-}]$ for the redox reaction of malachite green with metabisulphite ions 37

Figure 4.11: Pseudo-first order plot of log k_1 versus log $[SO_3^{2-}]$ for the redox reaction of malachite green with sulphite ions 38

Figure 4.12: Pseudo-first order plot of log k_1 versus log $[ClO_2^-]$ for the redox reaction of malachite green with chlorite ions 39

Figure 4.13: Plot of log k_1 versus log $[H^+]$ for the redox reaction of malachite green with bromate ions 41

Page

Figure 4.14: Plot of log k_1 versus log $[H^+]$ for the redox reaction of malachite green with metabisulphite ion 42

Figure 4.15: Plot of log k_1 versus log $[H^+]$ for the redox reaction of malachite green with sulphite ion 43

Figure 4.16: Plot of log k_1 versus log $[H^+]$ for the redox reaction of malachite green with chlorite ion 44

Figure 4.17: Plot of k_2 versus $[H^+]^2$ for the redox reaction of malachite green with bromate ion 45

Figure 4.18 Plot of k_2 versus $1/[H^+]$ for the redox reaction of malachite green with metabisulphite ion 46

Figure 4.19: Plot of k_2 versus $[H^+]$ for the redox reaction of malachite green with chlorite ion 47

Figure 4.20: Plot of log k_2 versus $\sqrt{I}$ for the redox reaction of malachite green with bromate ion 49

Figure 4.21: Plot of log k_2 versus $\sqrt{I}$ for the redox reaction of malachite green with metabisulphite ion 50

Figure 4.22: Plot of log k_2 versus $\sqrt{I}$ for the redox reaction of malachite green with sulphite ion 51

Figure 4.23: Plot of k_2 against 1/D for the redox reaction of malachite green with bromate ion 55

Figure 4.24: Plot of k_2 against 1/D for the redox reaction of malachite green with metabisulphite ion 56

Figure 4.25: Plot of k_2 versus $[NO_3^-]$ for the redox reaction of malachite green with bromate ion 61

Figure 4.26: Plot of k_2 versus $[NO_3^-]$ for the redox reaction of malachite green with metabisulphite ion 62

Page

Figure 4.27: Plot of k_2 versus $[HCOO^-]$ for the redox reaction of malachite green with metabisulphite ion 63

Figure 4.28: Plot of k_2 versus $[NO_3^-]$ for the redox reaction of malachite green with sulphite ion 64

Figure 4.29: Plot of k_2 versus $[NH_4^+]$ for the redox reaction of malachite green with bromate ion 69

Figure 4.30: Plot of k_2 versus $[Mg^{2+}]$ for the redox reaction of malachite green with bromate ion 70

Figure 4.31: Plot of k_2 versus $[NH_4^+]$ for the redox reaction of malachite green with metabisulphite ion 71

Figure 4.32: Plot of k_2 versus $[Mg^{2+}]$ for the redox reaction of malachite green with metabisulphite ion 72

Figure 4.33: Plot of k_2 versus $[NH_4^+]$ for the redox reaction of malachite green with sulphite ion 73

Figure 4.34: Plot of k_2 versus $[Mg^{2+}]$ for the redox reaction of malachite green with sulphite ion 74

Figure 4.35: Michaelis-Menten plot of $1/k_1$ versus $1/[BrO_3^-]$ for the redox reaction of malachite green with bromate ion 76

Figure 4.36: Michaelis-Menten plot of $1/k_1$ versus $1/[S_2O_5^{2-}]$ for the redox reaction of malachite green with metabisulphite ion 77

Figure 4.37: Michaelis-Menten plot of $1/k_1$ versus $1/[SO_3^{2-}]$ for the redox reaction of malachite green with sulphite ion 78

Figure 4.38: Michaelis-Menten plot of $1/k_1$ versus $1/[ClO_2^-]$ for the redox reaction of malachite green with chlorite ion 79

Figure 4.39: Spectra of malachite green and that of partially oxidized reaction mixture of malachite green and bromate ion 80

Page

Figure 4.40: Spectra of malachite green and that of partially oxidized reaction mixture of malachite green and metabisulphite ion 81

Figure 4.41: Spectra of malachite green and that of partially oxidized reaction mixture of malachite green and sulphite ion 82

Figure 4.42: Spectra of malachite green and that of partially oxidized reaction mixture of malachite green and chlorite ion 83

List of Tables **Page**

Table 4.1: Pseudo-first order and second order rate constants for the redox reaction of malachite green with bromate ions 32

Table 4.2: Pseudo-first order and second order rate constants for the redox reaction of malachite green with metabisulphite ions 33

Table 4.3: Pseudo-first order and second order rate constants for the redox reaction of malachite green with sulphite ions 34

Table 4.4: Pseudo-first order and second order rate constants for the redox reaction of malachite green with chlorite ions 35

Table 4.5: Pseudo-first order and second order rate constants for the effect of changes in dielectric constant on the rate of redox reaction of malachite green with bromate ions 53

Table 4.6: Pseudo-first order and second order rate constants for the effect of changes in dielectric constant on the rate of redox reaction of malachite green with metabisulphite ions 54

Table 4.7: Pseudo-first order and second order rate constants for the effect of added anions on the redox reaction of malachite green with bromate ions 57

Table 4.8: Pseudo-first order and second order rate constants for the effect of added anions on the redox reaction of malachite green with metabisulphite ions 58

Table 4.9: Pseudo-first order and second order rate constants for the effect of added anions on the redox reaction of malachite green with sulphite ions 59

Table 4.10: Pseudo-first order and second order rate constants for the effect of added anions on the redox reaction of malachite green with chlorite ions 60

Table 4.11: Pseudo-first order and second order rate constants for the effect of added cations on the redox reaction of malachite green with bromate ions 65

Table 4.12: Pseudo-first order and second order rate constants for the effect of added cations on the redox reaction of malachite green with metabisulphite ions 66

Page

Table 4.13: Pseudo-first order and second order rate constants for the effect of added cations on the redox reaction of malachite green with sulphite ions 67

Table 4.14: Pseudo-first order and second order rate constants for the effect of added cations on the redox reaction of malachite green with chlorite ions 68

Abbreviations

Abbreviations	Name
abs	Absorbance
aq	Aqueous
D	Dielectric constant
E_o	Redox Potential
Eq	Equation
ETR	Electron Transfer Reactions
Fig	Figure
k	Rate constant
K_{eq}	Equilibrium constant
M & B	May and Baker
MG^+	Malachite green
Ox	Oxidant
Red	Reductant
Sub	Substitution
λ_{max}	Wavelength of maximum absorption

CHAPTER ONE

1.0 INTRODUCTION

Inorganic Chemistry is a branch of Chemistry that deals with the behaviour of inorganic materials which is fundamental to the study of other areas of chemistry. It involves interpreting, correlating and predicting the properties and structures of these materials. Areas of study include; co-ordination chemistry, organometallic chemistry, acid-base chemistry, study of non-aqueous solvents and chemistry of elements other than carbon (House, 2008).

Kinetics of a reaction helps in determining the rate at which a reaction mixture approaches the state of equilibrium, yielding a certain reaction product (Asperger, 2003). A reaction mechanism is a detailed stepwise process involving molecules, atoms, radicals or ions that occur consecutively and culminates in the overall reaction observed (Cooke, 1979).

The knowledge of kinetics and mechanism of a reaction is fundamental to the adequate understanding of a wide area of science and technology. This ranges from the interplay between metabolic processes, where the intricate control of the rate of enzymatic processes is vital to the overall wellbeing of biological systems through the industrial synthesis of both fine and heavy chemicals. Hence, the understanding of the inherent processes and interactions is fundamental for the optimization of reaction conditions (Arnaut *et al*., 2006; Hamza, 2011).

1.1 Electron Transfer Reactions

Electron Transfer Reactions (ETR), are reactions of the oxidative-reductive type in which an electron is transferred from one specie (reductant) to another (oxidant). A loss of electron is accompanied by an increase in oxidation state to give an oxidized specie while a

gain of electron is accompanied by a decrease in oxidation state, giving rise to a reduced specie (Asperger, 2003).

Electron transfer reactions are important chemical processes as they play central roles in many biological, physical and chemical reactions (Finnegan *et al*., 2002). Reactions of metal ion complexes often involve electron transfer or ligand substitution or both.

The stability and reactivity of an ion in any oxidation state is greatly influenced by the presence of ligands in this reaction. A particular oxidation state may be said to be stable only when its redox reactions involve an unfavourable free energy change or the activation energies for the intramolecular electron transfer processes are too large (Sutin, 1968; Taube, 1968; Chaffee and Edwards, 1970; Bugaje, 2006; Abdulsalam, 2015). When these two factors are favourable, a redox process is spontaneous.

1.2 Types of Electron Transfer Reactions

a) Homonuclear (Self) Exchange Reactions

These are reactions which occur between two identical centres existing in different oxidation states. The reactants and products are the same and hence have the same concentrations. The free energy change for such a reaction is mainly due to mixing and is approximately zero. There is no net chemical change and K_{eq}= 1 (Sharpe 1982; Anweting, 2012). Examples of these reactions are given in Equations (1.1) and (1.2);

$$V^{2+} + {}^{*}V^{3+} \longrightarrow V^{3+} + {}^{*}V^{2+} \quad (1.1)$$

$$^{*}Fe(CN)_6^{2+} + Fe(CN)_6^{3+} \longrightarrow {}^{*}Fe(CN)_6^{3+} + Fe(CN)_6^{2+} \quad (1.2)$$

where * is an isotopic label

b) Heteronuclear (Cross) Exchange Reactions

This involves the transfer of electrons between different metal ion centres and hence products of reaction are chemically distinct from the reactants (Cooke, 1979). The net change in free energy in most cases is less than zero and $K_{eq} \neq 1$.

Examples of these reactions are given in Equations (1.3) and (1.4):

$$2Fe^{2+} + Tl^{3+} \longrightarrow 2Fe^{3+} + Tl^{+} \quad (1.3)$$

$$Co(NH_3)_5X^{2+} + Cr^{2+} + 5H^{+} \longrightarrow CrX^{2+} + Co^{2+} + 5NH^{4+} \quad (1.4)$$

Redox reactions can also be classified as **complementary and non-complementary reactions**

In complementary redox reactions, the oxidant and reductant both have equal changes in oxidation state and stoichiometry is always 1:1, whereas a non-complementary redox reaction results to an unequal change in oxidation state with an unbalanced stoichiometry.

Examples of such reactions are given below:

$$*Co(NH_3)_6^{3+} + Co(NH_3)_6^{2+} \longrightarrow *Co(NH_3)_6^{2+} + Co(NH_3)_6^{3+} \quad (1.5)$$

$$Sn(II) + Tl(III) \longrightarrow Sn(IV) + Tl(I) \text{ (complementary)} \quad (1.6)$$

$$2V^{2+} + Br_2 \longrightarrow 2V^{3+} + 2Br^{-} \text{ (non-complementary)} \quad (1.7)$$

where * is an isotopic label

1.3 Points of Mechanistic Interest in Electron Transfer Reactions

The following points are of great importance in the study of electron transfer (redox) reactions:

a) The stoichiometry of the reaction and the composition of the activated complex.

b) Whether the reaction is accompanied by transfer of electrons, atoms or other species.

c) The number of electrons transferred in each single step for a multi-step reaction.

d) The closeness of approach of reactants in the activated complex prior to electron transfer.

e) The comparison of the rate of electron transfer with rate of ligand substitution.

f) The importance of acid-base catalysis when observed. Could it be rationalized in terms of reactants, products or transition state.

g) Identification and isolation of reaction products and intermediates if any.

1.4 Mechanisms of Electron Transfer Reactions

1.4.1 Inner-sphere mechanism

This type of mechanism involves penetration into the inner-coordination sphere of reactants with the formation of a bridged activated intermediate (Candlin *et al*., 1968; Anweting, 2012). The mechanism normally follows three distinct steps; substitution to form a bridge between oxidant and reductant, actual electron transfer and separation of the products often with transfer of the bridging ligand (Taube *et al*., 1953; Abdulsalam, 2015). A typical inner-sphere reaction between Co(III) and Cr(II) is shown below:

$$[Co(NH_3)_5Cl]^{2+} + [Cr(H_2O)_6]^{2+} + 5H_2O \longrightarrow$$

$$[Co(H_2O)_6]^{2+} + [Cr(H_2O)_5Cl]^{2+} + 5NH_3 \qquad (1.8)$$

1.4.2 Outer-sphere mechanism

In this mechanism, the coordination shells of the complexes or metal ion remains intact, during the course of electron transfer. Outer-sphere electron transfer is generally enthalpically less favorable than inner-sphere electron transfer because the interaction through space between the redox centers in outer-sphere electron transfer is weaker than the interaction through the chemical bridge present in the inner-sphere mechanism. By the same token, outer-sphere electron transfer is usually entropically more favorable than inner-sphere electron transfer as the two sites involved do not have to go through the ordering processes associated with the formation of a bridge (Mcnaught and Wilkinson, 1997; Abdulsalam, 2015). Such a

mechanism is established when rapid electron transfer occurs between two substitution-inert complexes as shown in the examples below:

$$[Fe(CN)_6]^{4-} + [Mo(CN)_8]^{3-} \longrightarrow [Fe(CN)_6]^{3-} + [Mo(CN)_8]^{4-} \quad (1.9)$$

$$[Fe(CN)_6]^{4-} + [IrCl_6]^{2-} \longrightarrow [Fe(CN)_6]^{3-} + [IrCl_6]^{3-} \quad (1.10)$$

1.5 Justification of the Research

Malachite green (MG^+) dye has been widely used for the dyeing of leather, wool, jute and silk, in distilleries, as a fungicide and antiseptic in aquaculture industry to control fish parasites and disease (Zhang *et al.*, 2008). In spite of the outlined uses of this dye, literature reveals no report on the kinetics and mechanism of its redox reactions with these oxyanions; BrO_3^-, $S_2O_5^{2-}$, SO_3^{2-} and ClO_2^-. Data generated and the subsequent mechanisms proposed will assist in the better understanding and more efficient utilization of the reactions of this dye and also complement the much needed kinetic information which may throw more light on the staining properties, dye fastness and the redox properties of this dye.

1.6 Aim and Objectives of the Research

The aim of this research work is to study the kinetics of the redox reactions of malachite green with BrO_3^-, $S_2O_5^{2-}$, SO_3^{2-} and ClO_2^- in acidic medium and propose mechanisms for these reactions. This aim would be achieved through the following objectives:

a. determining the stoichiometry of the redox reaction,
b. estimating the rate constants as well as obtain the order of the reaction,
c. monitoring the effect of changes in acid concentration, ionic strength, dielectric constant and added ions on the reaction rates
d. testing for intermediate complex formation and presence of free radicals

e. qualitative analysis of the products of reactions and

f. proposal of plausible mechanisms for the reactions

CHAPTER TWO

2.0 LITERATURE REVIEW

2.1 Uses and Reactions of Malachite Green

Malachite Green dye also known as Aniline Green, Basic Green 4 or Victoria Green dye is a triarylmethane dye with the molecular formula $C_{23}H_{25}N_2Cl$.

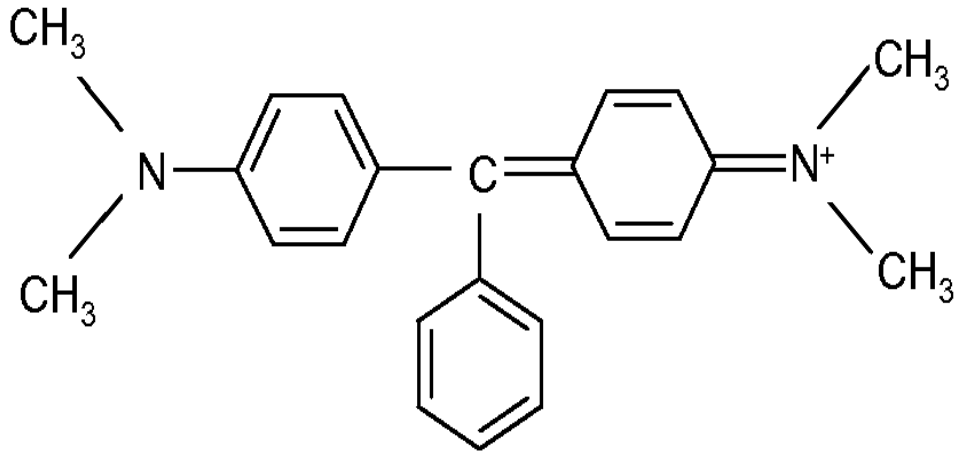


Figure 2.1: Structure of Malachite Green

Malachite green (MG^+) is the most widely used dye for colouring purposes with large industrial and medical applications (Crini *et al*., 2007). It is used as a biocide in the aquaculture industry world-wide due to its high effectiveness against parasitic invasion, fungal and bacterial infections in fish and fish eggs (Tsai and Chen, 2010). It is also used as a food colouring agent, food additive, medical disinfectant and anthelminthic as well as a dye in silk, wool, jute, leather, cotton, paper and acrylic industries (Chowdhury and Saha, 2010; Saha *et al*., 2010).

The kinetics of the oxidation of malachite green by dithionite ions, $S_2O_4^{2-}$ have been studied spectrophotometrically in an aqueous acid free medium under pseudo-first order conditions at a temperature of 25.5 ± 0.5°C, λ_{max} = 620 nm, and ionic strength of reaction medium, μ = 0.1moldm^{-3} (Idris *et al*., 2014). The reaction revealed a stoichiometry of 1:1 and reaction rate increases with increase in μ and dielectric constant. Added ion catalysis and result of Michealis-Menten analysis suggest that the reaction proceeded through the outer-sphere pathway.

Similarly, the reaction of malachite green with hydroxyl ion, OH^- in aqueous medium was reported to be first order with respect to both MG^+ and OH^- concentrations (Tanimu *et al*., 2012). The empirical rate law was given as:

$$-d[MG^+]/dt = k_2 [MG^+][OH^-] \qquad (2.1)$$

where k_2 = 47.36 ± 0.14 dm^{3}mol^{-1}min^{-1}. The reaction displayed a negative salt effect and the reaction rate decreases with increasing anion concentration.

Also, studies on the reaction of malachite green and permanganate ions carried out in aqueous acidic medium revealed a first order dependence in both [MG^+] and [MnO_4^-]. The rate of redox reaction showed dependence on acid concentration (Mohammed *et al*., 2009).

Rate equation for the reaction has been proposed as:

$$-d[MG^+]/dt = (a + b[H^+])[MG^+][MnO_4^-] \qquad (2.2)$$

The second order rate constant was found to be $(11.96 \pm 0.13) \times 10^{-3}$ $dm^3mol^{-1}s^{-1}$

In addition to the above mentioned, the kinetics of the redox reactions of the dye with ClO^- (hypochlorite), IO_4^- (periodate) and NO_2^- (nitrite) were also studied by Idris *et al*., (2015) and Mohammed *et al*., (2010).

2.2 Reactions of Bromate Ion (BrO_3^-)

Bromate is known to be an excellent oxidizing agent having E_o = 1.52 volts at 298K in an acid medium. Bromate has been widely used as an oxidant in the oxidation of large number of organic and inorganic compounds in acid medium and after the reaction itself reduced to bromide and molecular bromine. The bromate ion oxidation of metal ions has been investigated in the presence of different inorganic reductants (Knight and Thompson, 1973; Birk, 1978; Biswajit, 2014).

The kinetics of the oxidation of bromopyrollol red (BPR^{2-}) by BrO_3^- (Idris *et al.,* 2014) has been studied in aqueous hydrochloric acid medium at an ionic strength of I = 0.5 mol dm^{-3} (NaCl), $[H^+] = 1.0 \times 10^{-2}$ mol dm^{-3} (HCl), T = 30 ± 1°C and λ_{max} = 460nm. The reaction is first order in [BPR^{2-}] and [BrO_3^-] with a stoichiometry of 1:1. Rate of reaction increases with increase in [H^+] and I, but added cation and anion inhibited the reaction rate. Results of the Michealis-Menten plot gave no evidence

of intermediate complex formation during the reaction. Based on the results obtained, the outer-sphere mechanism was proposed for the reaction.

However, the reaction between bromate and thiourea studied in acidic medium by Rueben *et al*., (1994) gave the stoichiometry in excess thiourea as:

$$4BrO_3^- + SC(NH_2)_2 + 3H_2O \longrightarrow 3SO_4^{2-} + 3OC(NH_2)_2 + 4Br^- + 6H^+ \quad (2.3)$$

In excess of bromate, the stoichiometry is:

$$4BrO_3^- + 5SC(NH_2)_2 + H_2O \longrightarrow 5SO_4^{2-} + 5OC(NH_2)_2 + 4Br_2 + 2H^+ \quad (2.4)$$

No bromine was formed in excess thiourea. In excess bromate, the reaction displays an initial induction period. The formation of bromine (at the end of the induction period) did not involve the bromate-thiourea reaction. It was merely an indicator reaction that denotes the end of thiourea oxidation.

The kinetics of the oxidation of pyrocatechol violet by bromate ions has been carried out in aqueous hydrochloric acid medium (Adetoro *et al*., 2010). The reaction was first order with respect to oxidant and reductant concentrations. Changes in the concentration of hydrogen ions and the ionic strength of reaction medium were found to affect the reaction. Added anions and cations inhibited the reaction rate.

Also, the redox kinetics of the reaction of hydroxylamine hydrochloride ($H_2NOH.HCl$) and BrO_3^- carried out in aqueous acidic medium (Idris *et al*., 2010) had a stoichiometry of 1:1, first order kinetics in both [NH_3OH^+] and [BrO_3^-], dependent on acid concentrations, showed positive salt effect, catalysis due to anions and absence of evidence of intermediate complex formation.

Rate equation for the reaction has been proposed as:

$$-d[NH_3OH^+] / dt = (a[H^+])[NH_3OH^+][BrO_3^-] \quad (2.5)$$

The second order rate constant for the reaction was found to be 0.233 $dm^3\ mol^{-1}\ s^{-1}$.

2.3 Reactions of Metabisulphite Ion ($S_2O_5^{2-}$)

Metabisulphite ion or pyrosulphite ion is a good reducing agent whose compounds are used as preservative and antioxidant in food (EUFIC, 2007). Concentrated sodium metabisulphite can be used to remove tree stumps and it is used for wine and beer making to inhibit the growth of wild yeasts, bacteria and fungi (Miline, 2005). Some brands contain 98 sodium metabisulphite, and cause degradation of lignin in the stumps, facilitating its removal (OSHA, 2008).

In the study of the kinetics and mechanism of redox reaction of crystal violet (CV^+) with metabisulphite ion ($S_2O_5^{2-}$), a stoichiometry of 1:1 was reported (Abdulsalam, 2015). The influence of $[H^+]$ on reaction rate pointed to two parallel pathways conforming to the rate equation given below:

$$\frac{-d[CV^+]}{dt} = (a + b\,[H^+]^{-1})[CV^+][S_2O_5^{2-}] \quad (2.6)$$

The rate of the reaction displayed a negative salt effect with added anions inhibiting the rate of reaction. Spectroscopic investigations and Michaelis-Menten plot showed no evidence of intermediate complex formation for the reaction. Thus the outer-sphere mechanism was proposed for the reaction.

However, kinetics and mechanism of the reduction of methylene blue with metabisulphite ion in acidic medium investigated at 25 ± 1°C, $[H^+] = 1 \times 10^{-1}$ mol/dm^3,

I = 1.0 mol/dm^3 ($NaClO_4$) and λ_{max}= 663nm revealed a stoichiometry of 1:3. The kinetic studies indicated first order dependence in both methylene blue and metabisulphite ion (Babatunde *et al.*,

2013). The rate of reaction was enhanced by increase in hydrogen ion concentration which conforms to equation (2.3).

$$k_{2 =} a + b [H^+] \quad (2.7)$$

In the study of the kinetics of reduction of rosaniline with sodium metabisulphite, one mole of rosaniline was consumed by one mole of the metabisulphite ion (Onu and Iyun, 2001). Second order rate constant was determined and the effect of acid on the rate of reaction showed two pathways, one which is acid dependent and the other which is acid independent.

$$k_{obs} = k_1 + k_2 [H^+]^{-1} \quad (2.8)$$

The rate of reaction displayed negative salt effect and there was no evidence of intermediate complex formation. Anions were found to catalyze the reaction, hence outer-sphere mechanism was proposed for the reaction.

Additionally, the study of kinetics of the reduction of potassium hexacyanoferrate(III) with sodium metabisulphite as a function of pH (varied between 2.6 to 4.7 using citric acid buffer system) and at temperatures (15-30)^oC, ionic strength maintained at 1.0 mol dm^{-3} (KCl), a second order observed rate constant was found to follow two path; acid dependent and an inverse acid dependent paths (Abbas and Nabeel, 2010).

2.4 Reactions of Sulphite Ion

The sulphite ion is a powerful reducing agent. It is used as a preservative to prevent spoilage and oxidation at several stages of wine production. Also in dried fruits and potato products (Edokpayi, 2010).

The stoichiometry and products of reactions involving sulphite allows a distinction to be made between one-equivalent or two-equivalent oxidizing agents. The possible reaction paths are reflected in the equations below:

$$SO_3^{2-} \longrightarrow SO_4^{2-} \qquad \xrightarrow{1/2} S_2O_6^{2-} \qquad (2.9)$$

$$SO_3^{2-} \longrightarrow SO_4^{2-} \qquad (2.10)$$

Report shows that free SO_3^{2-} is always oxidized to SO_4^{2-} without $S_2O_6^{2-}$ or with very negligible amount of it (Babatunde and Iyun, 2009).

The kinetics of decolourization of methylene blue, MB^+ with sodium sulphite in aqueous acidic medium was investigated over a temperature range of 20-40°C. The studies were carried out as a function of different variables like concentration, pH and temperature on the rate of decolourisation. The rate of reaction was found to be $[H^+]$ dependent and first order in both $[MB^+]$ and reductant (Olajire and Olajide, 2014). The empirical rate law conforms to the equation:

$$-d[MB^+]/dt = -(k_3 + k_2K_1[H^+])\,[MB^+][SO_3^{2-}] \qquad (2.11)$$

where K_1 is the protonation constant and

k_2 and k_3 are the pseudo-second order rate constants for the protonation and deprotonation of MB^+.

Conversely, the redox reaction between indigo carmine and sulphite ions shows a first order dependence on both [IC] and $[SO_3^{2-}]$. Hydrogen ion concentration and effect of added anions and cations exerted no effect on the rate of the reaction. Results of the michealis-menten analysis gave evidence of intermediate complex formation and therefore the inner-sphere mechanism was proposed for the reaction (Edokpayi *et al*., 2010).

Babatunde (2005) studied the kinetics of the electron transfer reaction of rosaniline hydrochloride (referred to as Ros) with SO_3^{2-} in aqueous medium at 30°C, I=1.0 mol/dm^3 and $[H^+] = 1 \times 10^{-4}$ mol/dm^3. The reaction is first order in [Ros] and zero order in $[SO_3^{2-}]$. The rate of reaction showed an inverse dependence on acid concentration and the overall rate equation for the reaction is given as:

$$-d\,[Ros]/dt = (a + b[H^+]^{-1})\,[Ros][\,SO_3^{2-}] \qquad (2.12)$$

2.5 Reactions of Chlorite Ion

The kinetics and mechanism of oxidation of brilliant cresyl blue (7-amino-3-diethylamino-8-methyl-phenoxazine chloride) (BB^+) by chlorite in the presence of acid has been reported. During the reaction, chlorite ion disproportionates, resulting in accumulation of chlorine dioxide. The overall reaction is third-order with first-order dependence on both H^+ and ClO_2^- ions. The rate coefficient for the overall reaction is (0.158 ± 0.003) l^2 mol^{-2}s^{-1}. The stoichiometry of the reaction is;

$$BB^+ + 7ClO_2^- + 2H^+ \xrightarrow{2P} 2CH_3COOH + 4ClO_2 + 3Cl^- \qquad (2.13)$$

where P=7-amino-3-ethylamino-8-methyl-phenoxazine-10-N-oxide, and it varied with the initial concentrations of chlorite and acid (Qwabe *et al*., 2005). Near neutral pH, the hypochlorite-initiated oxidation of BB^+ proceeded through two second-order pathways, one driven by OCl^- ion and the other by HOCl. The latter reaction is much faster, with k = (1.26 ± 0.04) × 10^3 L mol^{-1} s^{-1}. At low pH, the reaction was much faster and had first-order dependence on the concentrations of BB^+, H^+ and HOCl.

Similarly, kinetics of oxidation-reduction reaction of $[Co(EDTA)]^{2-}$ with ClO_2^- have been studied in aqueous medium at 300K. The stoichiometric studies shows that two moles of $[Co(EDTA)]^{2-}$ consumed one mole of ClO_2^- (Bugaje, 2006).

The reaction was found to be first order in $[Co(EDTA)]^{2-}$ and half order in $[ClO_2^-]$. The rate of redox reaction showed two parallel acid pathways conforming to the rate equation below:

$$-d[Co(EDTA)]^{2-}/dt = (a + b[H^+])\,[Co(EDTA)]^{2-}\,[ClO_2^-]^{1/2} \qquad (2.14)$$

The rate of reaction showed a positive salt effect. Added anions and cations were found not to affect the reaction rate. Spectrophotometric investigation and Michealis-Menten plot showed intermediate complex formation for the reaction. From this result, the inner-sphere mechanism was proposed for the reaction.

Kudesia (2010) also studied the kinetics of oxidation of formaldehyde by chlorite ion in aqueous solution. The reaction was found to be of the first order with respect to formaldehyde and first order with respect to chlorite ion. Arrhenius equation is found to be valid for the reaction between 25°C and 55°C. The values of activation energy, $\Delta E^{\neq}$; frequency factor, A; heat of activation, $\Delta H^{\neq}$; entropy of activation, $-\Delta S^{\neq}$ and free energy of activation, $\Delta G^{\neq}$ (at 25°) are found to be 15.86 kcals/mol, 9.42 ± 107 L mol^{-1} sec^{-1}, 15.92 kcals/mol, 10.7 e. u. and 12.7 kcals/mol respectively.

And at I = 0.50 mol dm^{-3} (NaCl), T = 21 ± 1°C, $[H^+]$ = (0.6-1.8) × 10^{-2} mol dm^{-3}, the oxidation-reduction reaction between pyrocatechol violet (PCVH) and chlorite ions studied has a stoichiometry of 1:1. The reaction is second-order overall, first order in both oxidant and reductant. The reaction occurs by parallel acid independent and acid-dependent pathways suggesting $HClO^-$ and ClO_2^- as the principal reactant chlorite species. The second order rate constant increases with increase in acid concentration and decrease with an increase in ionic strength of the reaction medium. The reaction rate was mildly reduced by anions SO_4^{2-} and $HCOO^-$. The test for free radicals was negative (Adetoro *et al*., 2010). The kinetic data are consistent with the following equation:

$$-d[PCVH]/dt = (a + b[H^+])[PCVH][ClO_2^-] \qquad (2.15)$$

The experimental results are in favour of the outer-sphere mechanism.

CHAPTER THREE

3.0 MATERIALS AND METHODS

3.1 Materials

All solutions were prepared with distilled water except otherwise stated. Analytical grade reagents were used throughout this work without further purification. Sulphuric acid was used to investigate the effect of hydrogen ion on the rate of reaction for the malachite green-bromate and malachite green-chlorite systems while hydrochloric acid was used for malachite green-metabisulphite and malachite green-sulphite system. Sodium sulphate was used to maintain a

constant ionic strength of the reaction medium for the malachite green-bromate and malachite green-chlorite systems while sodium chloride was used for malachite green-metabisulphite and malachite green-sulphite system. Potassium bromate, sodium metabisulphite, sodium sulphite and sodium chlorite were the redox reagents used.

3.1.1 Preparation of malachite green solution

The malachite green dye was obtained from Aldrich Chemical Company (Analar grade). Stock solution of concentration of 1×10^{-3} mol dm^{-3} was prepared by weighing 0.0927 g of the dye, dissolved with distilled water in a 100 cm^3 volumetric flask and made up to the mark. The electronic spectrum of the solution was obtained by measuring its absorbance using Corning Colorimeter 252, within a wavelength range of 400-700 nm. From the spectrum, the wavelength of maximum absorption (λ_{max}) of 620 nm was obtained. This is close to the value of 616 nm reported in literature (Dixon *et al*., 2005).

3.1.2 Preparation of potassium bromate solution

A stock solution of 0.3 mol dm^{-3} ($KBrO_3$) was prepared by weighing 5.01g of the salt after drying in an oven for one hour at 110^{o}C and dissolved in a 100 cm^3 volumetric flask. The solution was made up to mark with distilled water.

3.1.3 Preparation of sodium metabisulphite solution

Stock solution of $Na_2S_2O_5$ (1.0 mol dm^{-3}) was prepared by dissolving 9.50g of the salt in a 50 cm^3 volumetric flask and made up to the mark with distilled water.

3.1.4 Preparation of sodium sulphite solution

Stock solution of Na_2SO_3 **(**1.0 mol dm^{-3}) was prepared by dissolving 12.60g of Na_2SO_3 salt in a 100 cm^3 volumetric flask and made up to mark with distilled water.

3.1.5 Preparation of sodium chlorite solution

Stock solution of 1.0 mol dm^{-3} $NaClO_2$ was prepared by accurately weighing 9.05g of the salt and dissolving it in distilled water in a 100 cm^3 volumetric flask.

3.1.6 Preparation of standard sulphuric acid solution

A stock solution of 1.0 mol dm^{-3} of H_2SO_4 was prepared by transferring 5.56 ml of 96.50% (w/w) H_2SO_4 (specific gravity 1.83) into a 100 cm^3 volumetric flask and making up to the mark with distilled water. The sulphuric acid was standardized volumetrically using sodium carbonate (Na_2CO_3) as primary standard and methyl orange as indicator.

3.1.7 Preparation of standard hydrochloric acid solution

A stock solution of 1.0 mol dm^{-3} hydrochloric acid was made by transferring 8.36ml of 37% (w/w) HCl (specific gravity 1.18) into a 100 cm^3 volumetric flask and making up to the mark with distilled water. The solution was standardized volumetrically using sodium carbonate (Na_2CO_3) as primary standard and methyl orange as indicator.

3.1.8 Preparation of sodium carbonate solution

Stock solution of 0.1 mol dm^{-3} sodium carbonate was obtained by dissolving 1.06g of Na_2CO_3 in 100 cm^3 volumetric flask and made up to the mark with distilled water. This solution was used as a primary standard in the standardization of sulphuric and hydrochloric acid.

3.1.9 Preparation of sodium sulphate solution

Sodium sulphate salt (Na_2SO_4) of mass 28.40g was weighed and dissolved with distilled water in a 100 cm^3 volumetric flask to obtain a 2.0 mol dm^{-3} standard solution.

3.1.10 Preparation of sodium chloride solution

Sodium chloride was prepared by dissolving 11.70 g of the salt with distilled water in 100 cm^3 volumetric flask to obtain 2.0 mol dm^{-3} standard solution.

3.1.11 Preparation of other salt solutions

Stock solutions of magnesium chloride ($MgCl_2$), magnesium sulphate ($MgSO_4$), sodium nitrate ($NaNO_3$), ammonium sulphate ($(NH_4)_2SO_4$), ammonium chloride (NH_4Cl) and sodium ethanoate (CH_3COONa), were prepared by dissolving a known amount of each salt in a known volume of distilled water.

3.2 Methods

3.2.1 Stoichiometric study

The stoichiometry of the reactions was determined by spectrophotometric titration using the mole ratio method. The concentration of malachite green was kept constant at 1.0×10^{-4} mol dm^{-3} while that of oxidants/reductants were varied as follows;

i. For MG^+ - BrO_3^- system; $[BrO_3^-]$ = (1.0×10^{-5} - 2.0×10^{-4} mol dm^{-3}),

$[H^+] = 1.0 \times 10^{-2}$ mol dm^{-3} (H_2SO_4), I = 0.5 mol dm^{-3} (Na_2SO_4)

ii. For MG^+ - $S_2O_5^{2-}$ system; $[S_2O_5^{2-}] = (0.25 – 4) \times 10^{-4}$ mol dm^{-3},

$[H^+] = 1.0 \times 10^{-3}$ mol dm^{-3} (HCl), I = 0.5 mol dm^{-3} (NaCl)

iii. For MG^+ - SO_3^{2-} system; $[SO_3^{2-}] = (0.25 – 4) \times 10^{-4}$ mol dm^{-3},

$[H^+] = 5.0 \times 10^{-3}$ mol dm^{-3} (HCl), I = 0.1 mol dm^{-3} (NaCl)

iv. For MG^+ - ClO_2^- system; $[ClO_2^-] = (0.25 – 4) \times 10^{-4}$ mol dm^{-3},

$[H^+] = 1.0 \times 10^{-2}$ mol dm^{-3} (H_2SO_4), I = 0.3 mol dm^{-3}, (Na_2SO_4)

The reacting mixtures were allowed to go to completion as indicated by constant values of absorbance observed in a two hourly interval over a period of two days. These values were recorded and the graphs of absorbance against mole ratio were plotted, the stoichiometry was then evaluated from the graphs.

3.2.2 Kinetic measurements

The rates of the redox reaction were studied by monitoring the decrease in absorbance of the dye at 620 nm using Corning Colorimeter 252. All kinetic measurements were performed under pseudo-first order conditions with the concentration of malachite green kept constant at 1.0×10^{-4} mol dm^{-3} and that of the other oxidants/reductants maintained at a concentration of at least 30 fold excess over that of the dye. The experimental conditions for the kinetic measurements were;

v. For MG^+ - BrO_3^- system; $[BrO_3^-] = (9.0 – 16.0) \times 10^{-2}$ mol dm^{-3},

$[H^+] = 1.0 \times 10^{-2}$ mol dm^{-3} (H_2SO_4), I = 0.5 mol dm^{-3} (Na_2SO_4) and T = 28 ± 1°C

vi. For MG^+ - $S_2O_5^{2-}$ system; $[S_2O_5^{2-}] = (5.0 – 12.0) \times 10^{-3}$ mol dm^{-3},

$[H^+] = 5.0 \times 10^{-3}$ mol dm^{-3} (HCl), I = 0.5 mol dm^{-3} (NaCl) and T = 28 ± 1°C

vii. For MG^+ - SO_3^{2-} system; $[SO_3^{2-}] = (3.0 – 6.0) \times 10^{-3}$ mol dm^{-3},

$[H^+] = 5.0 \times 10^{-3}$ mol dm^{-3} (HCl), I = 0.1 mol dm^{-3} (NaCl) and T = 27 ± 1°C

viii. For MG^+ - ClO_2^- system; $[ClO_2^-] = (4.0 – 10.0) \times 10^{-3}$ mol dm^{-3},

$[H^+] = 1.0 \times 10^{-2}$ mol dm^{-3} (H_2SO_4), I = 0.3 mol dm^{-3} (Na_2SO_4) and T = 26 ± 1°C

The pseudo first order rate constants for the reactions were obtained from the plots of the log (A_t - A_∞) versus time, t (where A_∞ and A_t are the absorbance at the end of the reaction and at time, t) and from the slope of the plots, the pseudo-first order rate constants (k_1) were determined. The second order rate constants (k_2) were obtained from the relation:

$$k_2 = k_1 / [\text{Oxyanions}] \qquad 3.1$$

3.2.3 Effect of $[H^+]$ on the reaction rate

The effect of $[H^+]$ on the rate of the reactions was investigated keeping the concentration of all other reactants constant while varying the $[H^+]$. The following experimental conditions were maintained for the four systems:

i. For MG^+ - BrO_3^- system; $[BrO_3^-] = 13.0 \times 10^{-2}$ mol dm^{-3}, $[H^+] = (0.6 – 1.6) \times 10^{-2}$ mol dm^{-3} (H_2SO_4), I = 0.5 mol dm^{-3} (Na_2SO_4) and T = 28 ± 1°C

ii. For MG^+ - $S_2O_5^{2-}$ system; $[S_2O_5^{2-}] = 10.0 \times 10^{-3}$ mol dm^{-3}, $[H^+] = (5.0 – 12.0) \times 10^{-3}$ mol dm^{-3} (HCl), I = 0.5 mol dm^{-3} (NaCl) and T = 28 ± 1°C

iii. For MG^+ - SO_3^{2-} system; $[SO_3^{2-}] = 5.6 \times 10^{-3}$ mol dm^{-3}, $[H^+] = (0.6 – 8.0) \times 10^{-3}$ mol dm^{-3} (HCl), I = 0.1 mol dm^{-3} (NaCl) and T = 27 ± 1°C

iv. For MG^+ - ClO_2^- system; $[ClO_2^-] = 6.0 \times 10^{-3}$ mol dm^{-3}, $[H^+] = (0.7 – 1.6) \times 10^{-2}$ mol dm^{-3} (H_2SO_4), I = 0.3 mol dm^{-3} (Na_2SO_4) and T = 26 ± 1°C

The order of reaction with respect to hydrogen ion concentration was obtained as the slope of the plot of log k_1, against log $[H^+]$. Variation of acid dependent rate constant with $[H^+]$ was obtained by plotting k_2 against $[H^+]$.

3.2.4 Effect of ionic strength and dielectric constant of reaction medium on the reaction rate

The effect of ionic strength on the rate of the reaction was investigated over a range of (0.2 – 1.0) and (0.1 – 0.7) mol dm^{-3} using Na_2SO_4 for BrO_3^- and ClO_2^-, (0.1 -0.8) and (0.05 – 0.5) using NaCl for $S_2O_5^{2-}$ and SO_3^{2-} while other reaction conditions were kept constant. A plot of log k_2 against $\sqrt{I}$ gives the relationship between the reaction rate with changes in ionic strength.

Effect of changes in dielectric constant of the reaction medium on the reaction rate was investigated by adding 0.10 – 0.80 cm^3 (accounting for 2 – 16%) acetone to the reaction mixture, while all other conditions were kept constant. A plot of k_2 against 1/D gives the relationship between the second order rate constant and the dielectric constant D.

3.2.5 Effect of added ions on the reaction rate

The effect of added ions on the reaction rate was studied by addition of $(10 – 100) \times 10^{-3}$ mol dm^{-3} of the ions (Mg^{2+}, NH_4^+, SO_4^{2-} and CH_3COO^-) while keeping all other parameters constant.

3.2.6 Test for intermediate complex formation

The spectra of the reaction mixtures were obtained over a wavelength range of (480–700) nm immediately after the initiation of the reaction. This was carried out in order to determine whether there is significant shift in λ_{max} or enhancement of peak resulted as the reaction progressed.

Michaelis-Menten plot of $1/k_1$ versus 1/[oxidant] or 1/[reductant] were also made.

3.2.7 Test for the presence of free radicals

To a partially oxidized reaction mixture containing various concentrations of oxidant, reductant and hydrogen ion for each system, about 5 cm^3 of acrylamide was added followed by excess of methanol to initiate free radical polymerization. A control experiment was carried out by adding acrylamide to each of the reactants separately. Formation of gelatinous precipitate indicates presence of free radical in the reaction.

3.2.8 Product analysis

Presence of Br_2 or Br^- (reduction product of BrO_3^-), SO_4^{2-} (oxidation product of $S_2O_5^{2-}$ and SO_3^{2-}), and Cl^- (reduction product of ClO_2^-) were tested by qualitative inorganic analysis (Vogel, 1961).

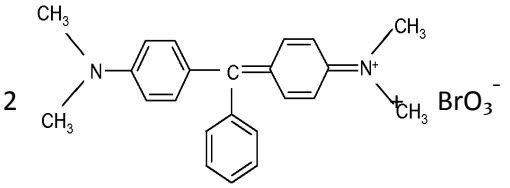
CHAPTER FOUR

4.0 RESULTS

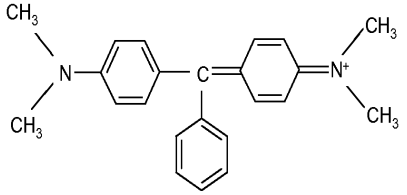
4.1 Stoichiometry

The results of the stoichiometric investigations indicate that two moles of malachite green consumed one mole of bromate ion, while one mole of malachite green consumed one mole each of metabisulphite ion, sulphite ion and chlorite ion respectively. The titration curves from which the stoichiometry of each of the systems was determined are presented in Figures 4.1 – 4.4.

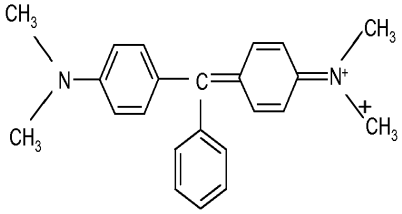
Based on the above results, the overall equations for the redox reactions can be represented in Equations 4.1 – 4.4.



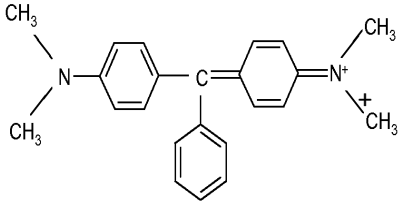
(4.1)



+ $S_2O_5^{2-}$ ⟶ Products (4.2)



+ SO_3^{2-} ⟶ Products (4.3)



+ ClO_2^- ⟶ Products (4.4)

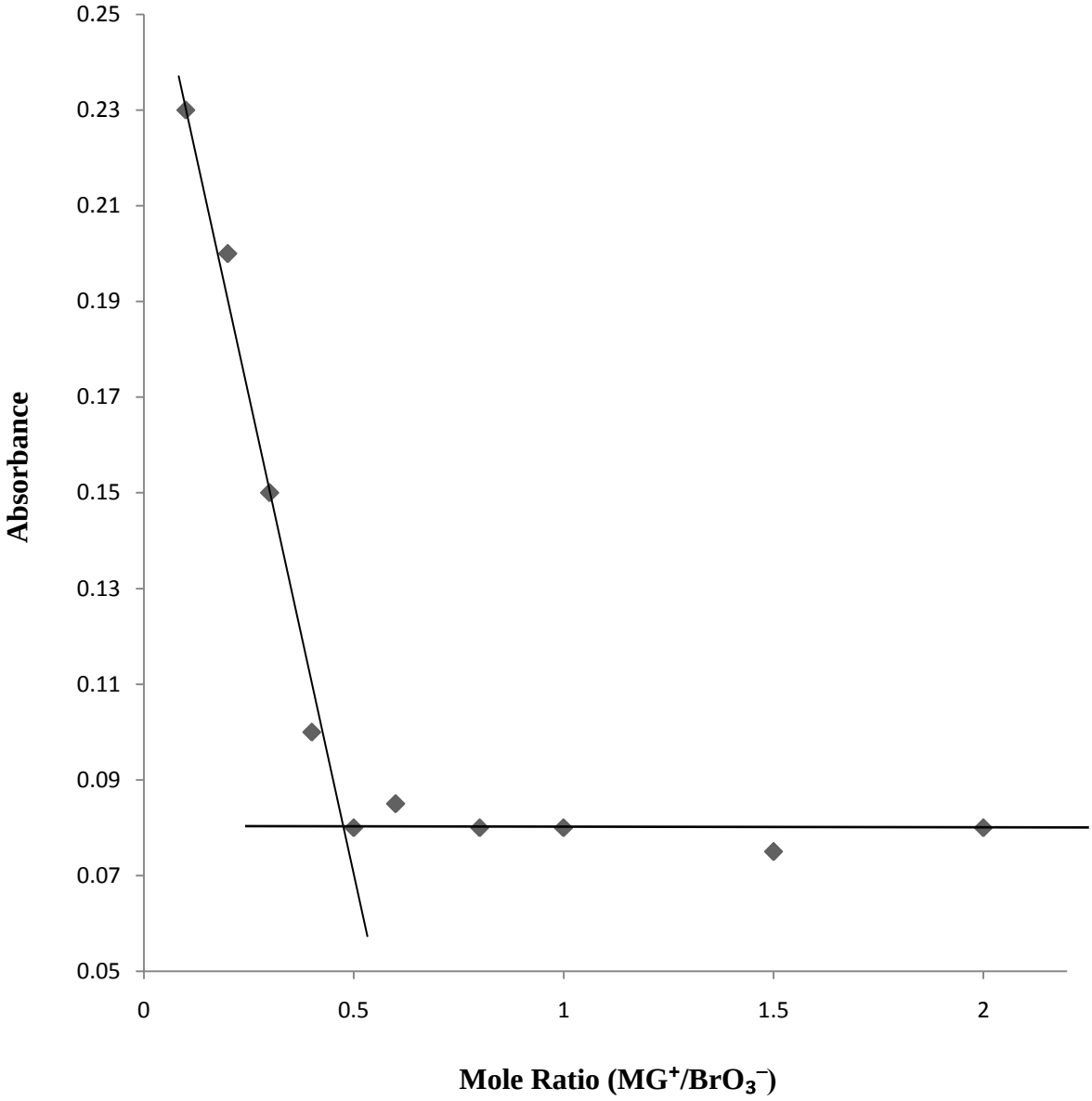


Figure 4.1: Plot of absorbance versus mole ratio for the redox reaction of malachite green with bromate ion at $[MG^+] = 1.0 \times 10^{-4}$ mol dm^{-3}, $[H^+] = 1.0 \times 10^{-2}$ mol dm^{-3}, I = 0.5 mol dm^{-3} and T = 28 ± 1ºC

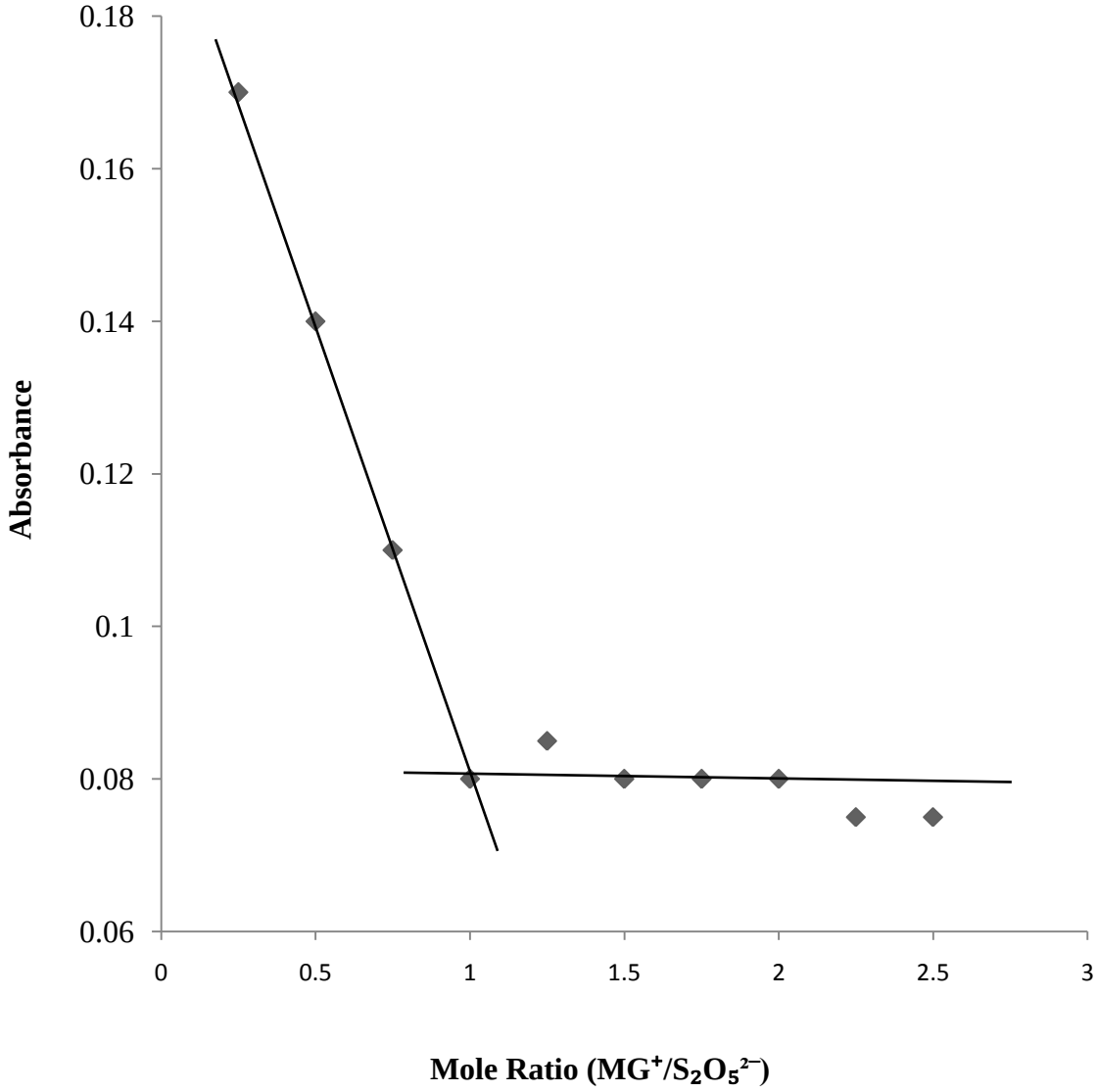


Figure 4.2: Plot of absorbance versus mole ratio for the redox reaction of malachite green with metabisulphite ion at $[MG^+] = 1.0 \times 10^{-4}$ mol dm^{-3},

$[H^+] = 5.0 \times 10^{-3}$ mol dm^{-3}, I = 0.50 mol dm^{-3} and T = 28 ± 1ºC

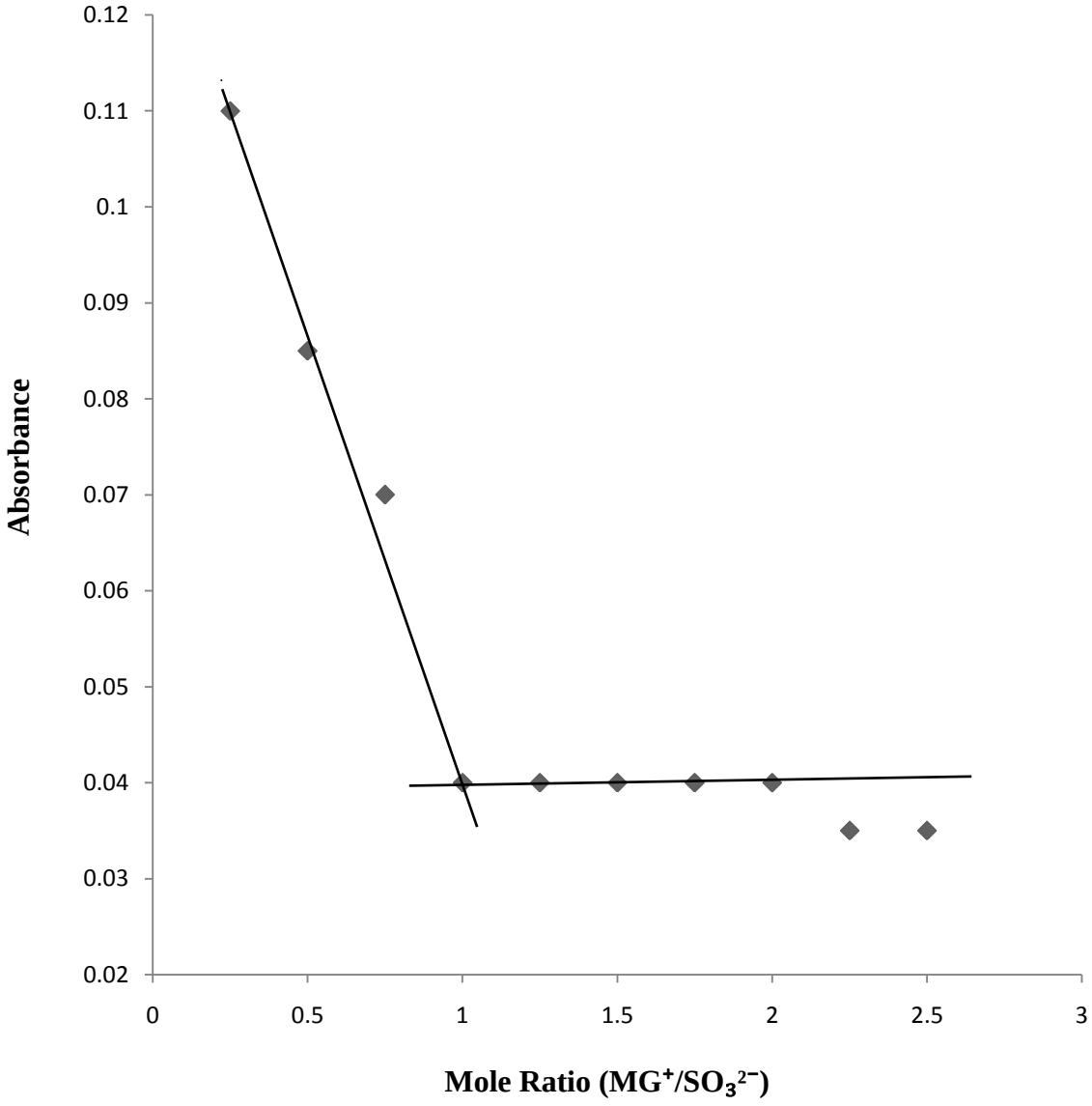


Figure 4.3: Plot of absorbance versus mole ratio for the redox reaction of malachite green with sulphite ion at $[MG^+] = 1.0 \times 10^{-4}$ mol dm^{-3}, $[H^+] = 5.0 \times 10^{-3}$ mol dm^{-3}, I = 0.10 mol dm^{-3} and T = 27 ± 1ºC

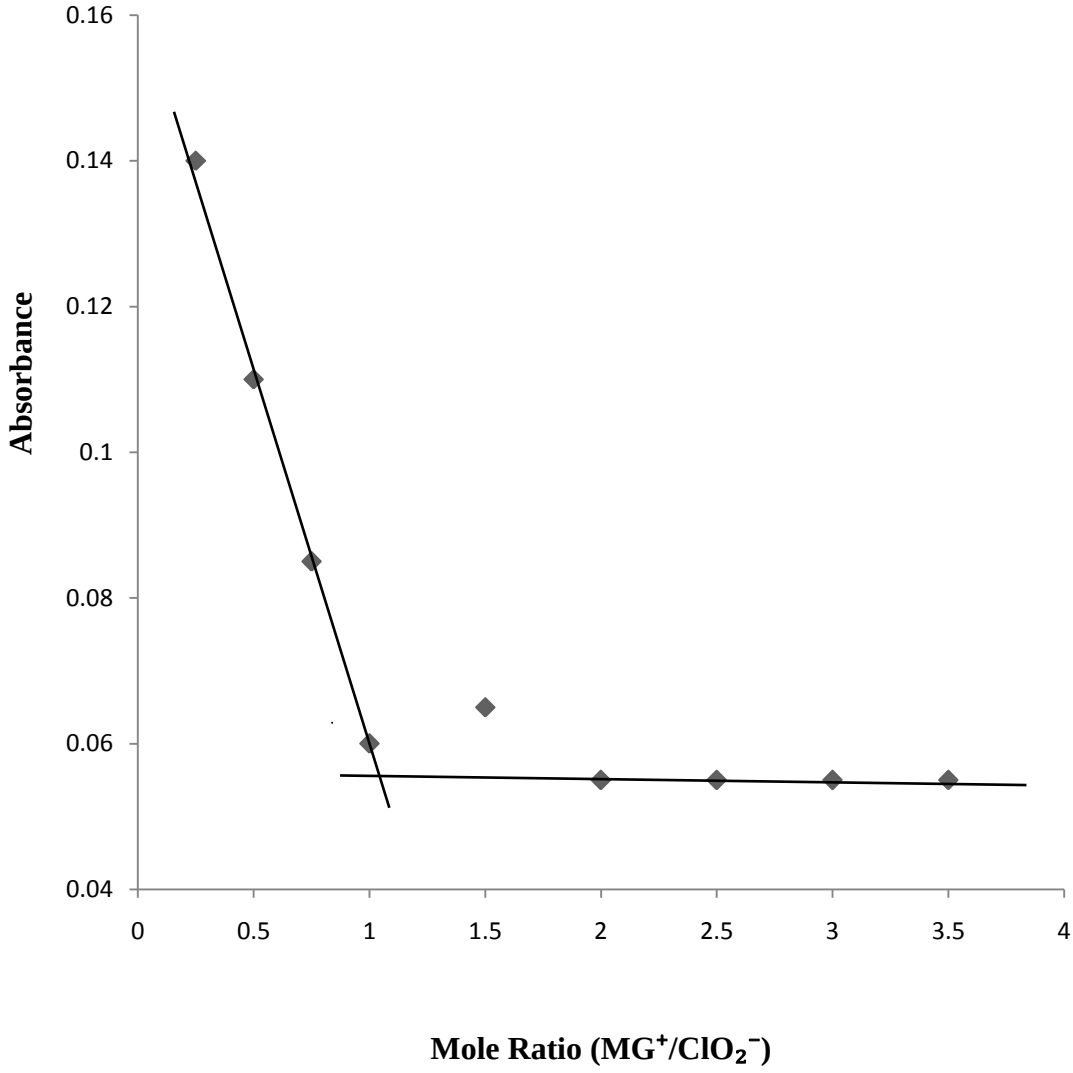


Figure 4.4: Plot of absorbance versus mole ratio for the redox reaction of malachite green with chlorite ion at $[MG^+] = 1.0 \times 10^{-4}$ mol dm^{-3}, $[H^+] = 1.0 \times 10^{-2}$ mol dm^{-3}, I = 0.30 mol dm^{-3} and T = 26 ± 1ºC

4.2 Determination of Order of the Reactions with Respect to the Reactants

The pseudo-first order plot of log (A_t - A_∞) versus time were linear to about 90% extent of the reaction (A_t and A_∞ are the absorbance at time t and at the end of the reaction respectively). The linearity of these plots indicates that these reactions are first order with respect to [MG^+]. Typical pseudo-first order plots are shown in Figures 4.5 - 4.8. Pseudo-first order rate constants, k_1 were calculated from the slopes of these plots and are reported on Tables 4.1 - 4.4. Least square plots of log k_1 versus log [oxyanion] at constant [H^+] were linear, with slopes of 1.04 for MG^+ - BrO_3^- system, 0.99 for MG^+ - $S_2O_5^{2-}$ system, 0.99 for MG^+ - SO_3^{2-} system and 0.93 for MG^+ – ClO_2^- system. This observation showed that the order of reaction with respect to [BrO_3^-], [$S_2O_5^{2-}$], [SO_3^{2-}] and [ClO_2^-] is one. The plots are represented in Figures 4.9 - 4.12.

Therefore the reaction is second order overall in all the systems, and the second order rate constants were determined from the relation;

$$k_2 = k_1 / [\text{oxyanion}] \qquad (4.5)$$

(oxyanion = BrO_3^-, $S_2O_5^{2-}$, SO_3^{2-} and ClO_2^-)

The rate laws for these reactions can therefore be written as:

$$\frac{-d[MG^+]}{dt} = k_2[MG^+][\text{oxyanion}] \qquad (4.6)$$

The second order rate constant for the various systems were found to be:

$k_2 = (30.81 \pm 0.36) \times 10^{-3}$ dm^3 mol^{-1} s^{-1} for MG^+ - BrO_3^- system

$k_2 = (38.04 \pm 0.30) \times 10^{-2}$ dm^3 mol^{-1} s^{-1} for MG^+ - $S_2O_5^{2-}$ system

$k_2 = (24.56 \pm 0.37) \times 10^{-2}$ dm^3 mol^{-1} s^{-1} for MG^+ - SO_3^{2-} system

$k_2 = (94.05 \pm 0.19) \times 10^{-2}$ dm^3 mol^{-1} s^{-1} for MG^+ - ClO_2^- system

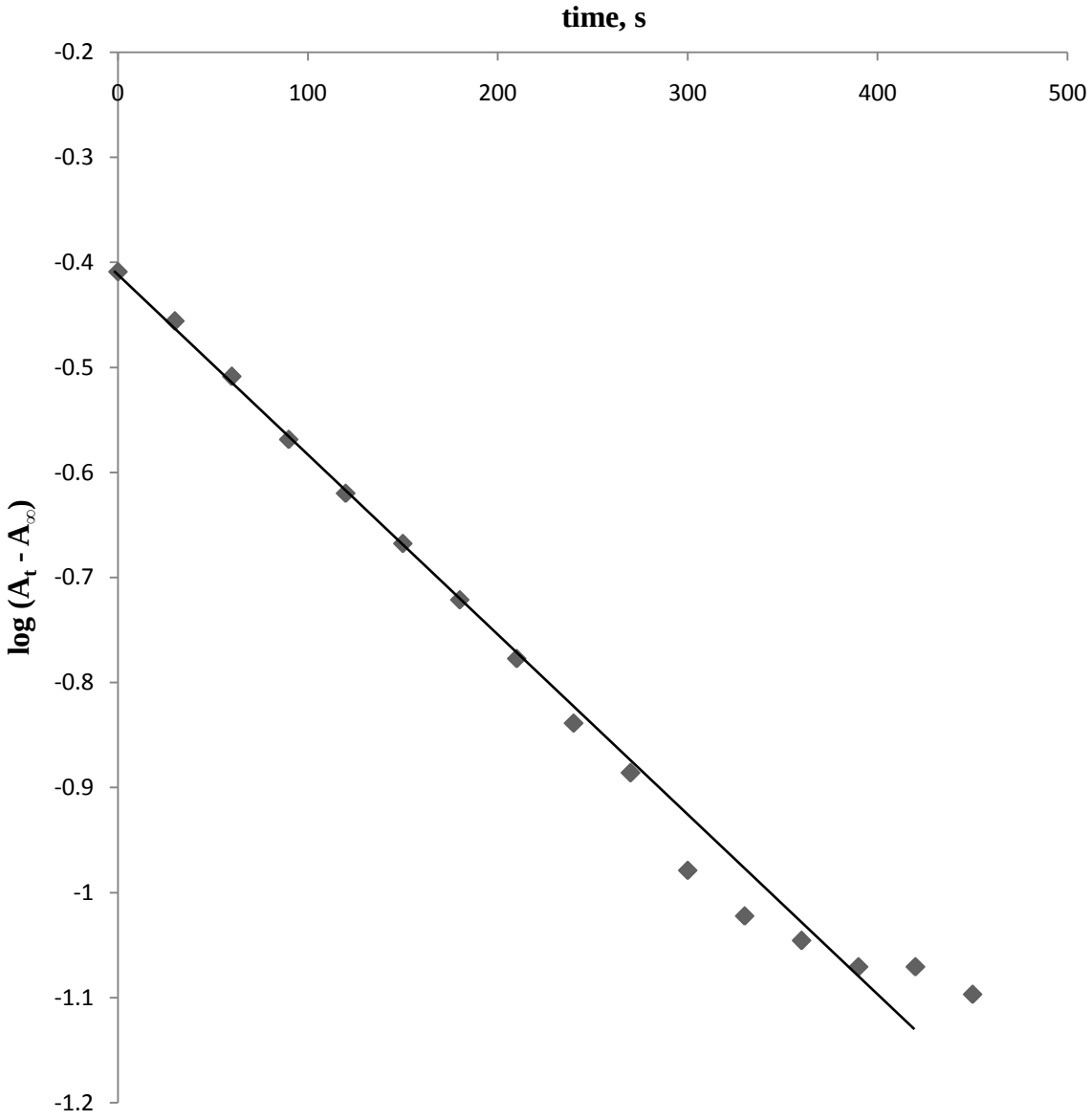


Figure 4.5: Typical pseudo-first order plot for the redox reaction of malachite green with bromate ion at $[MG^+] = 1.0 \times 10^{-4}$ mol dm^{-3}, $[BrO_3^-] = 13.0 \times 10^{-2}$ mol dm^{-3}, $[H^+] = 1.0 \times 10^{-2}$ mol dm^{-3}, I = 0.50 mol dm^{-3} and T = 28 ± 1 ºC

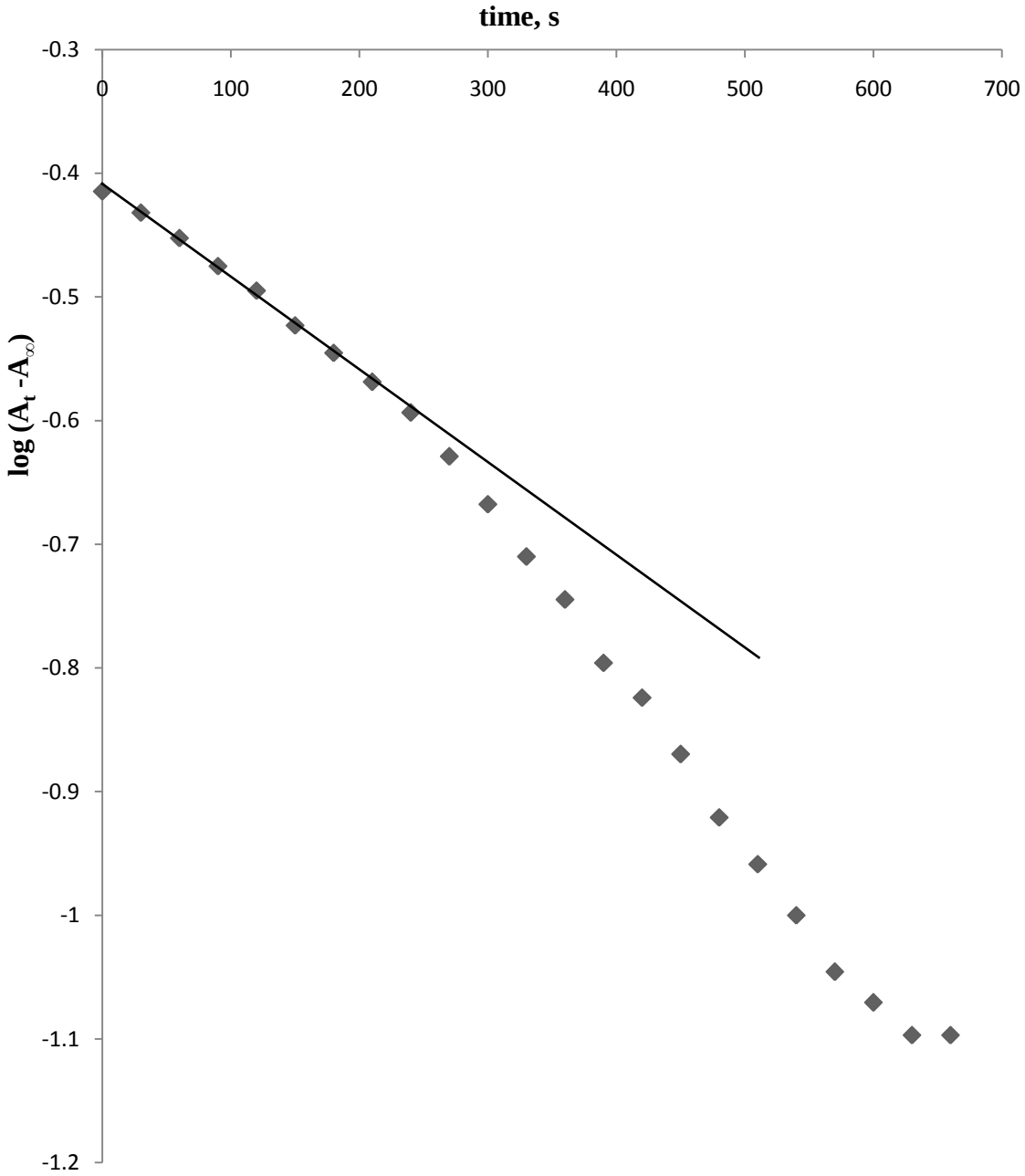


Figure 4.6: Typical pseudo-first order plot for the redox reaction of malachite green with metabisulphite ion at $[MG^+] = 1.0 \times 10^{-4}$ mol dm^{-3}, $[S_2O_5^{2-}] = 10.0 \times 10^{-3}$ mol dm^{-3}, $[H^+] = 5.0 \times 10^{-3}$ mol dm^{-3}, I = 0.50 mol dm^{-3} and T = 28 ± 1 ºC

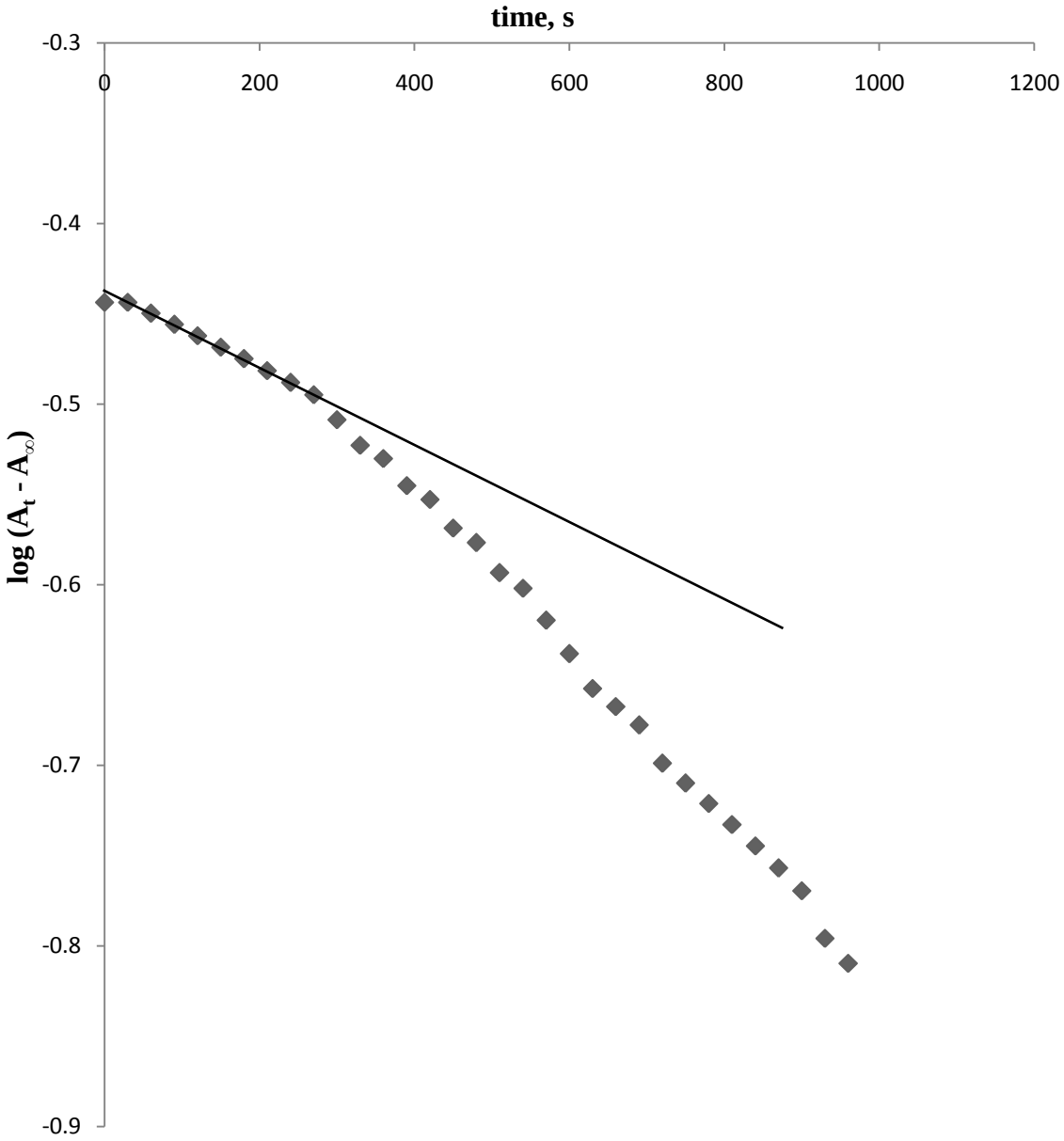


Figure 4.7: Typical pseudo-first order plot for the redox reaction of malachite green with sulphite ion at $[MG^{+}] = 1.0 \times 10^{-4}$ mol dm^{-3}, $[SO_3^{2-}] = 5.6 \times 10^{-3}$ mol dm^{-3},

$[H^+] = 5.0 \times 10^{-3}$ mol dm^{-3}, I = 0.10 mol dm^{-3} and T= 27 ± 1 ºC

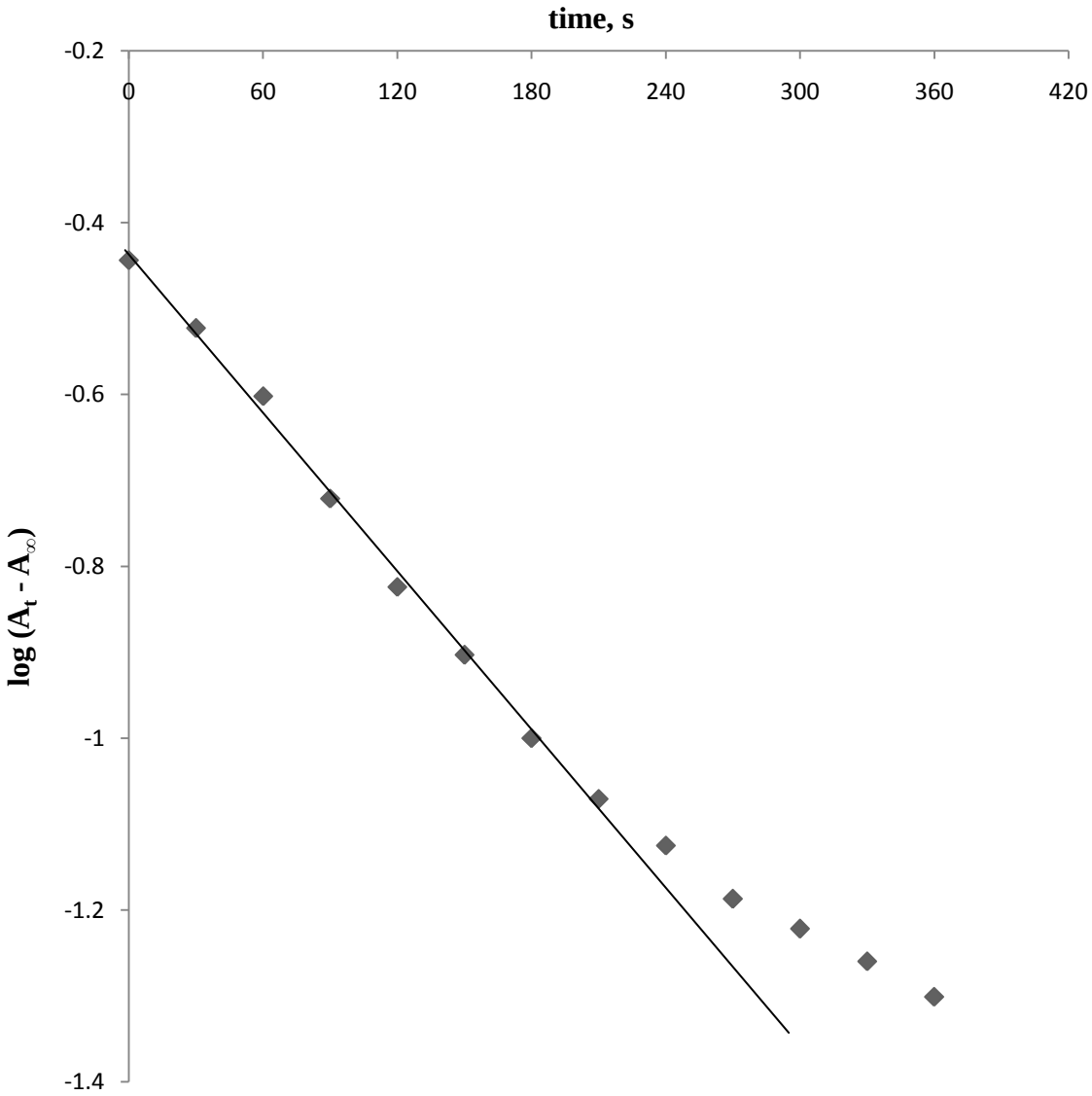


Figure 4.8: Typical pseudo-first order plot for the redox reaction of malachite green with chlorite ion at $[MG^+] = 1.0 \times 10^{-4}$ mol dm^{-3}, $[ClO_2^-] = 6.0 \times 10^{-3}$ mol dm^{-3}, $[H^+] = 1.0 \times 10^{-2}$ mol dm^{-3}, I = 0.30 mol dm^{-3} and T= 26 ± 1 ºC

Table 4.1: Pseudo-first order and second order rate constants for the redox reaction of malachite green with bromate ion in aqueous H_2SO_4 medium at $[MG^+] = 1.0 \times 10^{-4}$ mol dm^{-3}, T= 28 ± 1˚C and λ_{max}= 620 nm

$10^2[BrO_3^-]$, mol dm^{-3}	$10^2[H^+]$, mol dm^{-3}	I, mol dm^{-3}	$10^3 k_1$, s^{-1}	$10^2 k_2$, dm^3 mol^{-1} s^{-1}
9.00	1.00	0.50	2.78	3.10
10.00	1.00	0.50	3.07	3.07
11.00	1.00	0.50	3.37	3.07
12.00	1.00	0.50	3.68	3.08
13.00	1.00	0.50	4.07	3.13
14.00	1.00	0.50	4.22	3.02
15.00	1.00	0.50	4.60	3.07
16.00	1.00	0.50	4.98	3.12

13.00	0.60	0.50	1.42	1.10
13.00	0.70	0.50	2.12	1.62
13.00	0.80	0.50	2.82	2.17
13.00	1.00	0.50	4.03	3.10
13.00	1.20	0.50	4.80	4.53
13.00	1.30	0.50	6.13	4.73
13.00	1.50	0.50	8.72	6.70
13.00	1.60	0.50	9.60	7.38
13.00	1.00	0.20	1.35	1.03
13.00	1.00	0.30	1.92	1.48
13.00	1.00	0.40	2.68	2.07
13.00	1.00	0.50	4.03	3.10
13.00	1.00	0.60	4.98	3.83
13.00	1.00	0.70	6.53	5.03
13.00	1.00	0.80	8.07	6.20
13.00	1.00	1.00	12.67	9.75

Table 4.2: Pseudo-first order and second order rate constants for the redox reaction of malachite green with metabisulphite ion in aqueous HCl medium at $[MG^+] = 1.0 \times 10^{-4}$ mol dm^{-3}, T= 28 ± 1˚C and λ_{max}= 620 nm

$10^3[S_2O_5^{2-}]$, mol dm^{-3}	$10^3[H^+]$, mol dm^{-3}	I, mol dm^{-3}	$10^3 k_1$, s^{-1}	$10^1 k_2$, $dm^3 mol^{-1} s^{-1}$
5.00	5.00	0.50	1.88	3.77
6.00	5.00	0.50	2.30	3.83
7.00	5.00	0.50	2.68	3.84
8.00	5.00	0.50	3.03	3.79
9.00	5.00	0.50	3.38	3.76
10.00	5.00	0.50	3.80	3.80
11.00	5.00	0.50	4.10	3.81
12.00	5.00	0.50	4.60	3.83
10.00	5.00	0.50	3.77	3.77
10.00	6.00	0.50	3.28	3.28
10.00	7.00	0.50	2.97	2.97
10.00	8.00	0.50	2.82	2.82
10.00	10.00	0.50	2.40	2.40
10.00	11.00	0.50	2.23	2.23
10.00	12.00	0.50	2.10	2.10
10.00	5.00	0.10	1.62	1.62
10.00	5.00	0.20	2.12	2.12
10.00	5.00	0.30	2.48	2.48
10.00	5.00	0.40	3.42	3.42

10.00	5.00	0.50	3.80	3.80
10.00	5.00	0.60	4.10	4.10
10.00	5.00	0.70	4.42	4.42
10.00	5.00	0.80	4.53	4.53

Table 4.3: Pseudo-first order and second order rate constants for the redox reaction of malachite green with sulphite ion in aqueous HCl medium at

$[MG^+] = 1.0 \times 10^{-4}$ mol dm^{-3}, T= 27 ± 1˚C and λ_{max} = 620 nm

$10^3[SO_3^{2-}]$, mol dm^{-3}	$10^3[H^+]$, mol dm^{-3}	I, mol dm^{-3}	$10^4 k_1$, s^{-1}	$10^1 k_2$, $dm^3 mol^{-1} s^{-1}$
3.00	5.00	0.10	7.30	2.43
3.60	5.00	0.10	8.83	2.45
4.00	5.00	0.10	9.98	2.49
4.40	5.00	0.10	10.75	2.44
4.80	5.00	0.10	11.90	2.48
5.20	5.00	0.10	13.05	2.51
5.60	5.00	0.10	13.43	2.40
6.00	5.00	0.10	14.58	2.43
5.60	0.60	0.10	14.67	2.62
5.60	0.80	0.10	14.67	2.62
5.60	1.00	0.10	14.67	2.62
5.60	2.00	0.10	14.17	2.53
5.60	4.00	0.10	13.83	2.47
5.60	5.00	0.10	13.83	2.47
5.60	6.00	0.10	13.50	2.41
5.60	8.00	0.10	13.83	2.47
5.60	5.00	0.05	11.17	1.99

5.60	5.00	0.10	13.83	2.47
5.60	5.00	0.15	15.33	2.74
5.60	5.00	0.20	18.50	3.30
5.60	5.00	0.30	23.83	4.26
5.60	5.00	0.40	27.33	4.88
5.60	5.00	0.50	31.50	5.63

Table 4.4: Pseudo-first order and second order rate constants for the redox reaction of malachite green with chlorite ion in aqueous H_2SO_4 medium at

$[MG^+] = 1.0 \times 10^{-4}$ mol dm^{-3}, T= 26 ± 1˚C and λ_{max}= 620 nm

$10^3[ClO_2^-]$, mol dm^{-3}	$10^2[H^+]$, mol dm^{-3}	I, mol dm^{-3}	$10^3 k_1$, s^{-1}	$10^1 k_2$, dm^3 mol^{-1} s^{-1}

4.00	1.00	0.30	3.76	9.41
5.00	1.00	0.30	4,70	9.40
6.00	1.00	0.30	5.65	9.40
7.00	1.00	0.30	6.59	9.42
8.00	1.00	0.30	7.52	9.39
9.00	1.00	0.30	8.49	9.44
10.00	1.00	0.30	9.38	9.38
6.00	0.70	0.30	4.38	7.29
6.00	0.80	0.30	4.82	8.10
6.00	0.90	0.30	5.18	8.63
6.00	1.00	0.30	5.64	9.40
6.00	1.20	0.30	6.37	10.62
6.00	1.40	0.30	7.45	12.41
6.00	1.60	0.30	9.17	15.32
6.00	1.00	0.10	5.65	9.42
6.00	1.00	0.20	5.66	9.43
6.00	1.00	0.30	5.66	9.43
6.00	1.00	0.40	5.62	9.37
6.00	1.00	0.50	5.65	9.42
6.00	1.00	0.60	5.66	9.43
6.00	1.00	0.70	5.65	9.42

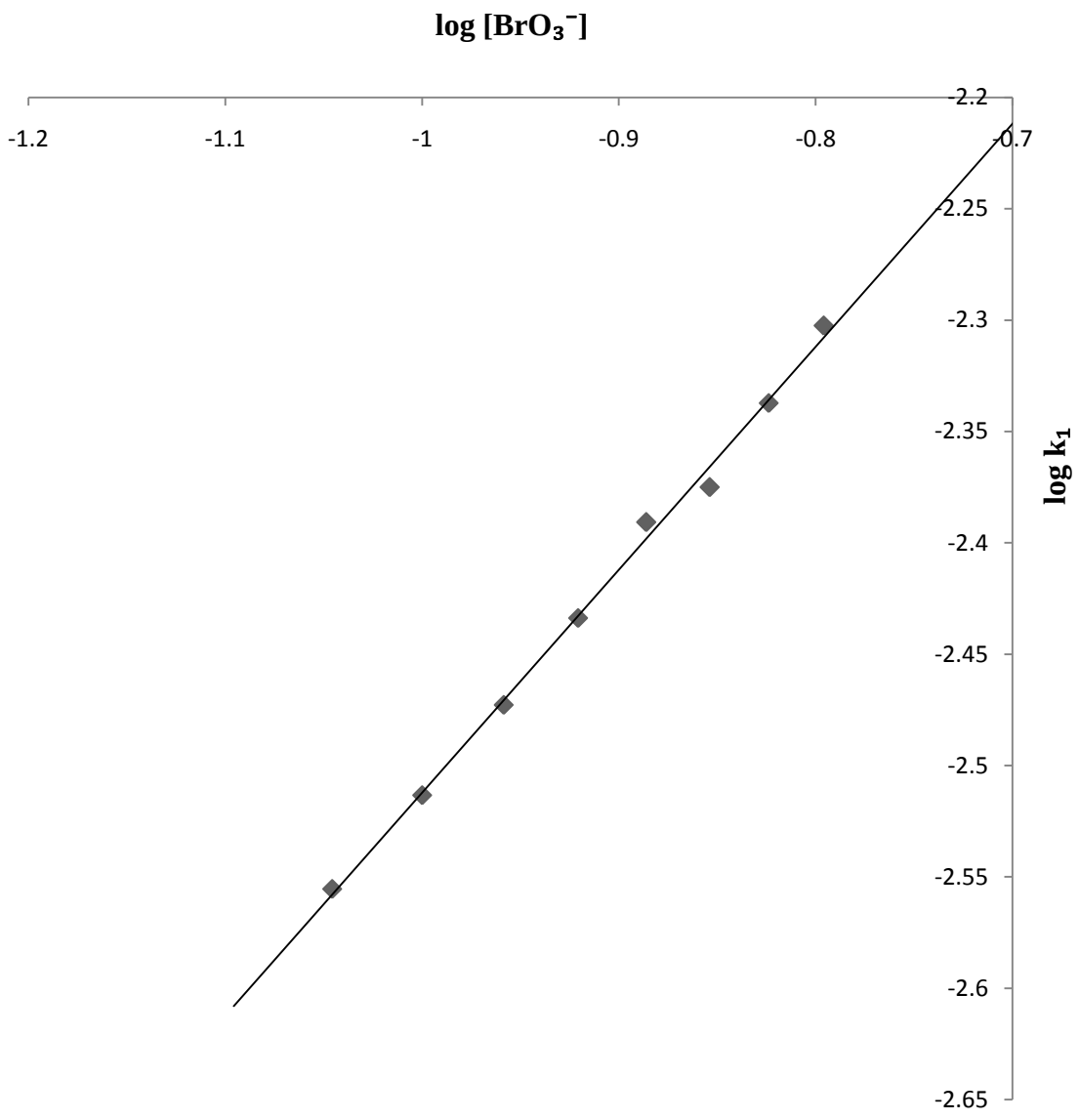


Figure 4.9: Pseudo-first order plot of log k_1 versus log [BrO_3^-] for the redox reaction of malachite green with bromate ion at [MG^+] = 1.0 × 10^{-4} mol dm^{-3},

[H^+] = 1.0 × 10^{-2} mol dm^{-3}, I = 0.50 mol dm^{-3}, λ_{max} = 620 nm and T= 28 ± 1 ºC

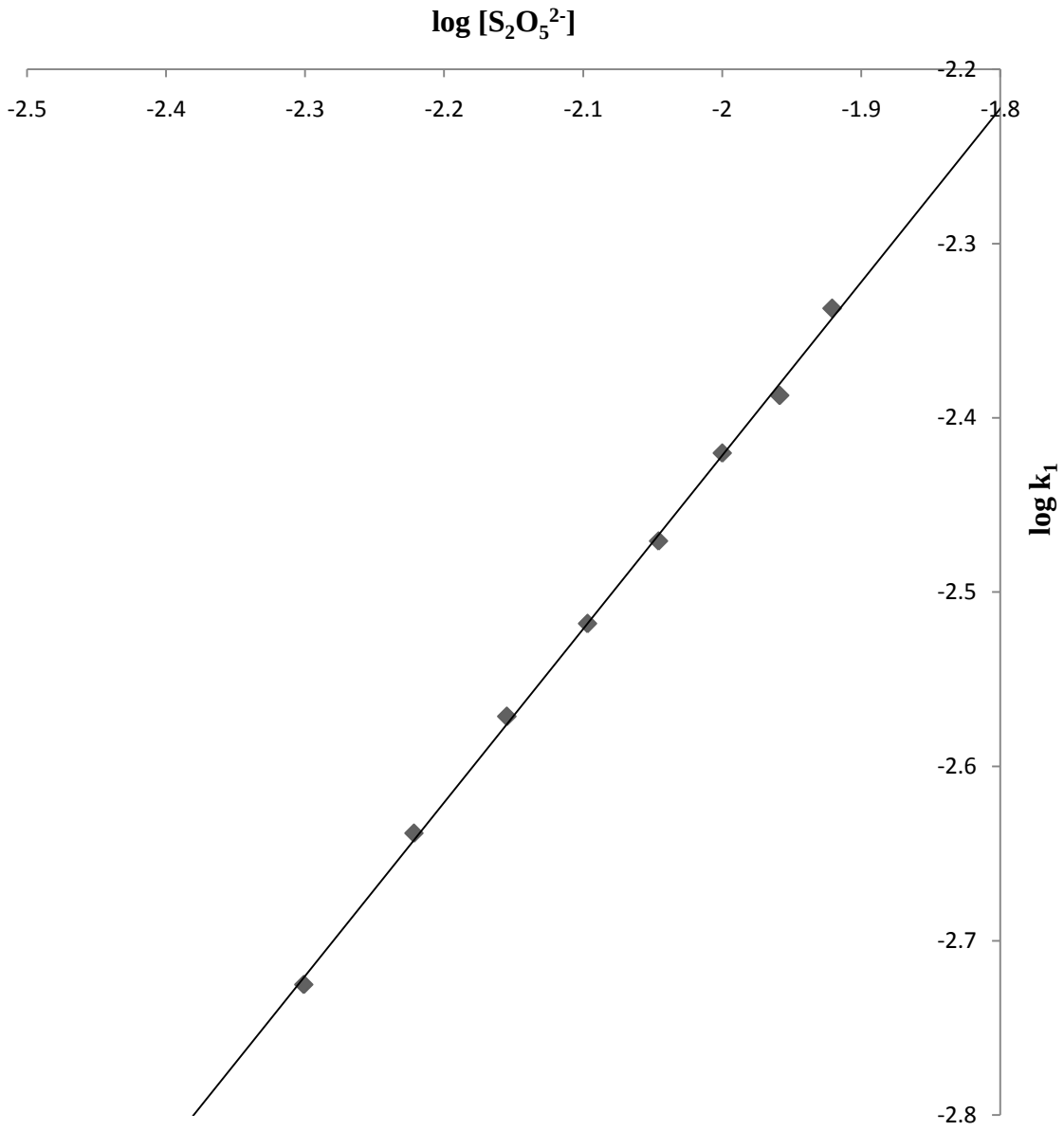


Figure 4.10: Pseudo-first order plot of log k_1 versus log $[S_2O_5^{2-}]$ for the redox reaction of malachite green with metabisulphite ion at $[MG^+] = 1.0 \times 10^{-4}$ mol dm^{-3},

$[H^+] = 5.0 \times 10^{-3}$ mol dm^{-3}, I = 0.50 mol dm^{-3}, λ_{max} = 620 nm and T= 28 ± 1 ºC

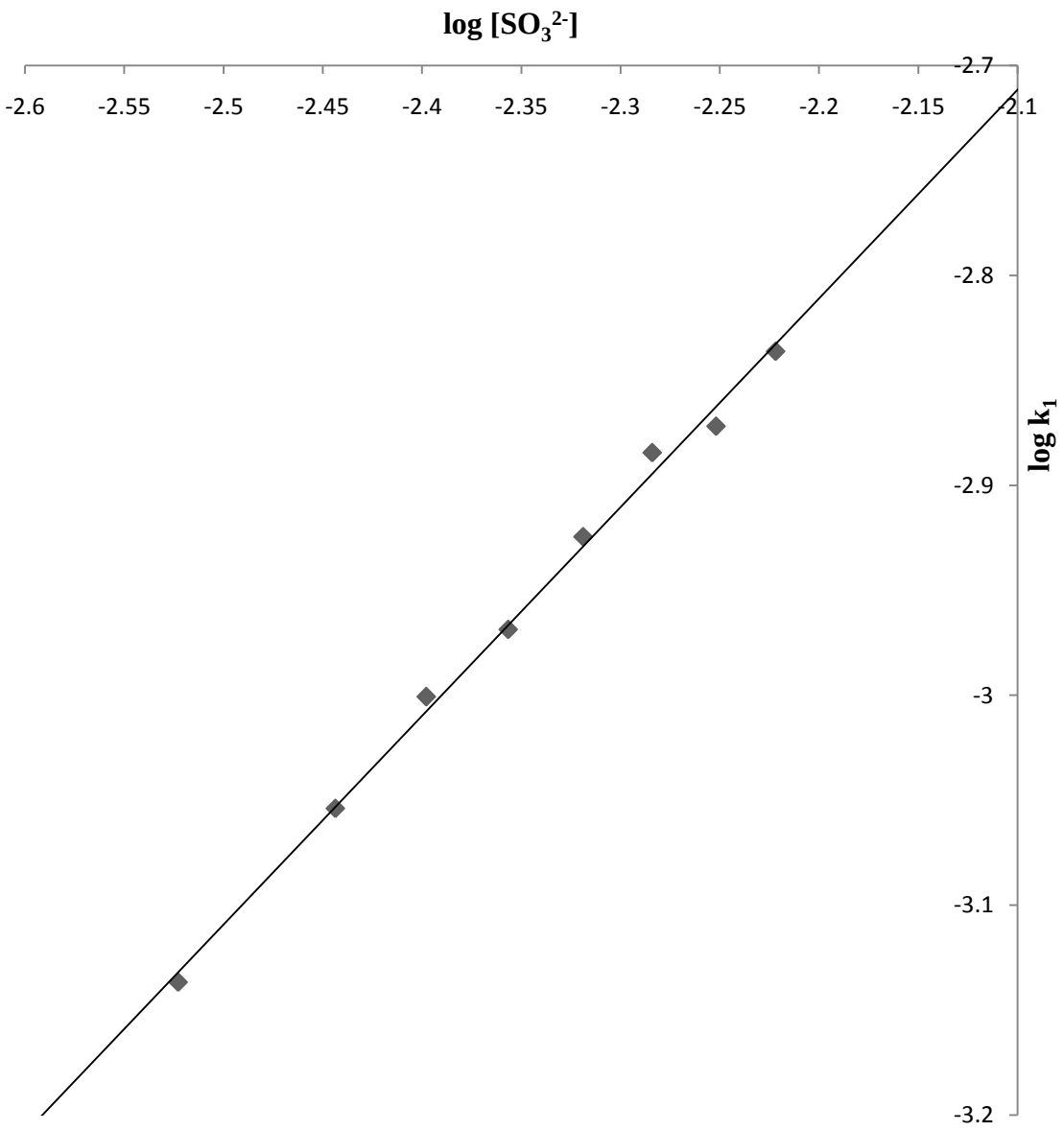


Figure 4.11: Pseudo-first order plot of log k_1 versus log $[SO_3^{2-}]$ for the redox reaction of malachite green with sulphite ion at $[MG^+] = 1.0 \times 10^{-4}$ mol dm^{-3}, $[H^+] = 5.0 \times 10^{-3}$ mol dm^{-3}, I = 0.10 mol dm^{-3}, λ_{max} = 620 nm and T= 27 ± 1 ºC

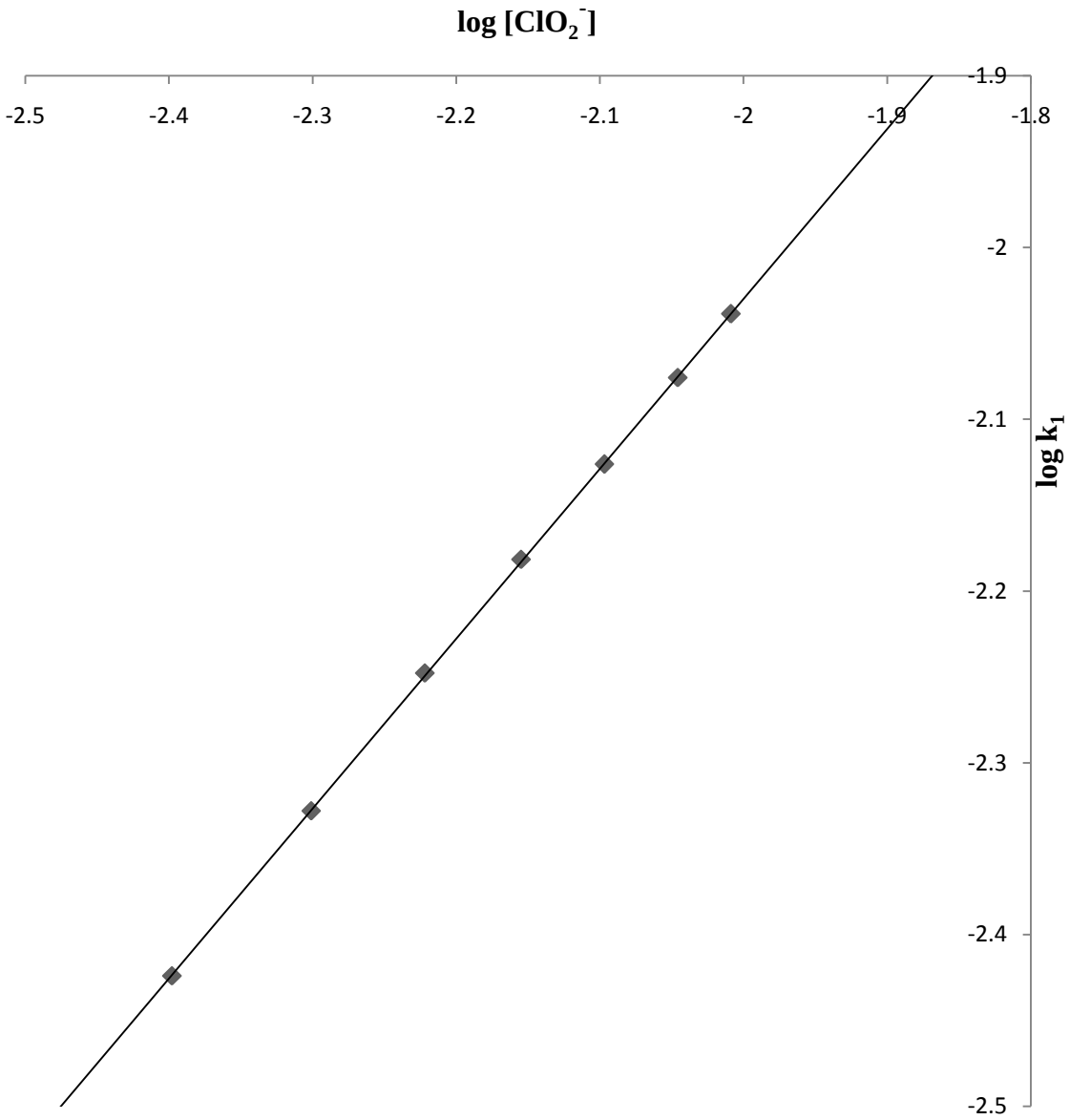


Figure 4.12: **Pseudo-first order plot of log k_1 versus log [ClO_2^-] for the redox reaction of malachite green with chlorite ion at [MG^+] = 1.0 $\times$ 10^{-4} mol dm^{-3},**

[H^+] = 1.0 $\times$ 10^{-2} mol dm^{-3}, I = 0.30 mol dm^{-3}, λ_{max} = 620 nm and T= 26 ± 1 ºC

4.3 Effect of Hydrogen ion Concentration on the Rates of the Reactions

For the MG^+ - BrO_3^- and MG^+ - ClO_2^- reaction, the rate of the reactions were found to increase with increase in hydrogen ion concentration in the range investigated, while for MG^+ - $S_2O_5^{2-}$ system, the rate of the reaction was found to be inversely influenced by hydrogen ion concentration. For MG^+ - SO_3^{2-} system, rate was found to be independent on hydrogen ion concentration (Tables 4.1 - 4.4).

Least square plots of log k_1 versus log $[H^+]$ were linear for all the systems with slopes of 1.82, -0.65, -0.03 and 0.85 for MG^+ - BrO_3^-, MG^+ - $S_2O_5^{2-}$ and MG^+ - ClO_2^- systems respectively (Figures 4.13 - 4.15). This indicates that the order with respect to $[H^+]$ is zero for MG^+ - SO_3^{2-} system, first order for MG^+- $S_2O_5^{2-}$ and MG^+ - ClO_2^- systems and second order for MG^+ - BrO_3^- system.

Plot of k_2 versus $[H^+]^2$ for the MG^+ - BrO_3^- system gave a straight line that passed through the origin (i.e intercept equal to zero) while plots of k_2 versus $[1/H^+]$ and k_2 versus $[H^+]$ for MG^+- $S_2O_5^{2-}$ and MG^+ - ClO_2^- systems had intercept (Figures 4.16 - 4.18).

The acid dependent rate constant can be represented by Equation (4.7) for MG^+ - BrO_3^- system, Equation (4.8) for MG^+ - $S_2O_5^{2-}$ system and Equation (4.9) for MG^+ - ClO_2^- system.

$$k_2 = a\,[H^+]^2 \qquad (4.7)$$

$$k_2 = (b + c\,[H^+]^{-1}) \qquad (4.8)$$

$$k_2 = (d + e\,[H^+]) \qquad (4.9)$$

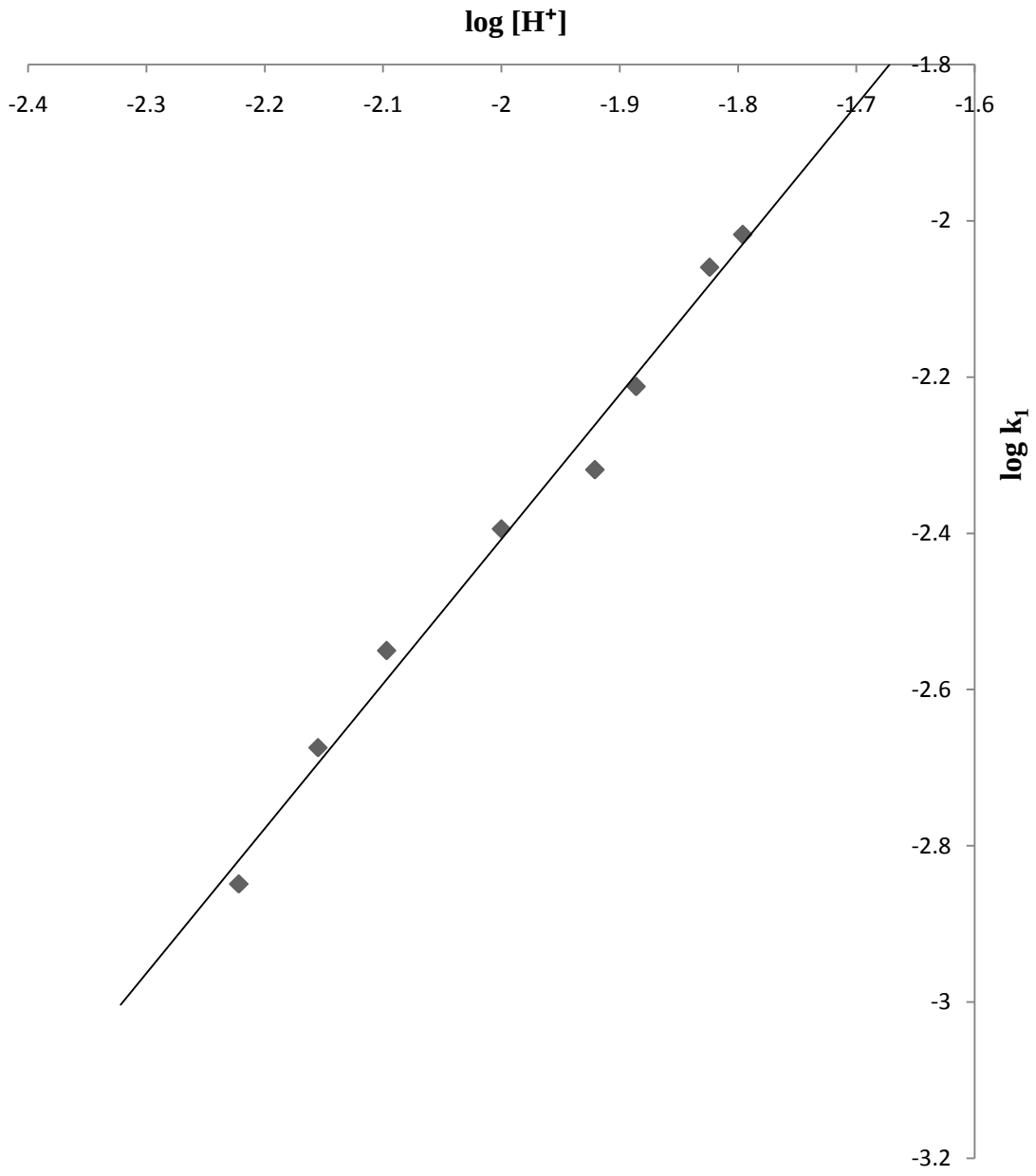


Figure 4.13: **Plot of log k_1 versus log $[H^+]$ for the redox reaction of malachite green with bromate ion at $[MG^+] = 1.0 \times 10^{-4}$ mol dm^{-3}, $[BrO_3^-] = 13.0 \times 10^{-2}$ mol dm^{-3},**

I = 0.50 mol $dm^{-3}$and T = 28 ± 1 ºC

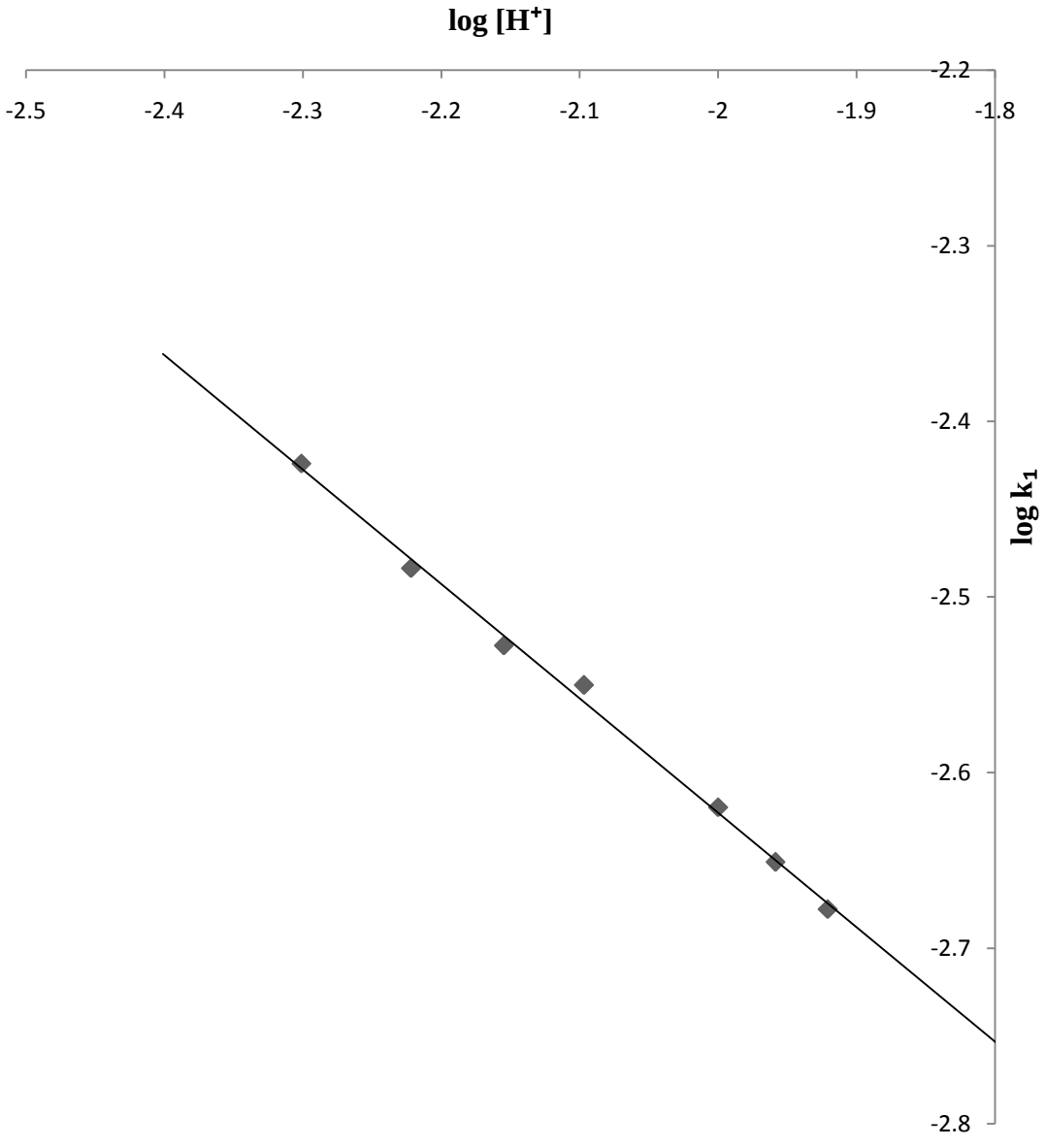


Figure 4.14: Plot of log k_1 versus log $[H^+]$ for the redox reaction of malachite green with metabisulphite ion at $[MG^+] = 1.0 \times 10^{-4}$ mol dm^{-3},

$[S_2O_5^{2-}]$ = 10.0 $\times$ 10^{-3} mol dm^{-3}, I = 0.50 mol $dm^{-3}$and T = 28 ± 1 ºC

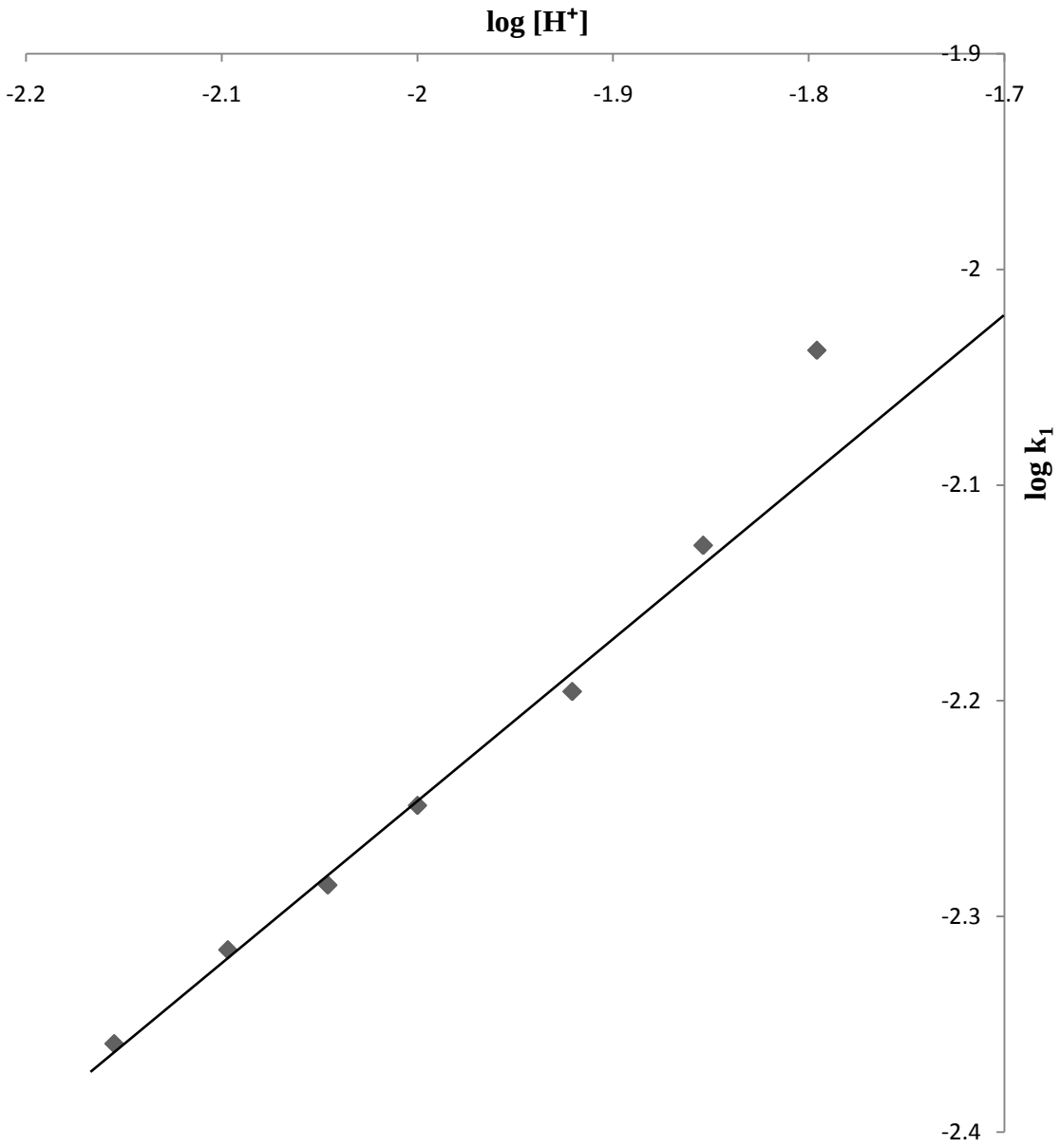


Figure 4.15: Plot of log k_1 versus log $[H^+]$ for the redox reaction of malachite green with chlorite ion at $[MG^+] = 1.0 \times 10^{-4}$ mol dm^{-3}, $[ClO_2^-] = 6.0 \times 10^{-3}$ mol dm^{-3}, I = 0.30 mol dm^{-3} and T = 26 ± 1 ºC

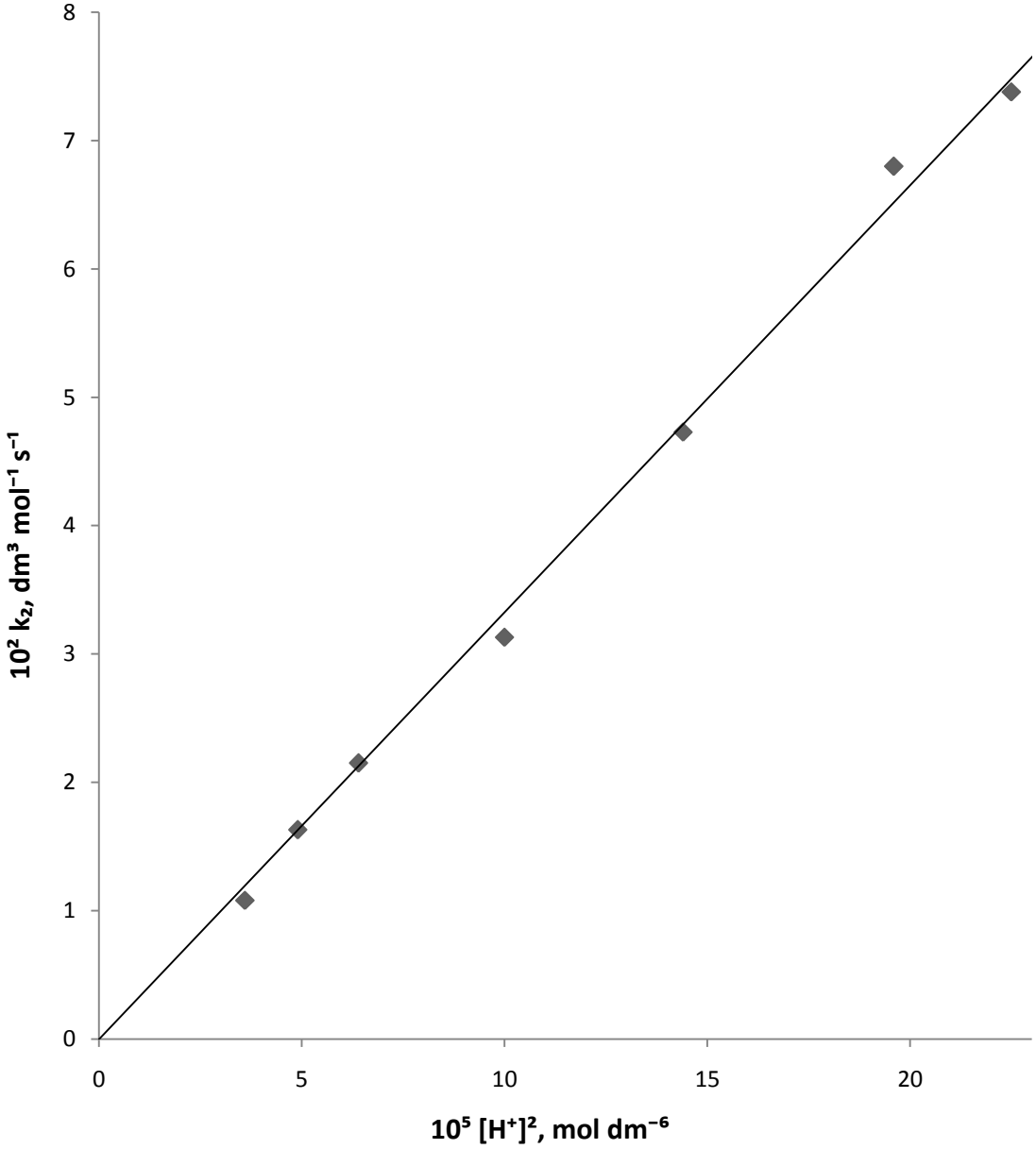


Figure 4.16: Plot of k_2 versus log $[H^+]^2$ for the redox reaction of malachite green with bromate ion at $[MG^+] = 1.0 \times 10^{-4}$ mol dm^{-3}, $[BrO_3^-] = 13.0 \times 10^{-2}$ mol dm^{-3},

I = 0.50 mol dm^{-3} and T = 28 ± 1 ºC

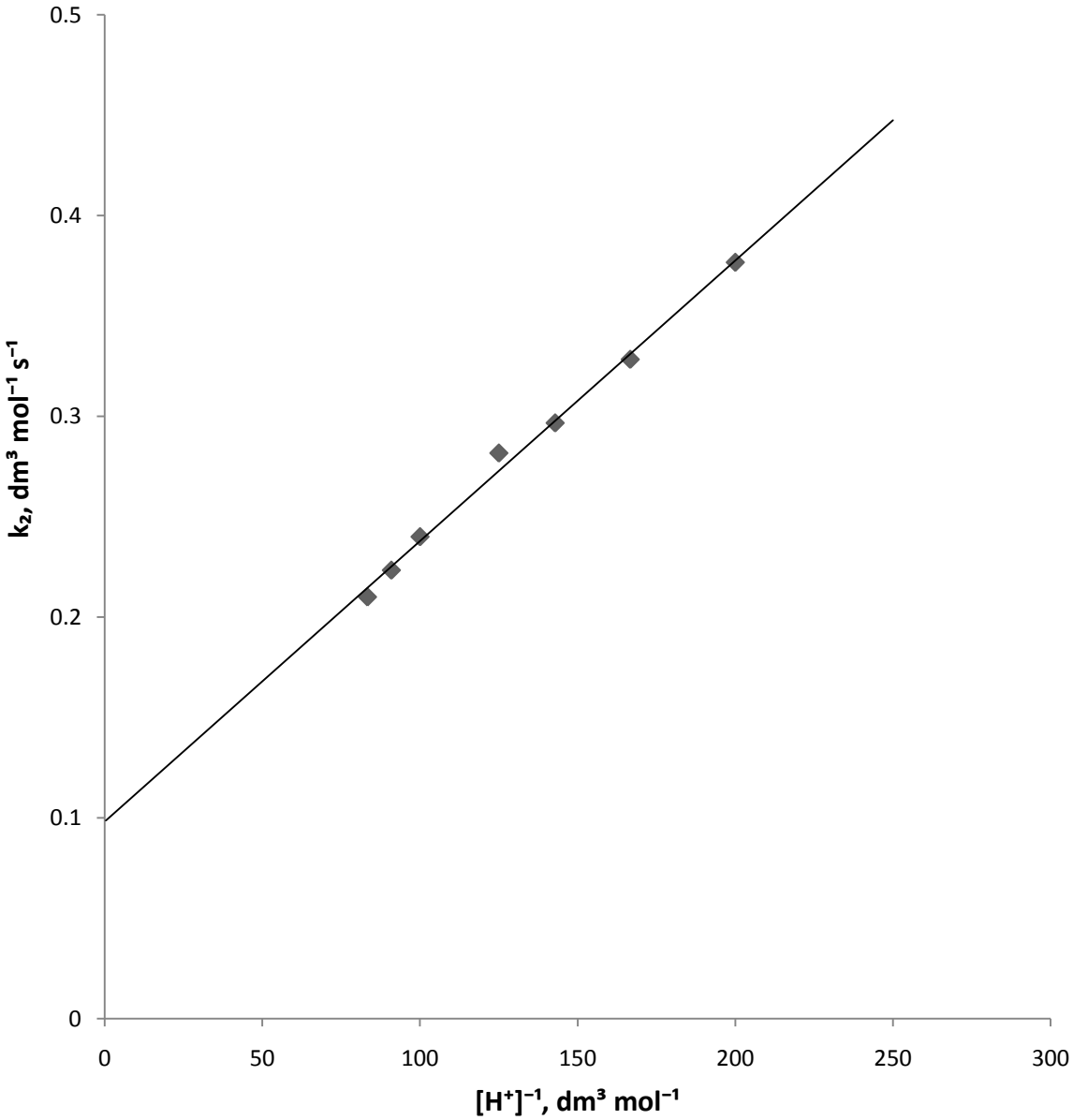


Figure 4.17: Plot of k_2 versus log $[H^+]^{-1}$ for the redox reaction of malachite green with metabisulphite ion at $[MG^+] = 1.0 \times 10^{-4}$ mol dm^{-3},

$[S_2O_5^{2-}] = 10.0 \times 10^{-3}$ mol dm^{-3}, I = 0.50 mol dm^{-3} and T = 28 ± 1 ºC

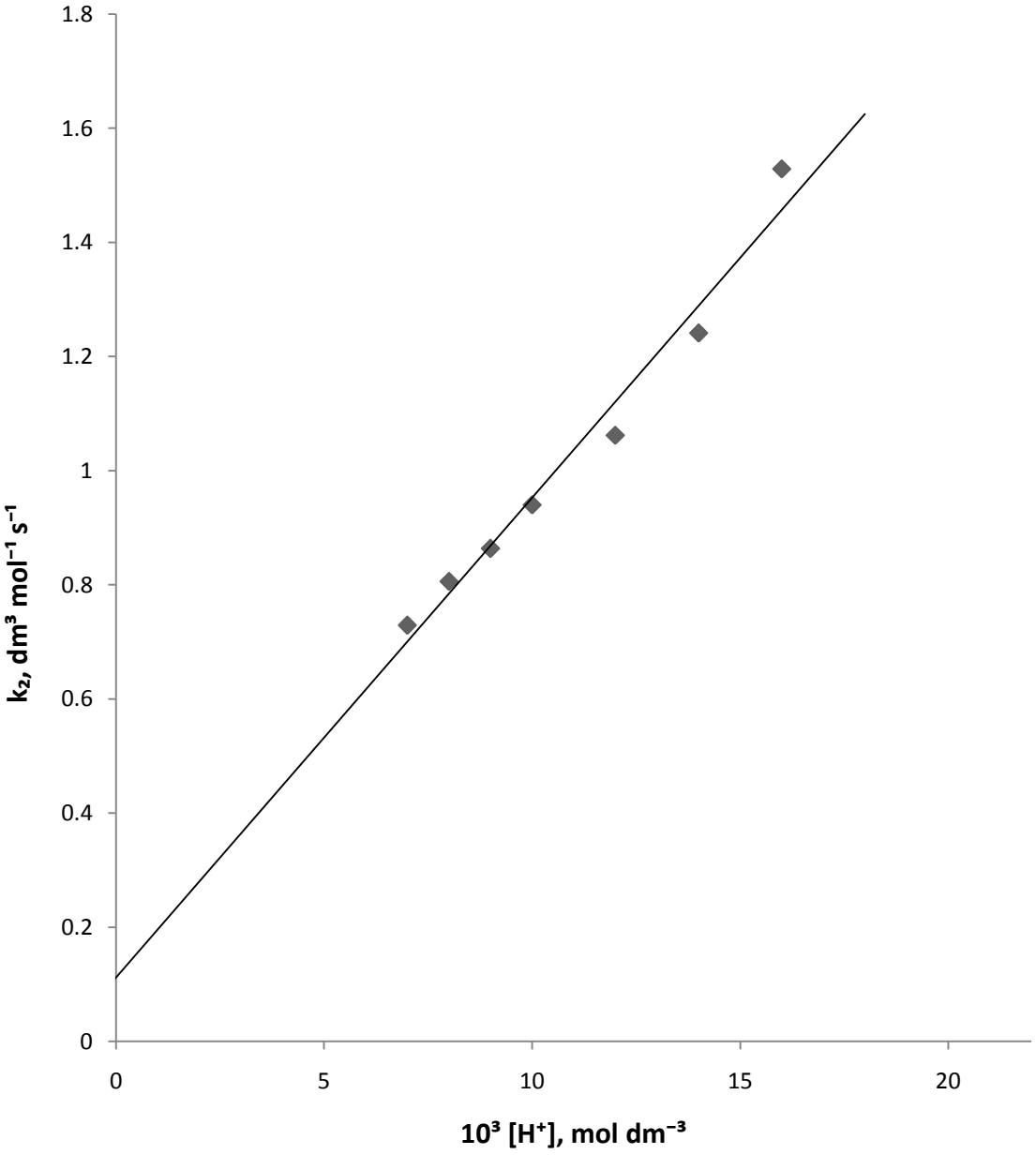


Figure 4.18: Plot of k_2 versus log $[H^+]$ for the redox reaction of malachite green with chlorite ion at $[MG^+] = 1.0 \times 10^{-4}$ mol dm^{-3}, $[ClO_2^-] = 6.0 \times 10^{-3}$ mol dm^{-3}, I = 0.30 mol dm^{-3} and T = 26 ± 1 ºC

where a = 3.32×10^{-1} dm^9 mol^{-3} s^{-1}, b = 9.80×10^{-2} dm^3 mol^{-1} s^{-1}, c = 1.38×10^{-3} s^{-1}, d = 0.11 dm^3 mol^{-1} s^{-1} and e = 8.40×10^{-2} s^{-1}.

The overall rate equations for these systems are represented in Equations 4.10 - 4.12.

$$\frac{-d[MG^+]}{dt} = (a\,[H^+]^2)[MG^+][BrO_3^-] \quad (4.10)$$

$$\frac{-d[MG^+]}{dt} = (b + c\,[H^+]^{-1})[MG^+][S_2O_5^{2-}] \quad (4.11)$$

$$\frac{-d[MG^+]}{dt} = [H^+]^0[MG^+][SO_3^{2-}] \quad (4.12)$$

$$\frac{-d[MG^+]}{dt} = (d + e\,[H^+])[MG^+][ClO_2^-] \quad (4.13)$$

4.4 Effect of Ionic Strength of the Reaction Medium on the Reaction Rate

The rates of the reactions were found to increase with increase in ionic strength of the reaction medium for the bromate, metabisulphite and sulphite systems, suggesting a positive

Bronsted-Debye salt effect. In the case of the chlorite system, increase in ionic strength of the reaction medium was found not to affect the rate of reaction.

The results are presented in Table 4.1 - 4.4. The logarithmic plots of k_2 against $\sqrt{I}$ are presented in Figures 4.19 - 4.21.

4.5 Effect of Changes in Dielectric Constant (D) of the Reaction Medium on the Rate of Reaction

From the results presented in Tables 4.5 and 4.6, the rate of the reaction decreased with increase in the amount of added acetone for the MG^+ - BrO_3^- system, increased with increase in amount of added acetone for MG^+ - $S_2O_5^{2-}$ system and has no effect on the rates of reactions for MG^+ - SO_3^{2-} and MG^+ - ClO_2^- systems. Plot of dielectric constant dependent rate constant (k_2) against 1/D for the BrO_3^- and $S_2O_5^{2-}$ systems are presented in Figures 4.22 and 4.23.

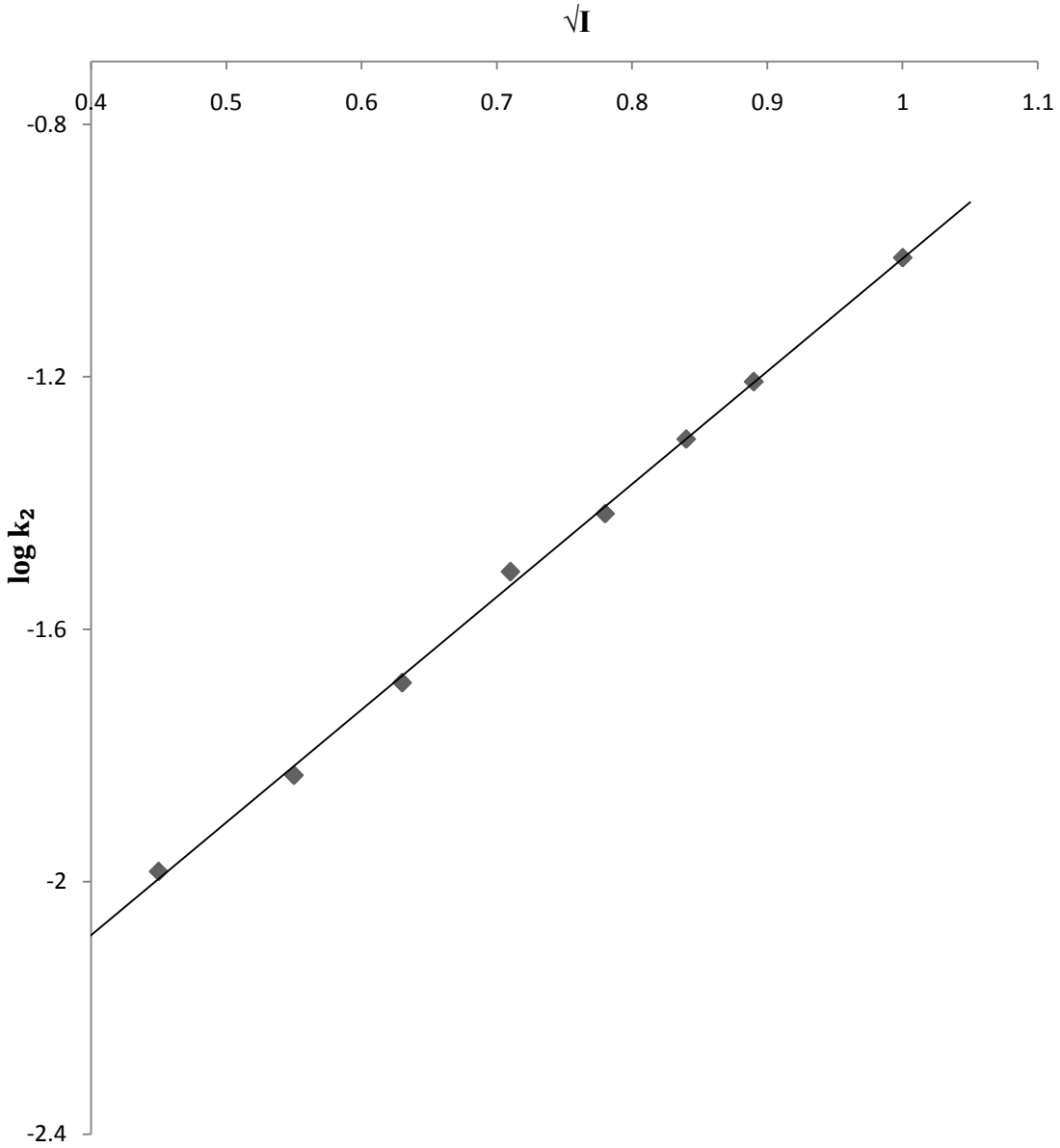


Figure 4.19: **Plot of log k_2 versus $\sqrt{I}$ for the redox reaction of malachite green with bromate ion at $[MG^+] = 1.0 \times 10^{-4}$ mol dm^{-3}, $[BrO_3^-] = 13.0 \times 10^{-2}$ mol dm^{-3}, $[H^+] = 1.0 \times 10^{-2}$ mol dm^{-3} and T= 28 ± 1 ºC**

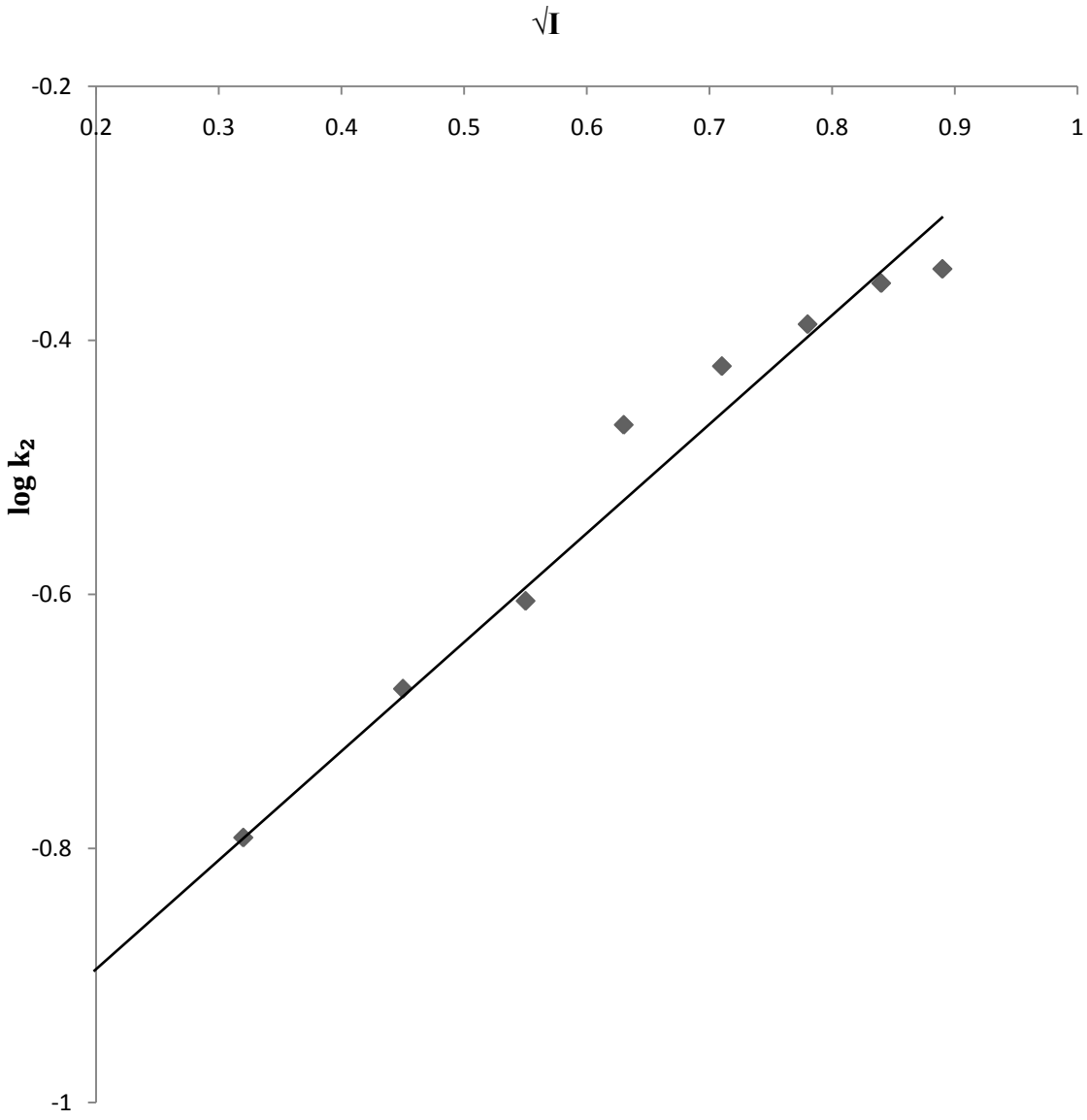


Figure 4.20: **Plot of log k_2 versus $\sqrt{I}$ for the redox reaction of malachite green with metabisulphite ion at $[MG^+] = 1.0 \times 10^{-4}$ mol dm^{-3}, $[S_2O_5^{2-}] = 10.0 \times 10^{-3}$ mol dm^{-3}, $[H^+] = 5.0 \times 10^{-3}$ mol dm^{-3} and T= 28 ± 1 ºC**

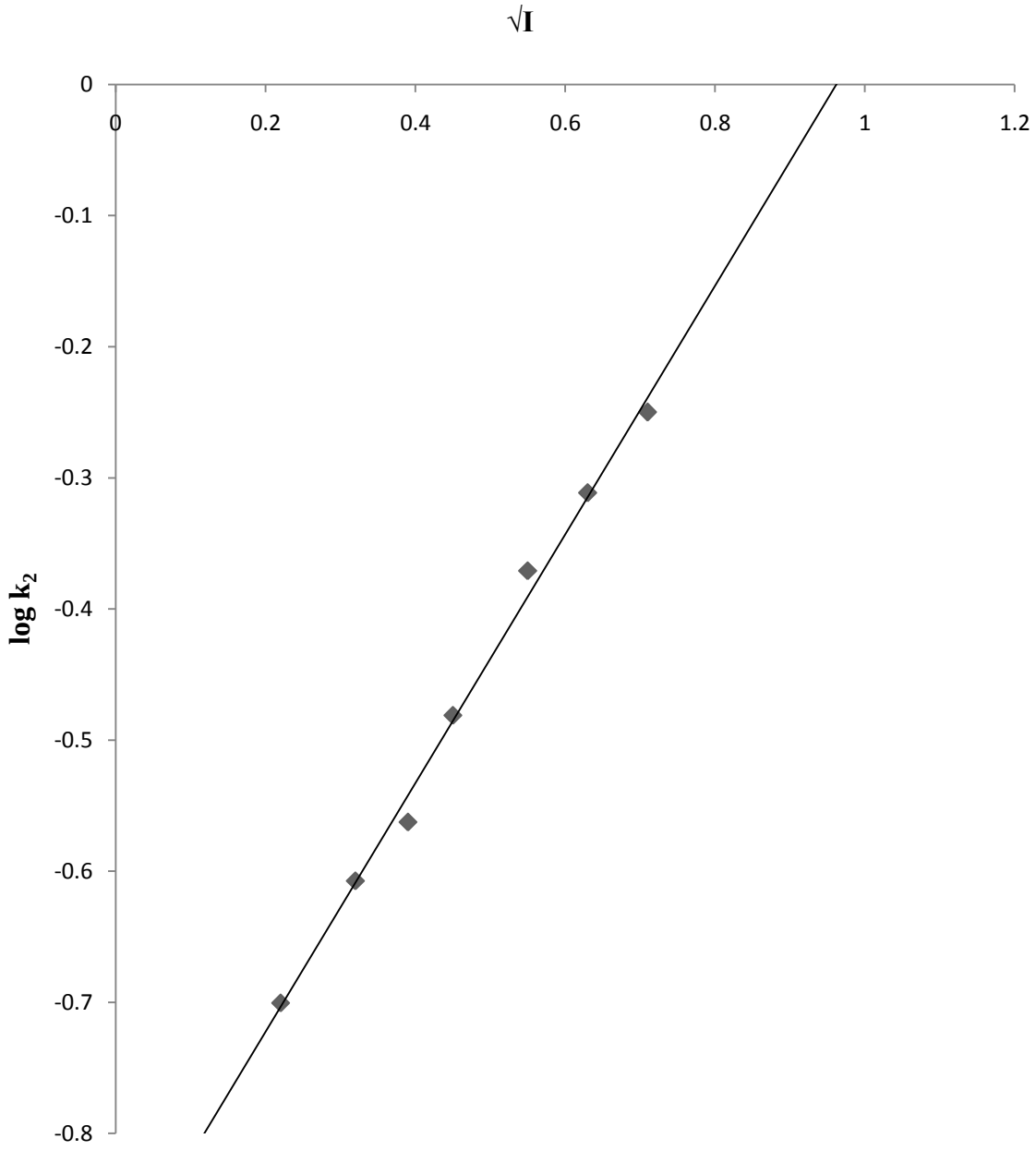


Figure 4.21: Plot of log k_2 versus $\sqrt{I}$ for the redox reaction of malachite green with sulphite ion at $[MG^+] = 1.0 \times 10^{-4}$ mol dm^{-3}, $[SO_3^{2-}] = 5.6 \times 10^{-3}$ mol dm^{-3} $[H^+] = 5.0 \times 10^{-3}$ mol dm^{-3} and T= 27 ± 1 ºC

Table 4.5: **Pseudo-first order and second order rate constants for the effect of changes in dielectric constant on the rate of redox reaction of malachite green with bromate ion at $[MG^+] = 1.0 \times 10^{-4}$ mol dm^{-3}, $[BrO_3^-] = 13.0 \times 10^{-2}$ mol dm^{-3}, I = 0.50 mol dm^{-3} and T= 28 ± 1 ºC**

D	$10^3$1/D	10^3 k_1, s^{-1}	10^2 k_2, dm^3 mol^{-1} s^{-1}
76.29	13.1	2.48	1.92
72.48	13.8	2.37	1.82
68.67	14.6	2.10	1.62
64.85	15.4	1.92	1.48
61.04	16.4	1.62	1.23
57.23	17.5	1.40	1.08
53.41	18.7	1.12	0.87
49.60	20.2	0.80	0.62

Table 4.6: Pseudo-first order and second order rate constants for the effect of changes in dielectric constant on the rate of redox reaction of malachite green with metabisulphite ion at $[MG^+] = 1.0 \times 10^{-4}$ moldm^{-3}, $[S_2O_5^{2-}] = 10.0 \times 10^{-3}$ mol dm^{-3}, I = 0.50 mol dm^{-3}and T = 28 ± 1ºC

D	$10^3$1/D	10^3 k_1, s^{-1}	10^1 k_2, dm^3 mol^{-1} s^{-1}

77.57	12.9	1.47	1.47
75.05	13.3	1.70	1.70
72.52	13.8	1.90	1.90
70.00	14.3	2.30	2.30
67.47	14.8	2.55	2.55
64.94	15.4	2.78	2.78
62.42	16.0	3.18	3.18
59.89	16.7	3.63	3.63

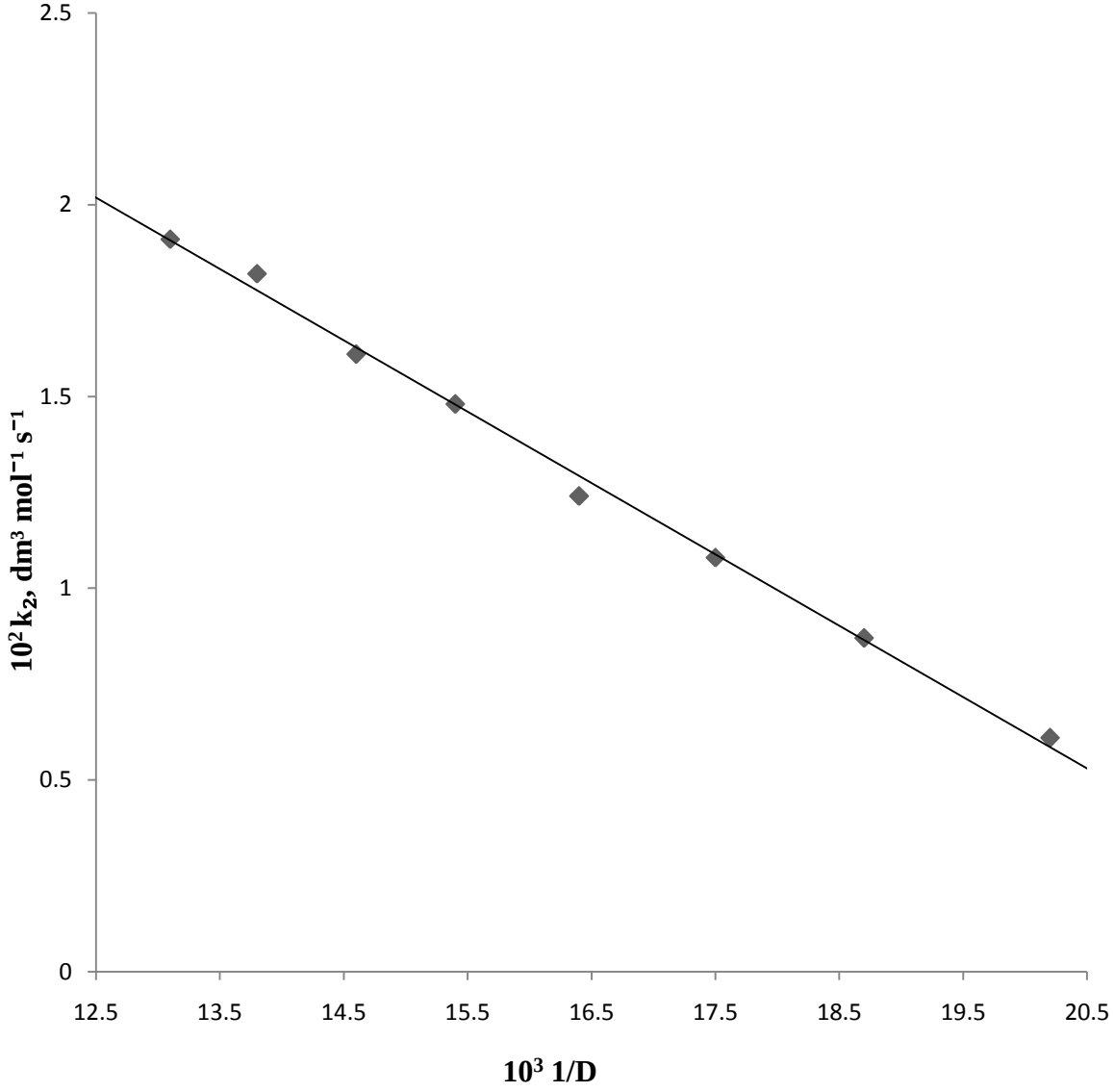


Figure 4.22: Plot of k_2 against 1/D for the redox reaction of malachite green with bromate ion at $[MG^+] = 1.0 \times 10^{-4}$ mol dm^{-3}, $[BrO_3^-] = 13.0 \times 10^{-2}$ mol dm^{-3}, $[H^+] = 1.0 \times 10^{-2}$ mol dm^{-3}, I = 0.50 mol dm^{-3} and T= 28 ± 1ºC

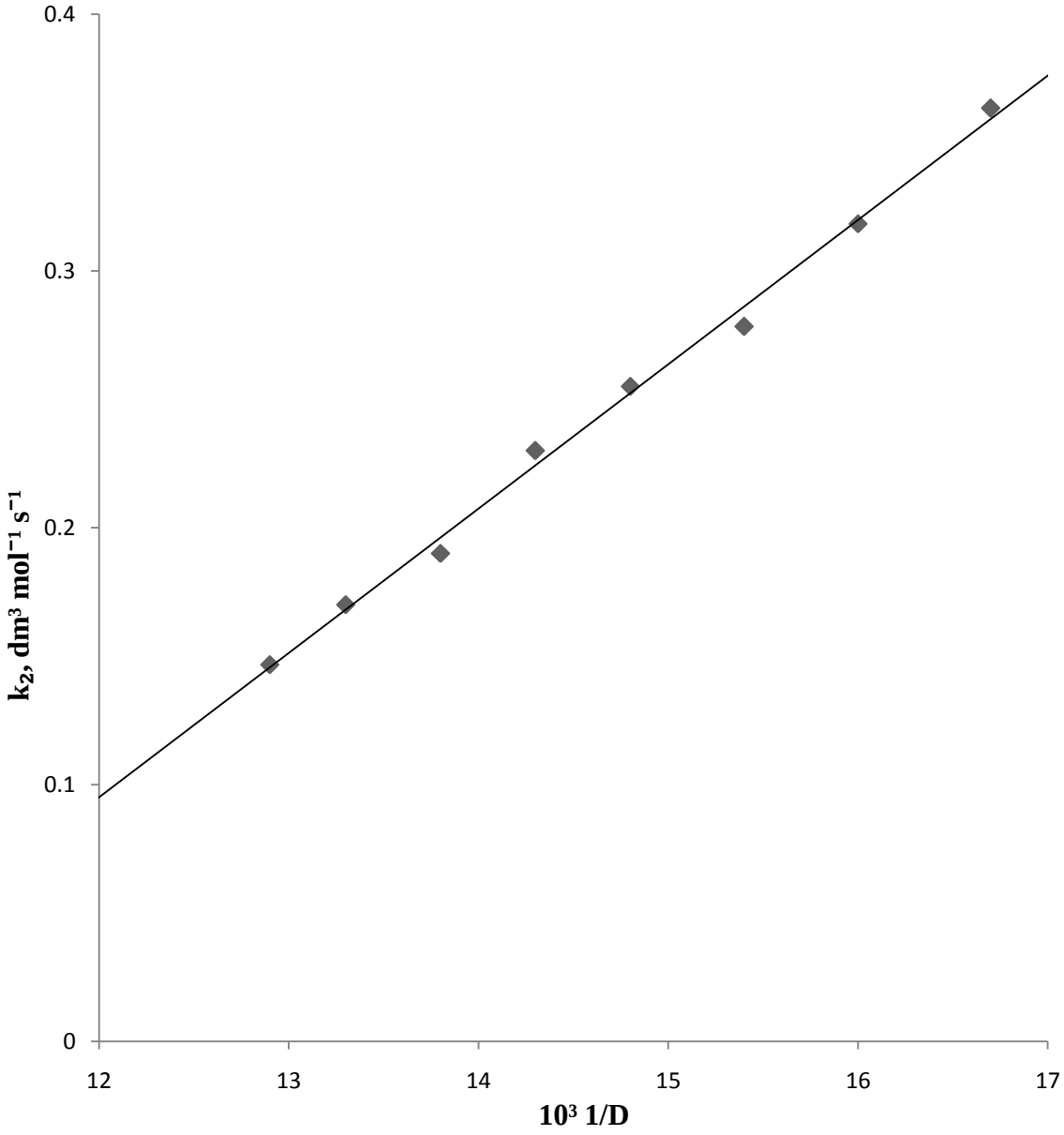


Figure 4.23: Plot of k_2 against 1/D for redox reaction of malachite green with metabisulphite ion at $[MG^+] = 1.0 \times 10^{-4}$ mol dm^{-3}, $[S_2O_5^{2-}] = 10.0 \times 10^{-3}$ mol dm^{-3}, $[H^+] = 5.0 \times 10^{-3}$ mol dm^{-3}, I = 0.50 mol dm^{-3} and T = 28 ± 1ºC

4.6 Effect of Added ions on the Reaction Rate

The results of the effects of added anions on the rate of reaction showed that the rate of reactions decreased with increase in the anion concentration for MG^+ - BrO_3^- and MG^+ - $S_2O_5^{2-}$ systems, increased with increase in the anion concentration for MG^+ - SO_3^{2-} system and had no effect on the rate of reaction for MG^+ - ClO_2^- system. These are presented in Tables 4.7 - 4.10. Plots of anion dependent rate constants against anion concentrations are presented in Figures 4.24 - 4.27.

Addition of Mg^{2+} and NH_4^+ ions decreased the rate of reaction for MG^+ - BrO_3^- and MG^+ - $S_2O_5^{2-}$ systems, inhibited the rate of reaction for MG^+ - SO_3^{2-} system and had no effect on the rate of reaction of the MG^+-ClO_2^- system. These results are presented in Tables 4.11 - 4.14. Plots of cation dependent rate constants against cation concentrations are presented in Figures 4.28 - 4.33.

4.7 Test for Intermediate Complex Formation

4.7.1 Test for the presence of free radicals

Addition of acrylamide showed no visible reaction on reactant sample solutions. The formation of a gelatinous precipitate was observed for MG^+ - BrO_3^-, MG^+ - $S_2O_5^{2-}$ and MG^+ - SO_3^{2-} systems but the MG^+ - ClO_2^- system gave no precipitate. This indicates that the involvement of free radicals in the ClO_2^- reaction is unlikely.

4.7.2 Michaelis - Menten plot

The Michaelis-Menten plots of $1/k_1$ versus 1/[oxyanion] were linear and passed through the origin for all the systems studied. These observations suggest the absence of intermediate complex formation prior to the rate determining step (Figures 4.34 - 4.37).

Table 4.7: Pseudo-first order and second order rate constants for the effect of added anion on the rate of redox reaction of malachite green with bromate ion at $[MG^+] = 1.0 \times 10^{-4}$ mol dm^{-3}, $[BrO_3^-] = 13.0 \times 10^{-2}$ mol dm^{-3},

I = 0.50 mol dm^{-3} and T = 28 ± 1 ºC

X	10^3 [X], mol dm^{-3}	$10^3 k_1$, s^{-1}	$10^2 k_2$, $dm^3 mol^{-1} s^{-1}$
NO_3^-	0	4.03	3.10
	10	0.76	0.58
	20	0.70	0.53
	30	0.65	0.50
	40	0.58	0.45
	50	0.47	0.37

	70	0.32	0.25
	80	0.23	0.18

Table 4.8: Pseudo-first order and second order rate constants for the effect of added anions on the rate of redox reaction of malachite green with metabisulphite ion at $[MG^+] = 1.0 \times 10^{-4}$ mol dm^{-3}, $[S_2O_5^{2-}] = 10.0 \times 10^{-3}$ mol dm^{-3},

I = 0.50 mol $dm^{-3}$and T= 28 ± 1 ºC

X	10^3 [X], mol dm^{-3}	10^3 k_1, s^{-1}	10^1 k_2, dm^3 mol^{-1} s^{-1}
NO_3^-	0	3.77	3.77
	20	3.62	3.62
	30	3.57	3.57
	40	3.45	3.50
	50	3.42	3.47
	60	3.38	3.38
	70	3.30	3.30
	80	3.27	3.27
$HCOO^-$	0	3.77	3.77
	10	3.68	3.68
	20	3.62	3.62
	40	3.50	3.55
	50	3.45	3.45
	60	3.38	3.38
	80	3.23	3.23

Table 4.9: Pseudo-first order and second order rate constants for the effect of added anion on the rate of redox reaction of malachite green with sulphite ion at $[MG^+] = 1.0 \times 10^{-4}$ mol dm^{-3}, $[SO_3^{2-}] = 5.6 \times 10^{-3}$ mol dm^{-3}, I = 0.10 mol dm^{-3} and T= 27 ± 1 ºC

X	10^4 [X], mol dm^{-3}	10^3 k_1, s^{-1}	10^1 k_2, dm^3 mol^{-1} s^{-1}
NO_3^-	0	1.38	2.47
	20	1.85	3.29
	30	2.00	3.58
	40	2.12	3.77
	50	2.15	3.84
	60	2.23	3.98
	70	2.30	4.11
	80	2.42	4.32

Table 4.10: **Pseudo-first order and second order rate constants for the effect of added anions on the rate of redox reaction of malachite green with chlorite ion at $[MG^{+}] = 1.0 \times 10^{-4}$ mol dm^{-3}, $[ClO_2^{-}] = 6.0 \times 10^{-3}$ mol dm^{-3},**

I = 0.30 mol dm^{-3} and T= 26 ± 1 ºC

X	10^4 [X], moldm^{-3}	10^3 k_1, s^{-1}	10^1 k_2, dm^3 mol^{-1} s^{-1}

NO_3^-	0	5.66	9.43
	10	5.65	9.42
	20	5.66	9.43
	30	5.64	9.40
	40	5.66	9.43
	50	5.62	9.37
	60	5.66	9.43
CH_3COO^-	0	5.66	9.43
	10	5.66	9.43
	20	5.66	9.43
	30	5.65	9.42
	40	5.64	9.40
	50	5.65	9.42
	60	5.65	9.42

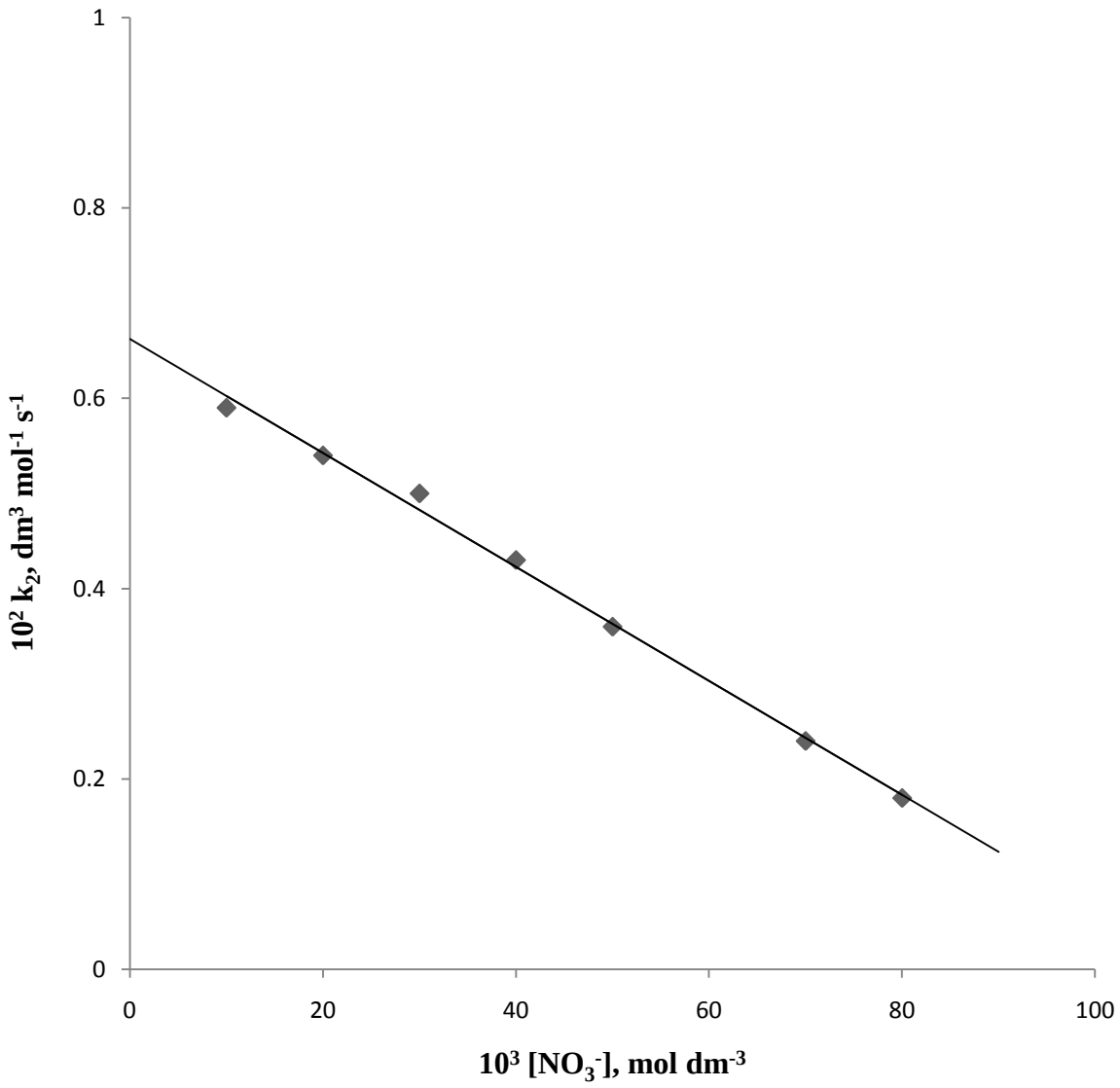


Figure 4.24: **Plot of k_2 versus $[NO_3^-]$ for the redox reaction malachite green with bromate ion at $[MG^+] = 1.0 \times 10^{-4}$ mol dm^{-3}, $[BrO_3^-] = 13.0 \times 10^{-2}$ mol dm^{-3}, I = 0.50 mol dm^{-3} and T = 28 ± 1 ºC**

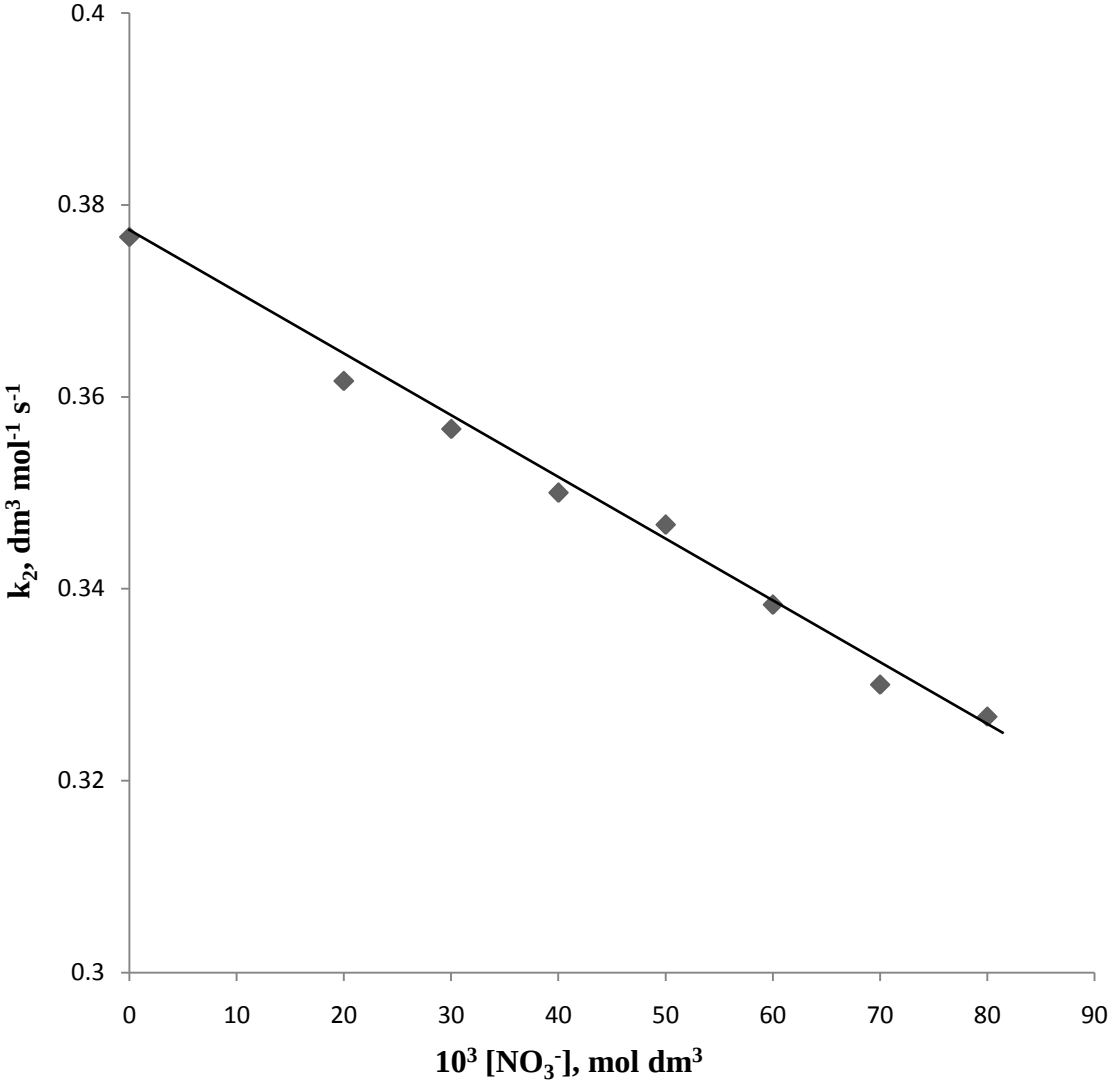


Figure 4.25: **Plot of k_2 versus $[NO_3^-]$ for the redox reaction malachite green with metabisulphite ion at $[MG^+] = 1.0 \times 10^{-4}$ mol dm^{-3}, $[S_2O_5^{2-}] = 10.0 \times 10^{-3}$ mol dm^{-3}, I = 0.50 mol dm^{-3} and T= 28 ± 1 ºC**

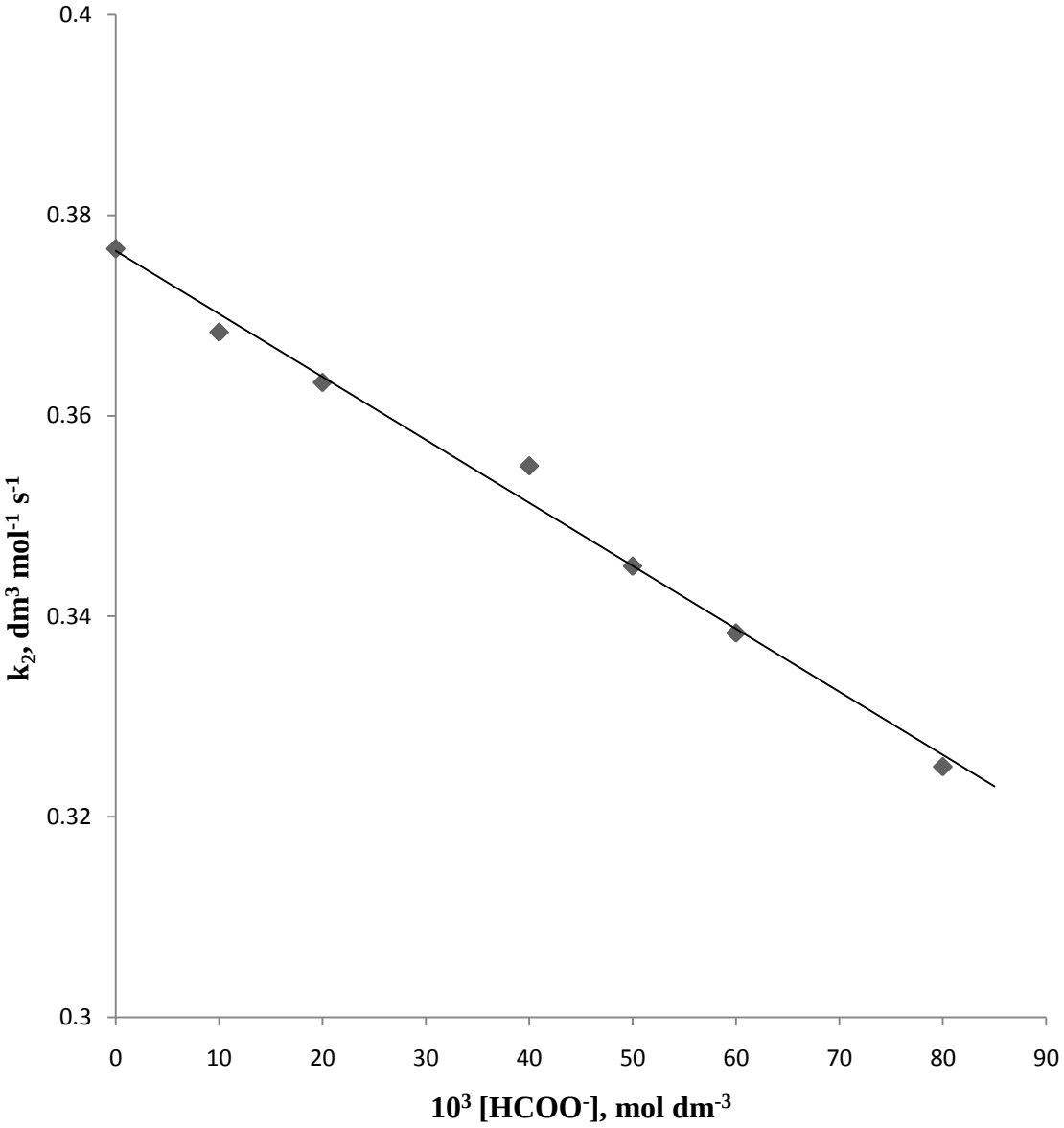


Figure 4.26: **Plot of k_2 versus $[HCOO^-]$ for the redox reaction of malachite green with metabisulphite ion at $[MG^+] = 1.0 \times 10^{-4}$ mol dm^{-3}, $[S_2O_5^{2-}] = 10.0 \times 10^{-3}$ mol dm^{-3}, I = 0.50 mol dm^{-3} and T= 28 ± 1 ºC**

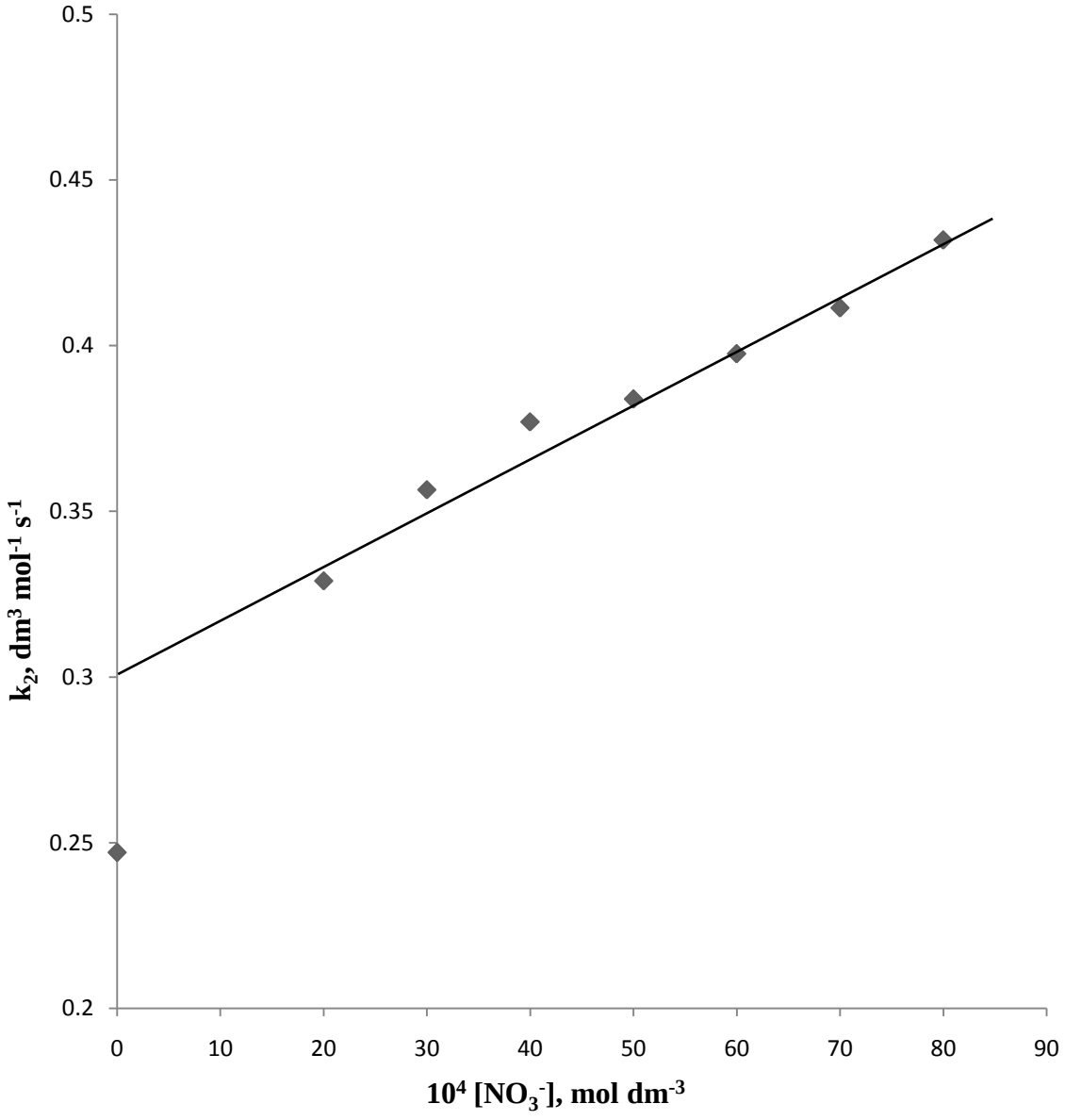


Figure 4.27: Plot of k_2 versus $[NO_3^-]$ for the redox reaction of malachite green with sulphite ion at $[MG^+] = 1.0 \times 10^{-4}$ mol dm^{-3}, $[SO_3^{2-}] = 5.6 \times 10^{-3}$ mol dm^{-3}, I = 0.10 mol dm^{-3} and T= 27 ± 1 ºC

Table 4.11: Pseudo-first order and second order rate constants for the effect of added cations on the rate of redox reaction of malachite green with bromate ion at $[MG^+] = 1.0 \times 10^{-4}$ mol dm^{-3}, $[BrO_3^-] = 13.0 \times 10^{-2}$ mol dm^{-3},

I = 0.50 mol dm^{-3} and T = 28 ± 1 ºC

X	10^3 [X], mol dm^{-3}	10^3 k_1, s^{-1}	$10^1 k_2$, dm^{-3} mol^{-1} s^{-1}
NH_4^+	0	4.03	3.10
	10	3.82	2.93
	20	3.65	2.80
	30	3.55	2.73
	40	3.38	2.60
	50	3.18	2.45
	60	3.05	2.35
	70	2.98	2.30
Mg^{2+}	0	4.03	3.10
	20	3.37	2.58

	30	2.87	2.20
	40	2.65	2.03
	50	2.45	1.88
	60	2.22	1.70
	70	1.88	1.45
	80	1.38	1.07

Table 4.12: Pseudo-first order and second order rate constants for the effect of added cations on the rate of redox reaction of malachite green with metabisulphite ion at $[MG^+] = 1.0 \times 10^{-4}$ mol dm^{-3}, $[S_2O_5^{2-}] = 10.0 \times 10^{-3}$ mol dm^{-3}, I = 0.50 mol dm^{-3} and T= 28 ± 1 ºC

X	10^3 [X], mol dm^{-3}	10^3 k_1, s^{-1}	10^1 k_2, dm^3 mol^{-1} s^{-1}
NH_4^+	0	3.77	3.77
	10	2.37	2.37
	20	2.18	2.18

	30	2.00	2.00
	40	1.80	1.80
	50	1.73	1.73
	60	0.16	1.57
	70	0.15	1.53
Mg^{2+}	0	3.77	3.77
	20	3.42	3.42
	30	3.17	3.17
	40	2.73	2.73
	50	2.67	2.67
	60	2.83	2.83
	70	2.53	2.53
	80	2.50	2.50

Table 4.13: Pseudo-first order and second order rate constants for the effect of added cations on the rate of redox reaction of malachite green with sulphite ion at $[MG^{+}] = 1.0 \times 10^{-4}$ mol dm^{-3}, $[SO_3^{2-}] = 5.6 \times 10^{-3}$ mol dm^{-3}, I = 0.10 mol dm^{-3} and T= 27 ± 1 ºC

X	10^4 [X], mol dm^{-3}	10^3 k_1, s^{-1}	10^1 k_2, dm^3 mol^{-1} s^{-1}
NH_4^+	0	1.35	2.40
	20	1.38	2.47
	30	1.42	2.54
	40	1.42	2.54
	50	1.47	2.61
	60	1.50	2.67
	70	1.50	2.67
	80	1.55	2.74
Mg^{2+}	0	1.35	2.40
	10	1.35	2.40
	20	1.38	2.47
	30	1.42	2.54
	40	1.42	2.54
	50	1.47	2.61

	60	1.50	2.67
	80	1.62	2.88

Table 4.14: Pseudo-first order and second order rate constants for the effect of added cations on the rate of redox reaction of malachite green with chlorite ion at $[MG^+] = 1.0 \times 10^{-4}$ mol dm^{-3}, $[ClO_2^-] = 6.0 \times 10^{-3}$ moldm^{-3}, I = 0.30 mol dm^{-3} and T= 26 ± 1 ºC

X	10^4 [X], mol dm^{-3}	$10^3 k_1$, s^{-1}	$10^1 k_2$, dm^3 mol^{-1} s^{-1}
NH_4^+	0	5.66	9.43
	10	5.66	9.43
	20	5.64	9.40
	40	5.65	9.42
	40	5.64	9.40
	50	5.66	9.43
	60	5.66	9.43
Mg^{2+}	0	5.66	9.43
	10	5.65	9.42

20	5.65	9.42
30	5.62	9.37
40	5.64	9.40
50	5.66	9.43
60	5.65	9.42

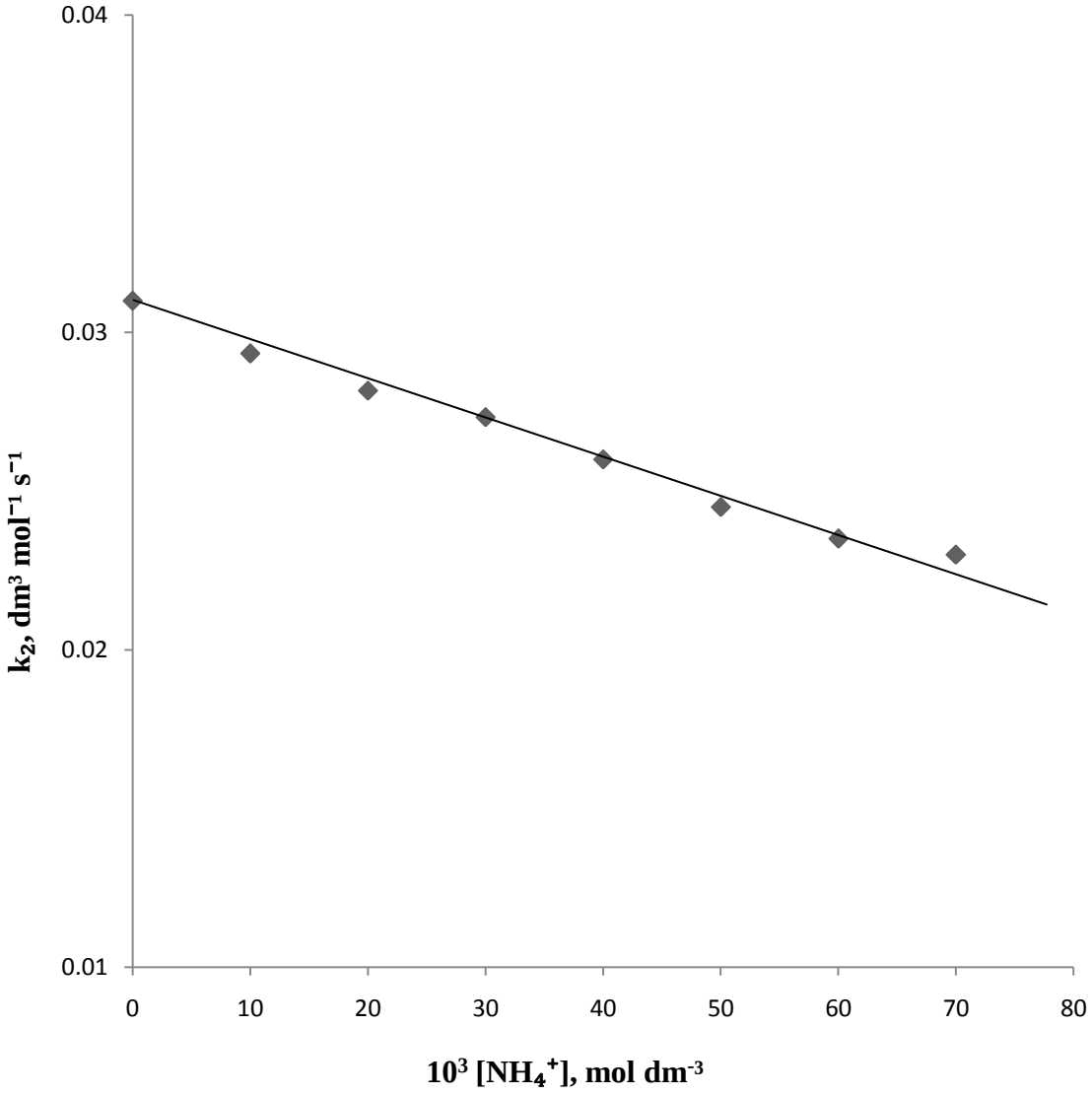


Figure 4.28: **Plot of k_2 versus $[NH_4^+]$ for the redox reaction malachite green with bromate ion at $[MG^+] = 1.0 \times 10^{-4}$ mol dm^{-3}, $[BrO_3^-] = 13.0 \times 10^{-2}$ mol dm^{-3}, I = 0.50 mol dm^{-3} and T = 28 ± 1ºC**

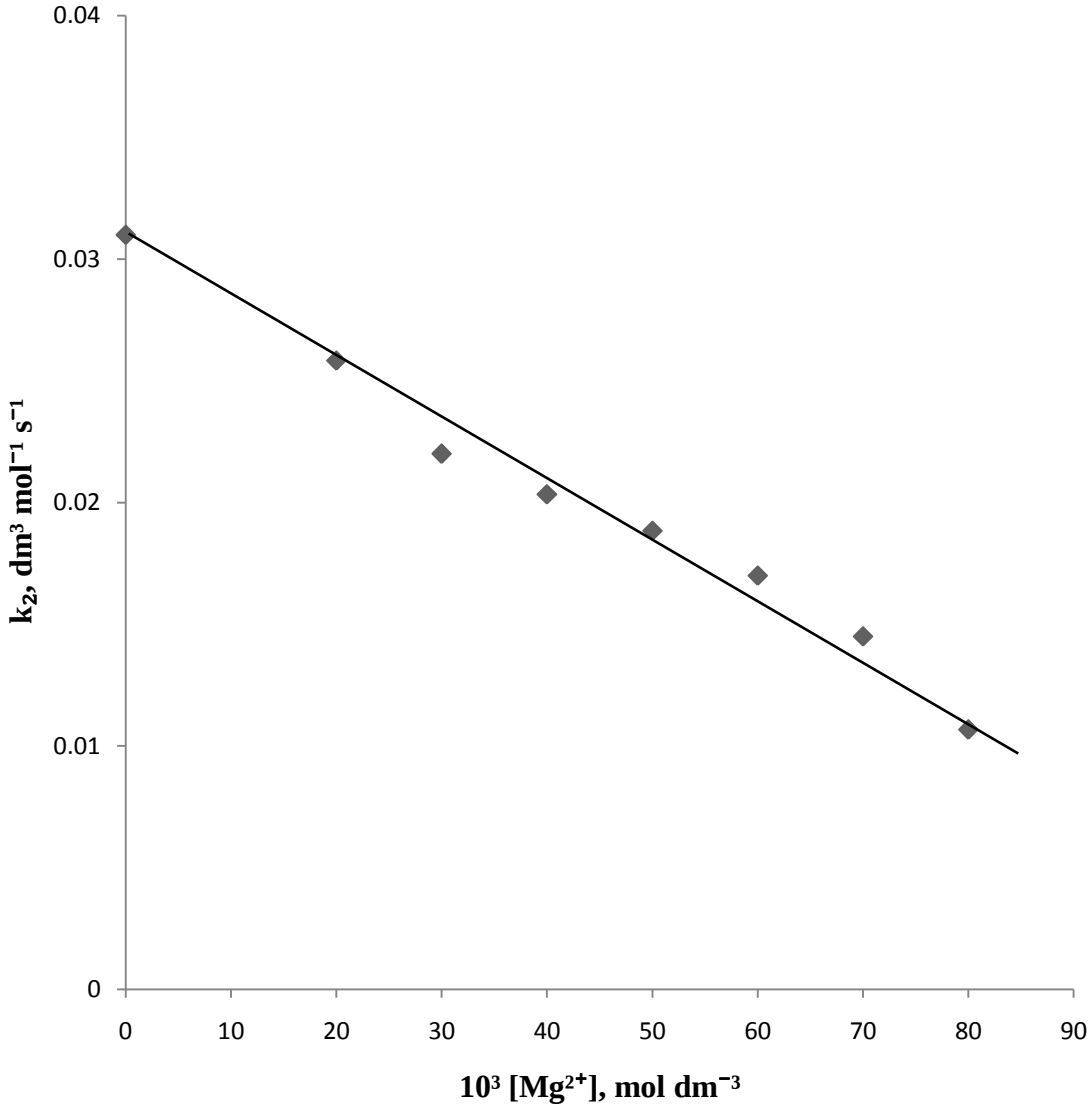


Figure 4.29: **Plot of k_2 versus [Mg^{2+}] for the redox reaction malachite green with bromate ion at [MG^+] = 1.0 × 10^{-4} mol dm^{-3}, [BrO_3^-] = 13.0 × 10^{-2} mol dm^{-3}, I = 0.50 mol dm^{-3} and T = 28 ± 1ºC**

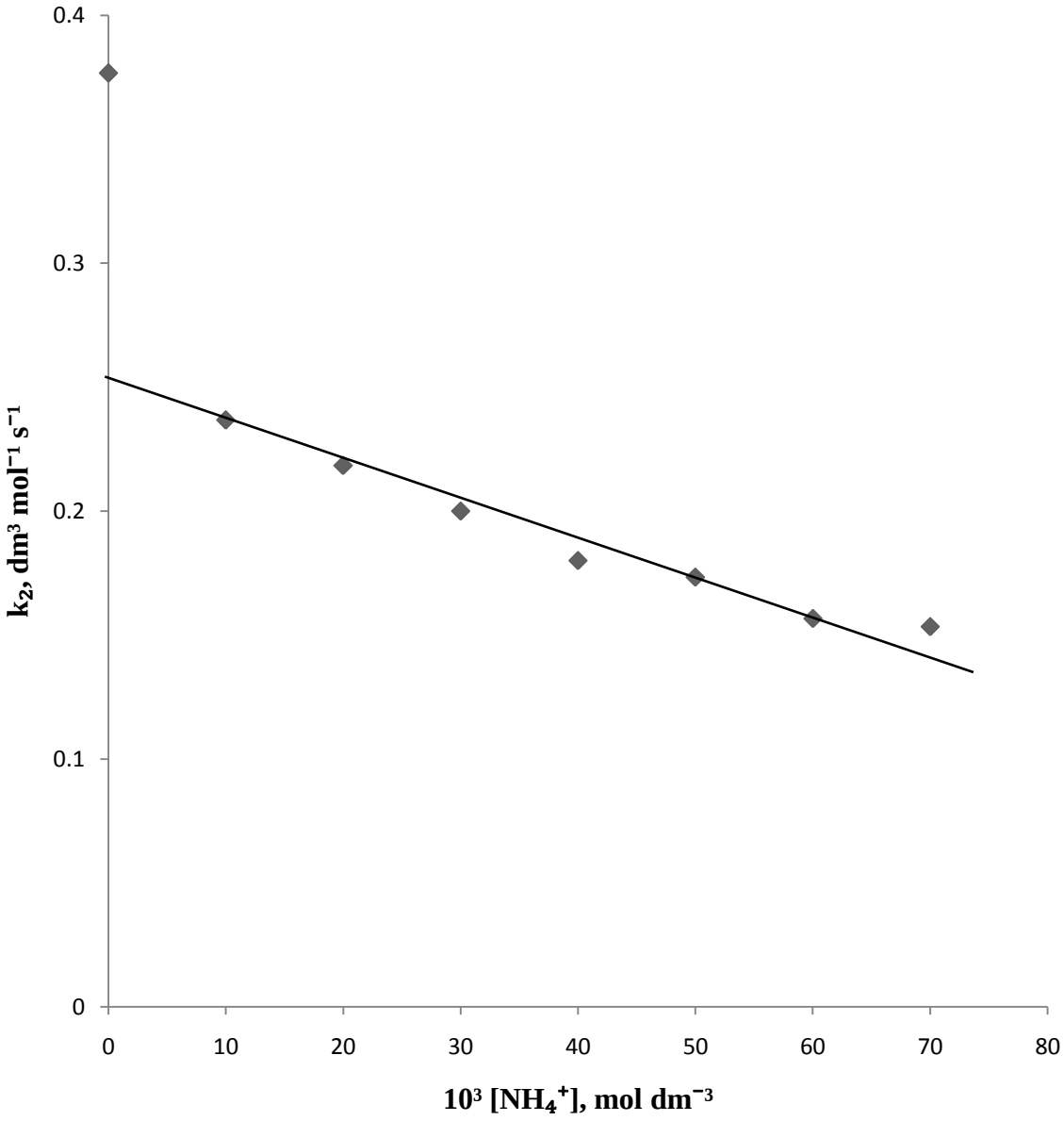


Figure 4.30: **Plot of k_2 versus [NH_4^+] for the redox reaction malachite green with metabisulphite ion at [MG^+] = 1.0 × 10^{-4} mol dm^{-3}, [$S_2O_5^{2-}$]= 10.0 × 10^{-3} mol dm^{-3}, I = 0.50 mol dm^{-3} and T = 28 ± 1ºC**

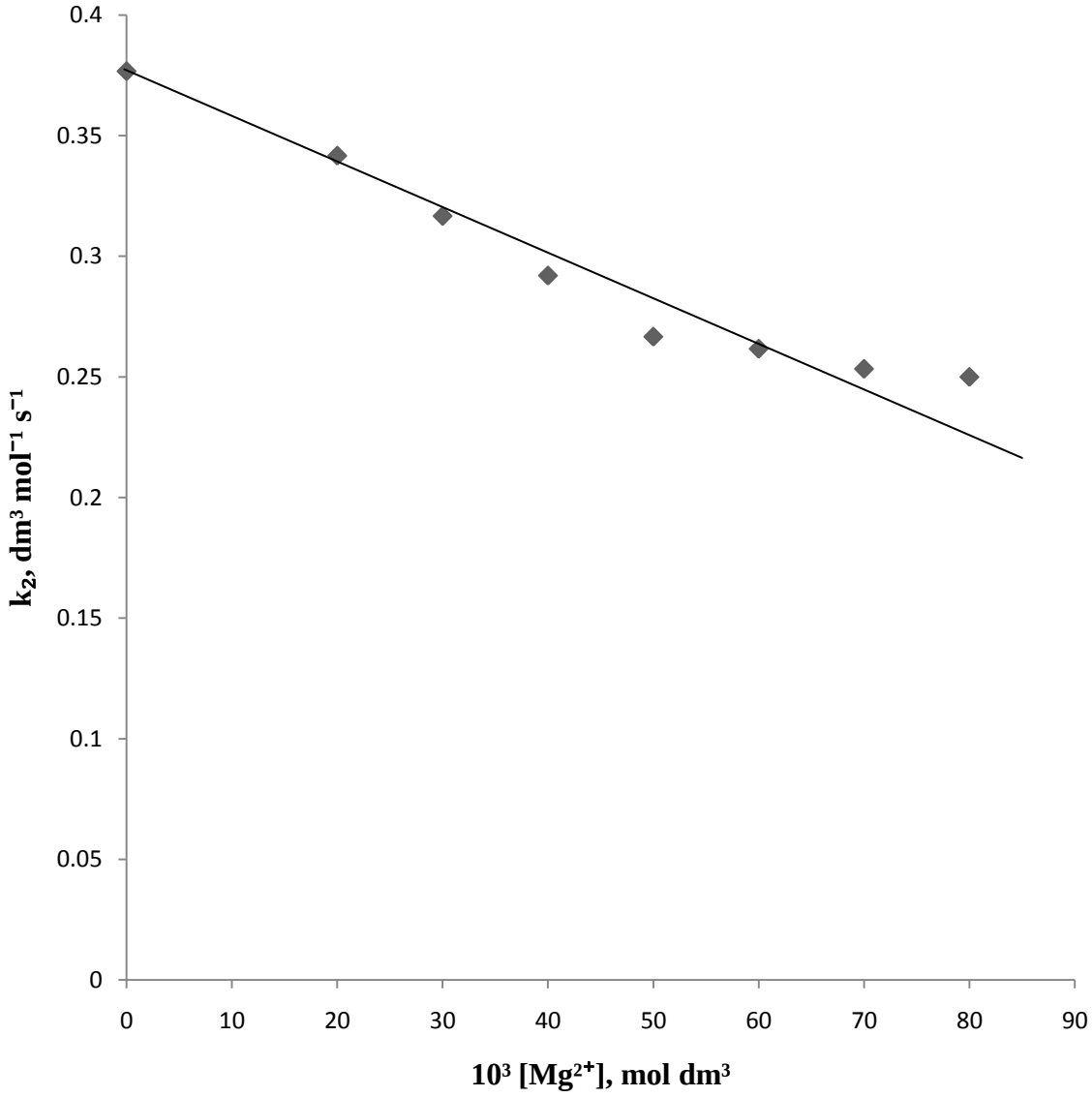


Figure 4.31: Plot of k_2 versus $[Mg^{2+}]$ for the redox reaction malachite green with metabisulphite ion at $[MG^{+}] = 1.0 \times 10^{-4}$ mol dm^{-3}, $[S_2O_5^{2-}] = 10.0 \times 10^{-3}$ mol dm^{-3}, I = 0.50 mol dm^{-3} and T = 28 ± 1ºC

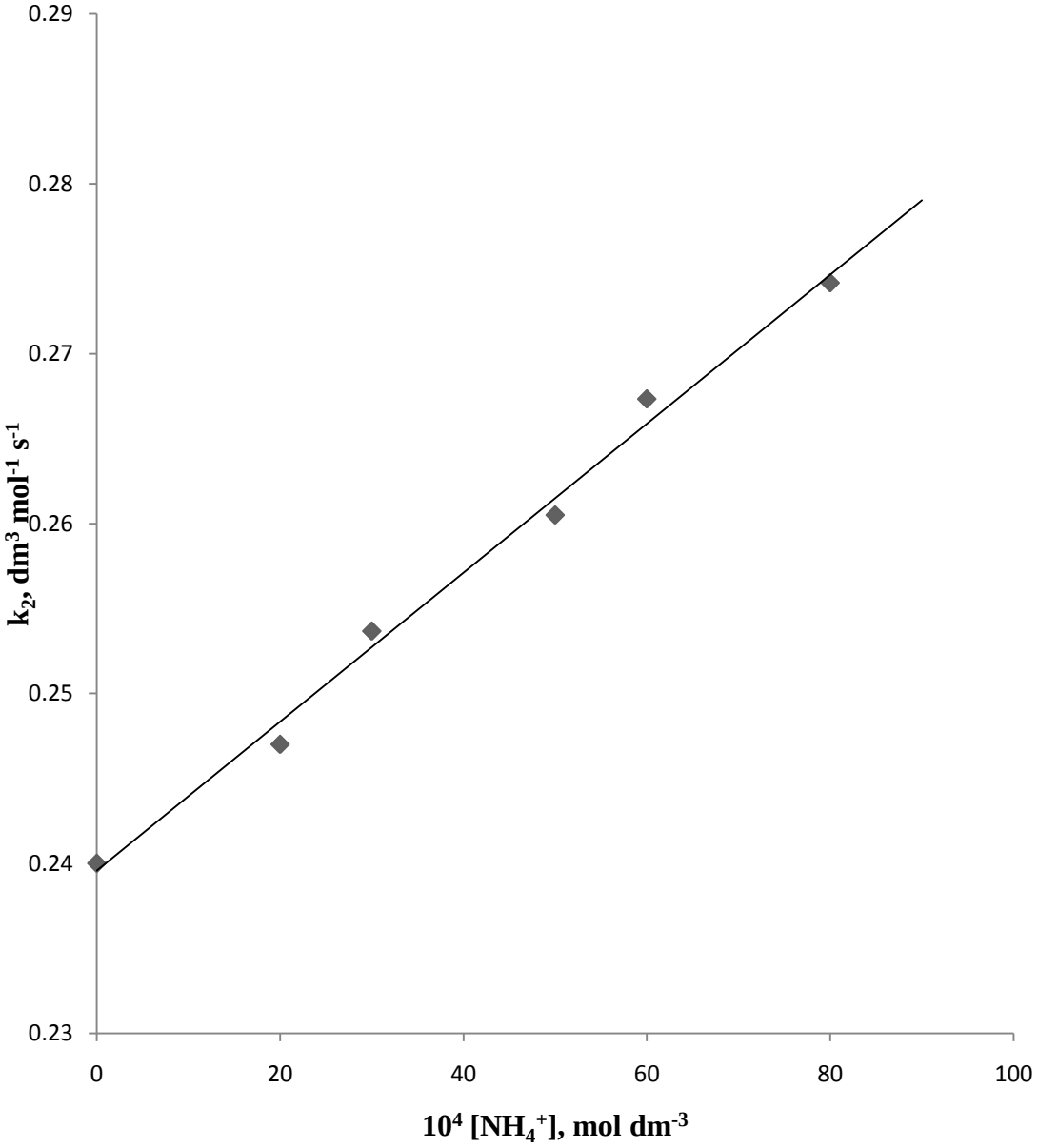


Figure 4.32: **Plot of k_2 versus [NH_4^+] for the redox reaction malachite green with sulphite ion at [MG^+] = 1.0 × 10^{-4} mol dm^{-3}, [SO_3^{2-}] = 5.6 × 10^{-3} mol dm^{-3},**

I = 0.10 mol dm^{-3} and T = 27 ± 1ºC

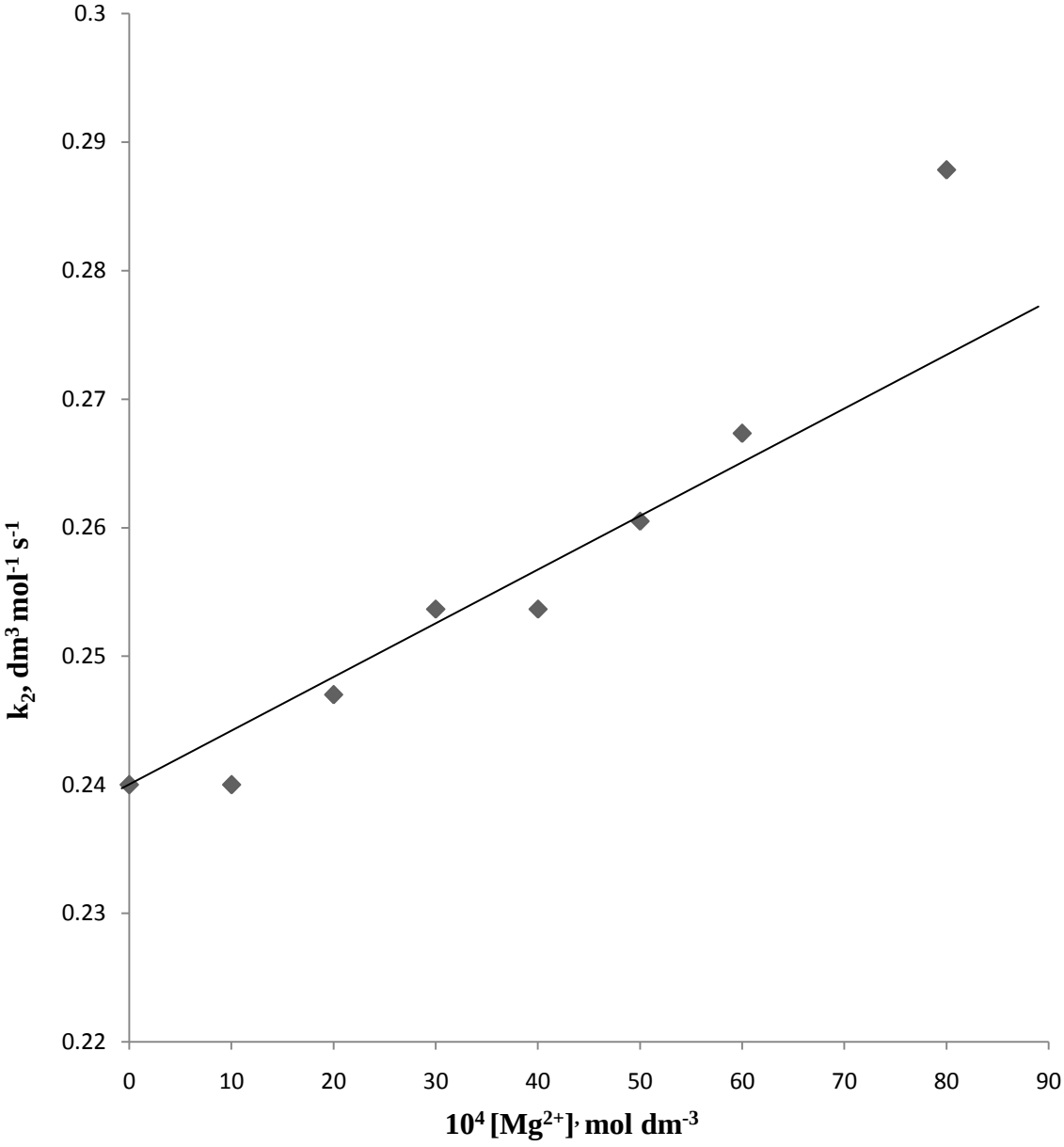


Figure 4.33: Plot of k_2 versus $[Mg^{2+}]$ for the redox reaction malachite green with sulphite ion at $[MG^{+}] = 1.0 \times 10^{-4}$ mol dm^{-3}, $[SO_3^{2-}] = 5.6 \times 10^{-3}$ mol dm^{-3}, I = 0.10 mol dm^{-3} and T = 27 ± 1ºC

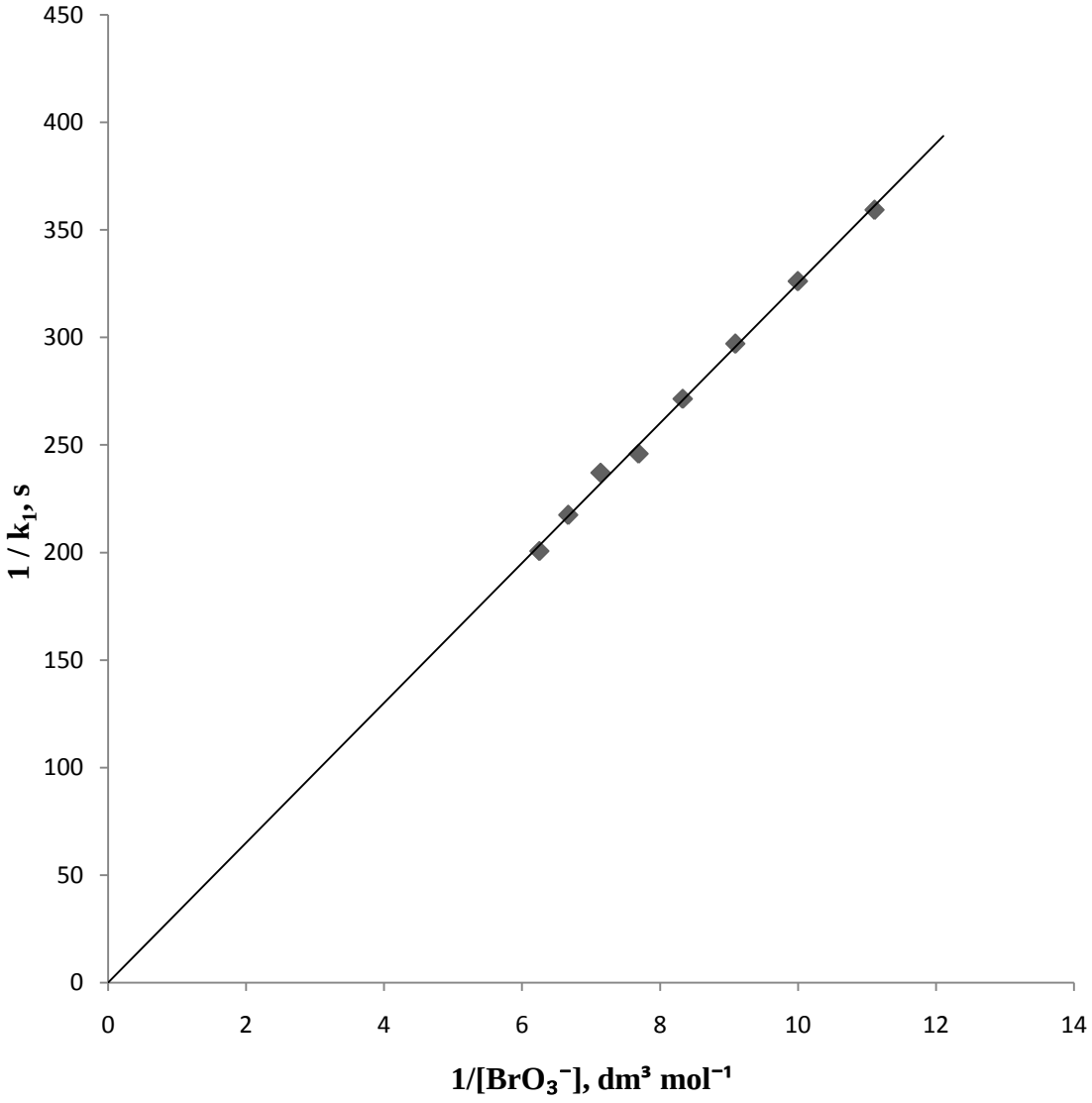


Figure 4.34: **Michaelis-Menten plot of $1/k_1$ versus $1/[BrO_3^-]$ for the redox reaction of malachite green with bromate ion at $[MG^+] = 1.0 \times 10^{-4}$ mol dm^{-3},**

$[H^+] = 1.0 \times 10^{-2}$ mol dm^{-3}, I = 0.50 mol dm^{-3} and T= 28 ± 1 ºC

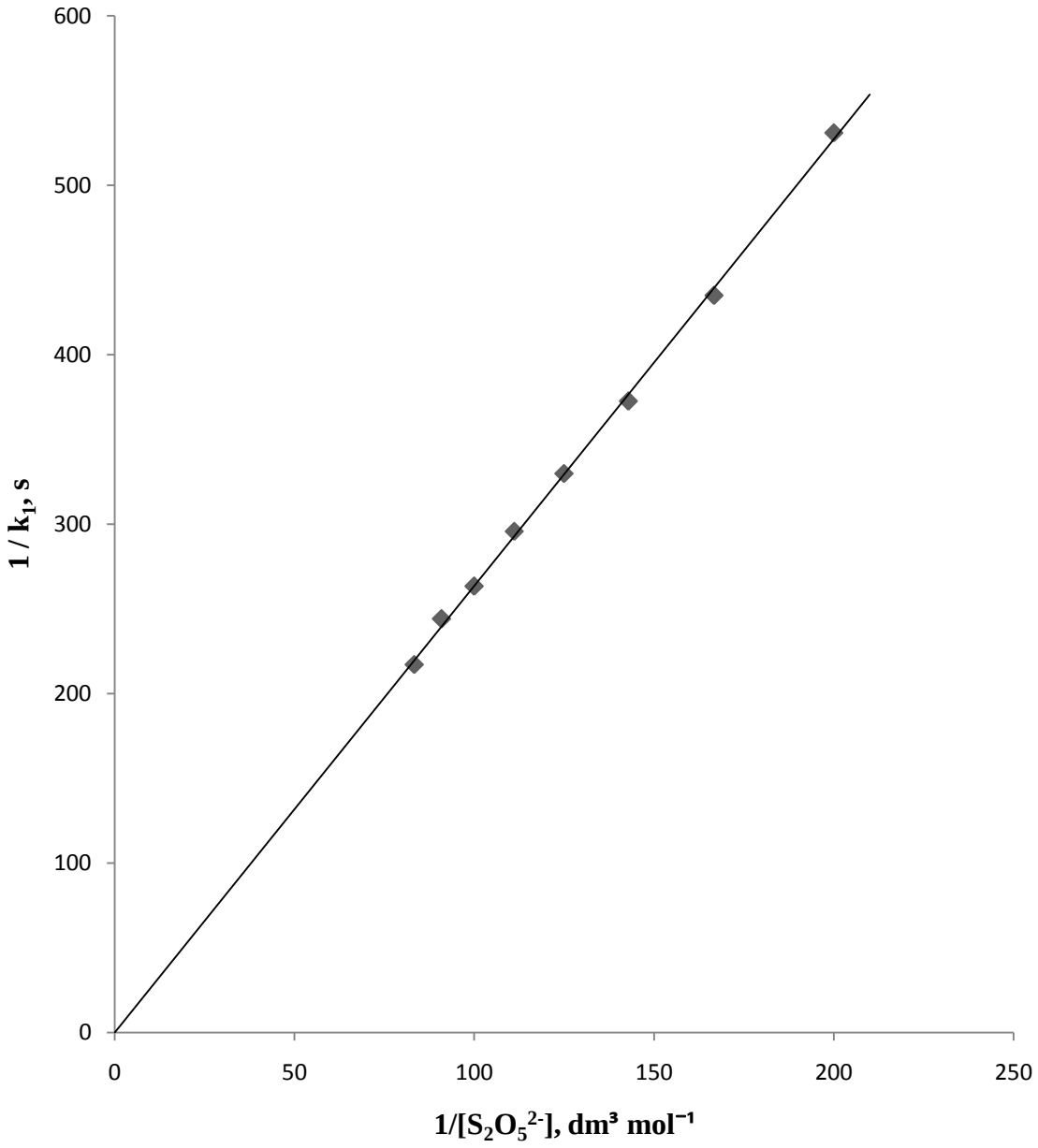


Figure 4.35: **Michaelis-Menten plot of $1/k_1$ versus $1/[S_2O_5^{2-}]$ for the redox reaction of malachite green with metabisulphite ion at $[MG^+] = 1.0 \times 10^{-4}$ mol dm^{-3}, $[H^+] = 5.0 \times 10^{-3}$ mol dm^{-3}, I = 0.50 mol $dm^{-3}$and T= 28 ± 1 ºC**

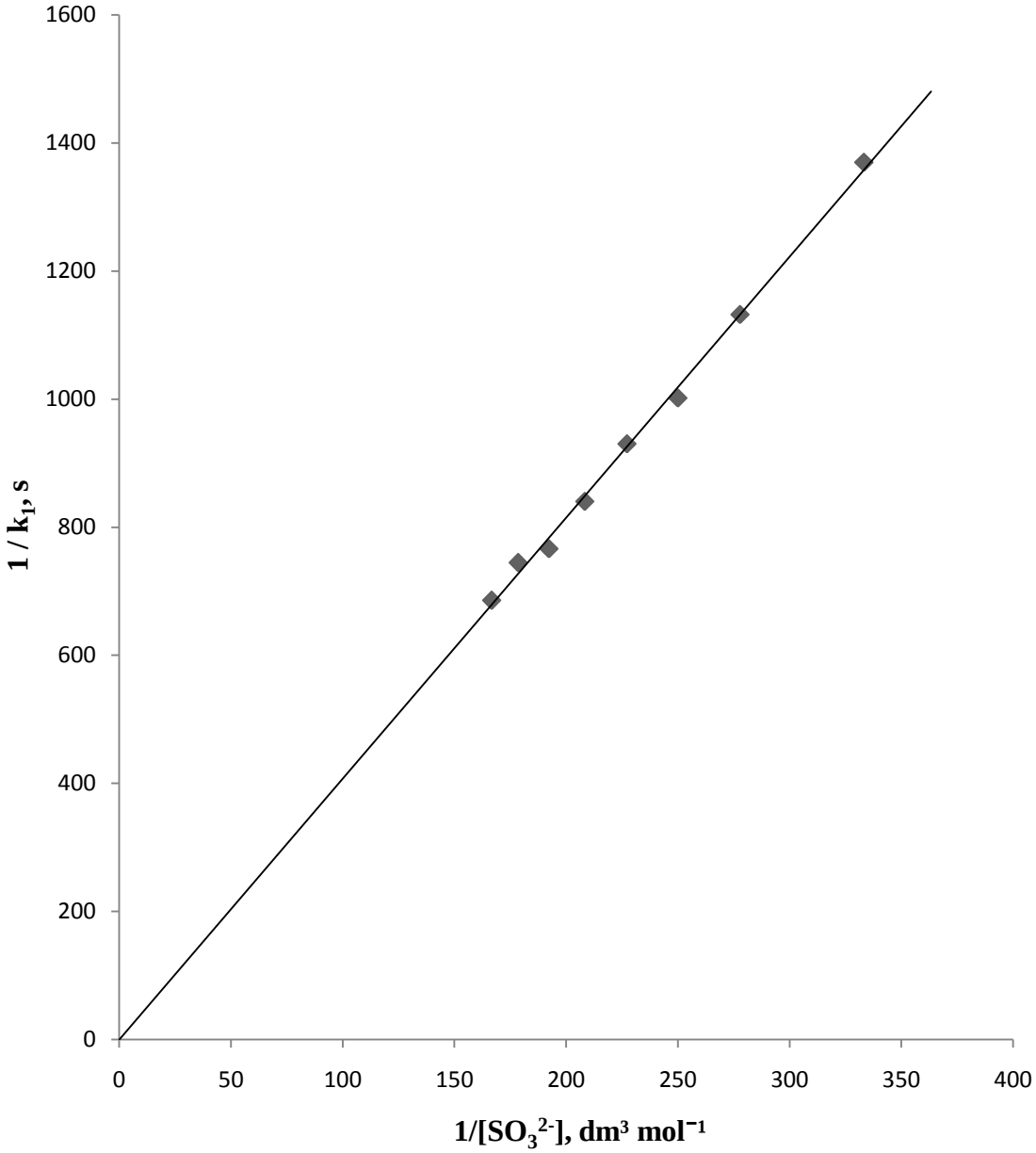


Figure 4.36: Michaelis-Menten plot of $1/k_1$ versus $1/[SO_3^{2-}]$ for the redox reaction of malachite green with sulphite ion at $[MG^+] = 1.0 \times 10^{-4}$ mol dm^{-3},

$[H^+]$ = 5.0 × 10^{-3} mol dm^{-3}, I = 0.10 mol dm^{-3} and T= 27 ± 1 ºC

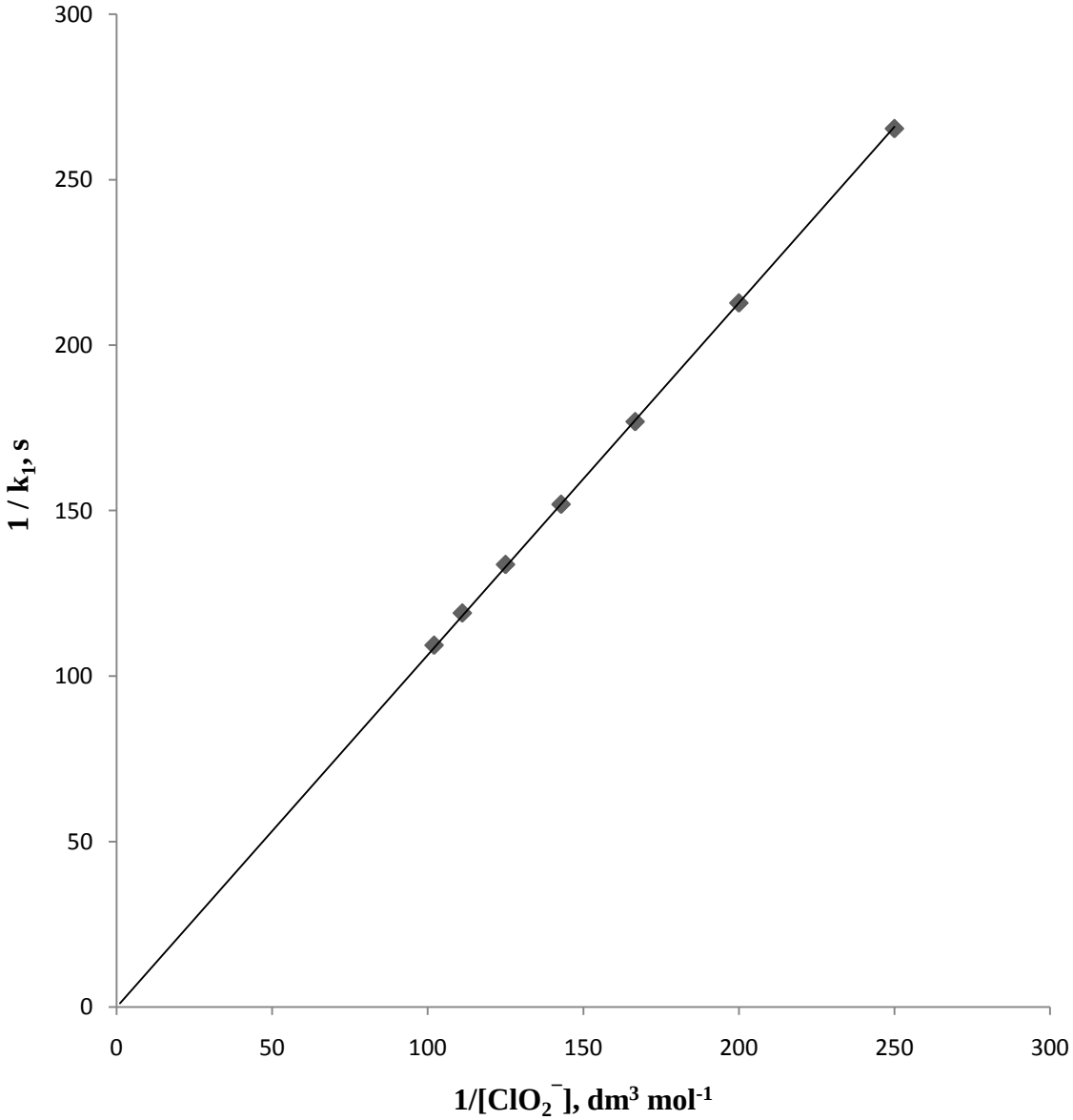


Figure 4.37: Michaelis-Menten plot of $1/k_1$ versus $1/[ClO_2^-]$ for the redox reaction of malachite green with chlorite ion at $[MG^+] = 1.0 \times 10^{-4}$ mol dm^{-3}, $[H^+] = 1.0 \times 10^{-2}$ mol dm^{-3}, I = 0.30 mol dm^{-3} and T= 26 ± 1 ºC

4.7.3 Spectrophotometric test

For all the systems studied, only the chlorite system revealed a shift in λ_{max} from 620 to 600 nm. The spectra are shown in Figures 4.38 - 4.41.

4.8 Products analysis

The products of these reactions were subjected to qualitative inorganic analysis.

a) Bromide was confirmed as one of the products of MG^+ - BrO_3^- reaction by addition of 1cm^3 HNO_3 solution to 2cm^3 of the reaction mixture, followed by $AgNO_3$ solution in drops and then in excess. Formation of a creamy white precipitate of AgBr which only dissolved in 15M NH_3 solution confirmed the presence of Br^-.

b) For the MG^+ - $S_2O_5^{2-}$ and MG^+ - SO_3^{2-} systems, sulphate ion was confirmed by the addition of $BaCl_2$ solution to the reaction mixture followed by excess dilute HCl. Formation of white precipitate of $BaSO_4$ which was insoluble in excess dilute HCl confirmed the presence of SO_4^{2-}.

c) Chloride was confirmed as one of the reaction products of MG^{+} - ClO_2^{-} oxidation by the addition of $1cm^3$ HNO_3 followed by few drops of $AgNO_3$. Formation of white precipitate of AgCl which dissolves in 2M NH_3 solution confirmed the presence of Cl^{-}.

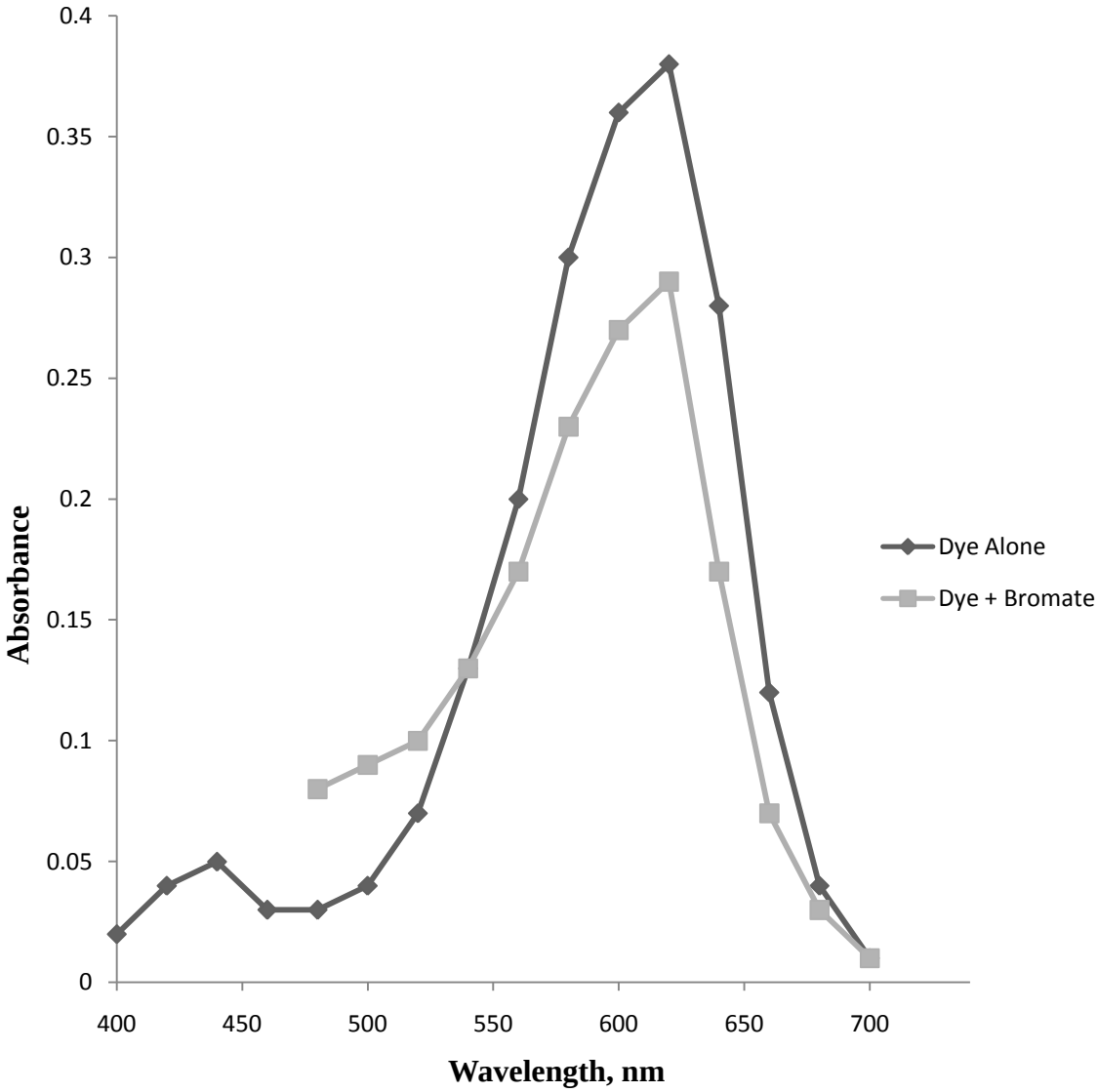


Figure 4.38: Spectra of malachite green and that of partially oxidized reaction mixture of malachite green and bromate ion at $[MG^+] = 1.0 \times 10^{-4}$ mol dm^{-3}, $[BrO_3^-] = 13.0 \times 10^{-2}$ mol dm^{-3}, $[H^+] = 1.0 \times 10^{-2}$ mol dm^{-3}, I = 0.50 mol dm^{-3}, λ_{max} = (400 - 670) nm and T= 28 ± 1 ºC

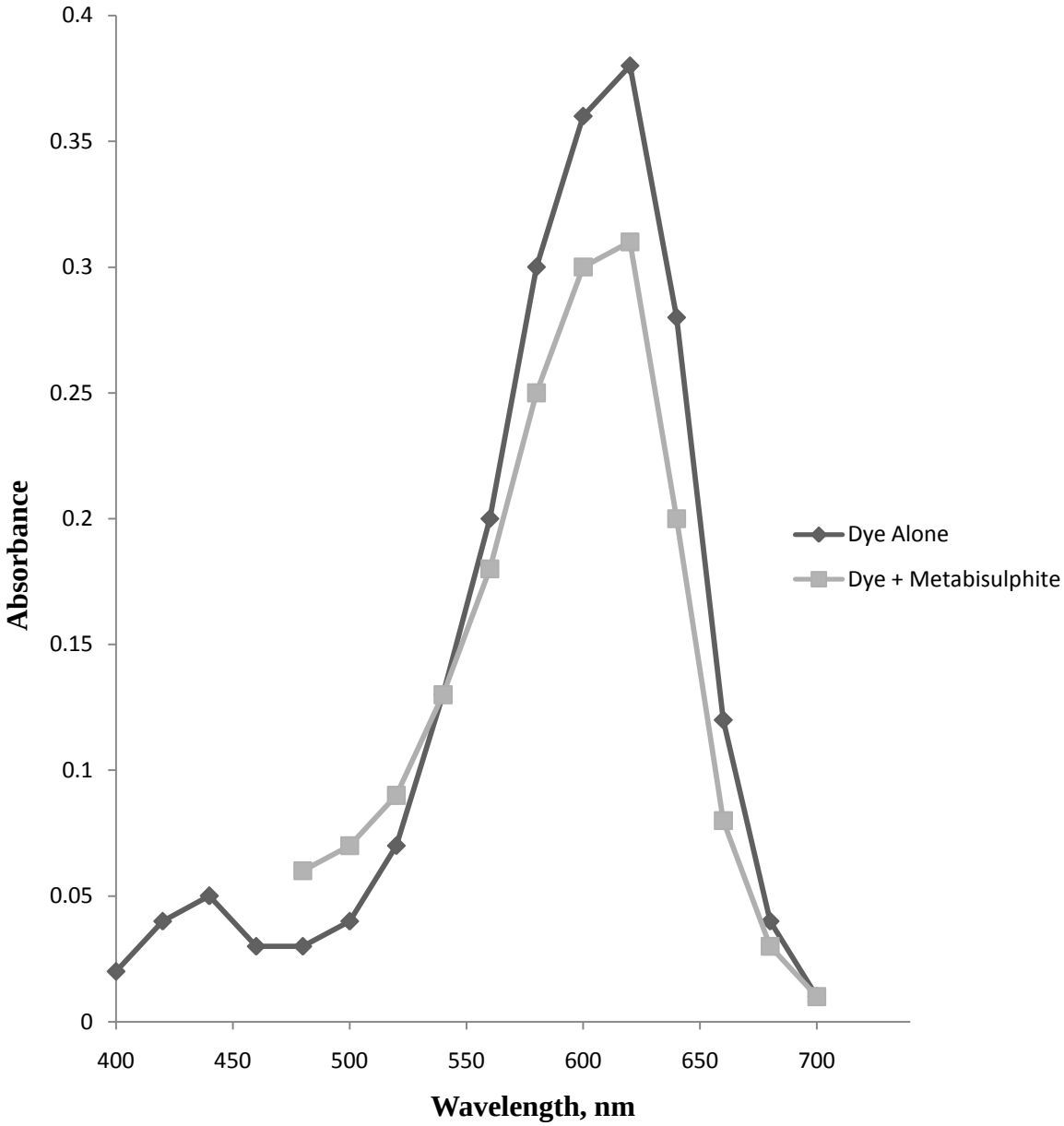


Figure 4.39: Spectra of malachite green and that of partially oxidized reaction mixture of malachite green and metabisulphite ion at $[MG^+] = 1.0 \times 10^{-4}$ mol dm^{-3}, $[S_2O_5^{2-}] = 10.0 \times 10^{-3}$ mol dm^{-3}, $[H^+] = 5.0 \times 10^{-3}$ moldm^{-3}, I = 0.50 mol dm^{-3}

λ_{max} = (400 - 670) nm and T= 28 ± 1 ºC

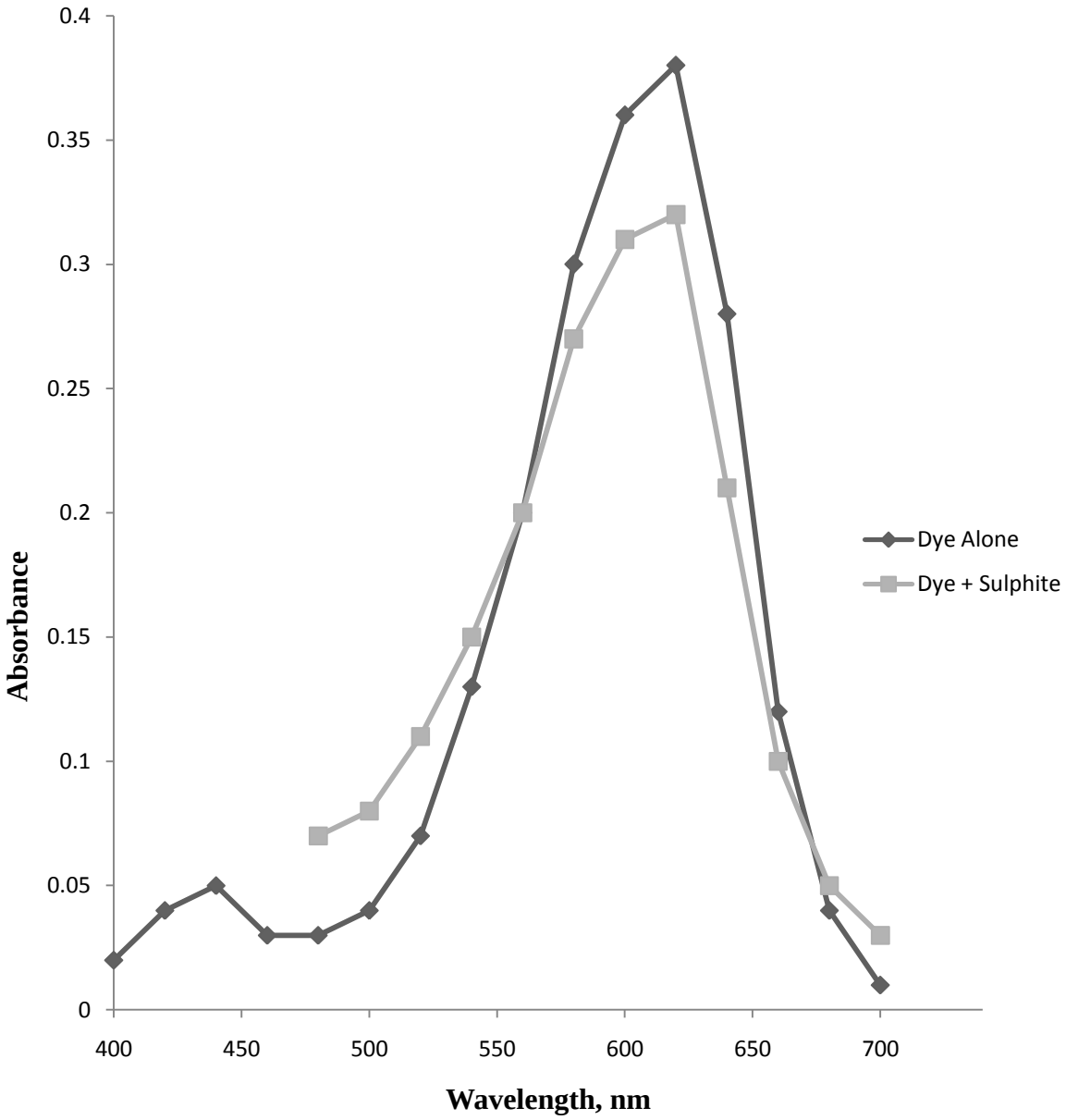


Figure 4.40: Spectra of malachite green and that of partially oxidized reaction mixture of malachite green and sulphite ion at $[MG^+] = 1.0 \times 10^{-4}$ mol dm^{-3}, $[SO_3^{2-}] = 5.6 \times 10^{-3}$ mol dm^{-3}, $[H^+] = 5.0 \times 10^{-3}$ mol dm^{-3}, I = 0.10 mol dm^{-3} λ_{max} = (400 - 670) nm and T= 27 ± 1 ºC

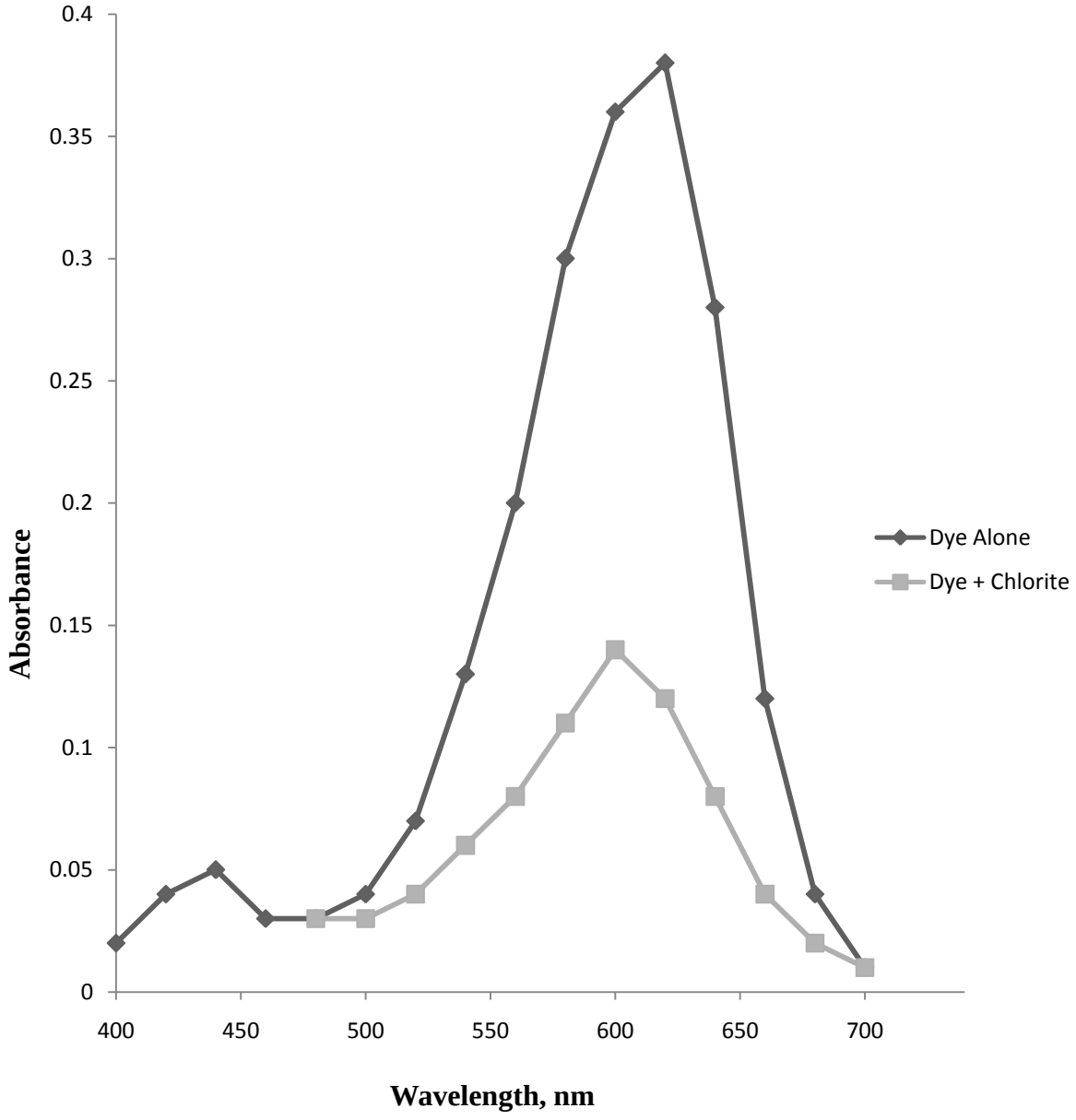


Figure 4.41: Spectra of malachite green and that of partially oxidized reaction mixture of malachite green and chlorite ion at $[MG^+] = 1.0 \times 10^{-4}$ mol dm^{-3},

$[ClO_2^-] = 6.0 \times 10^{-3}$ mol dm^{-3}, $[H^+] = 1.0 \times 10^{-2}$ mol dm^{-3}, I = 0.30 mol dm^{-3}

λ_{max} = (400 - 670) nm and T= 26 ± 1 ºC

CHAPTER FIVE

5.0 DISCUSSION

5.1 Malachite Green - Bromate Ion System

The result of the stoichiometric investigation indicated that two moles of malachite green (MG^+) was consumed by one mole of bromate ion. A stoichiometry of 1:1 was reported in the electron transfer reaction of crystal violet with bromate ion in aqueous hydrochloric acid medium (Adetoro *et al*., 2014) and also in the oxidation of toluidine blue by bromate ion (Hamza, 2010). Likewise, a stoichiometry of 5:2 was reported for the oxidation of rosalinine by bromate (Shallangwa, 2005) and also in the oxidation of acetaldehyde by bromate ion in aqueous perchloric acid medium (Lohdip and Iyun, 1993).

The order of the reaction with respect to both reactants was found to be one, hence the reaction is second order overall and the second order rate constant, k_2, was determined to be (30.81 ± 0.36) $\times 10^{-3}$ dm^3 mol^{-1} s^{-1} (Table 4.1). Similar second order dependence have been reported for the reaction of the same oxidant with crystal violet, methylene blue and tetrahedral cobalt(II) (Abdulsalam, 2015, Iyun and Asala, 1994 and Ayoko *et al.,* 1991) respectively.

The rate of the reaction increased with increase in acid concentration in the range investigated with slope of 1.82 (Figure 4.13). Plot of k_2 versus $[H^+]^2$ gave a straight line which passes

through the origin (Figure 4.16). This indicates that equilibrium between the protonated and deprotonated forms of the reactant prior to the slow step was rapid and that the equilibrium constant for protonation is small and incomplete at high acidities. Thus, only the protonated specie is reactive (Gupta and Gupta 1984).

Ionic strength effect on the rate of reaction showed that rate increases with increasing ionic strength. This suggests a positive Bronsted – Debye salt effect. Plot of log k_2 against $\sqrt{I}$ gave a slope of 1.80 (R^2 = 0.965) (Fig. 4.19). This implies that activated complex was formed from reactants of similar charges in the rate determining step and the product of the charges is +2. Reactions between two pairs of ions of like charge are usually accelerated by increasing ionic strength because of the favorable interactions of the activated complex with the denser ionic environment (Osunlaja, *et al*., 2012).

The observed inhibitive effect of added anions can only be explained in terms of ion pairing. The anions might have undergone extensive ion pairing with one of the reactant, thereby hindering the chances of the two reactants coming into contact. The inhibitive effect of the added cations could be explained in terms of columbic effects, as the activated complex in this reaction is made up of positively charged species, bringing in another positively charged specie would lead to overall repulsion, thereby decreasing the rate of reaction. The effect of these ions however suggests that outer-sphere mechanism might be operating in the system (Babatunde, 2009). The formation of a gelatinous precipitate on addition of acrylamide to the partially oxidized reaction mixture indicates the presence of free radicals in the reaction.

The spectra of the reaction mixture taken 2 minutes after the initiation of the reaction showed no shift from the λ_{max} of 620 nm characteristic of malachite green. This suggests that there is most likely no intermediate complex formation prior to the electron transfer step. Also Michaelis -

Menten plot of $1/k_1$ versus $1/[BrO_3^-]$ (Figure 4.34) was linear with zero intercept, further suggesting the absence of intermediate complex formation.

On the basis of the above, the scheme below is thus proposed for the reaction which is occurring via the outer-sphere mechanism.

$$BrO_3^- + 2H^+ \overset{K}{\rightleftharpoons} H_2BrO_3^+ \quad \text{(fast)} \qquad (5.1)$$

$$MG^+ + H_2BrO_3^+ \xrightarrow{k_3} [MG//H_2BrO_3]^{2+} \qquad (5.2)$$

$$[MG//H_2BrO_3]^{2+} + MG^+ \xrightarrow{k_4} \text{Products} + Br^- + 2OH^* \quad \text{(slow)} \qquad (5.3)$$

$$2OH^* \xrightarrow{k_5} H_2O + ½O_2 \qquad (5.4)$$

Equation 5.3 is the rate determining step. Therefore:

$$\text{Rate} = k_4 [MG//H_2BrO_3^{2+}] [MG^+] \qquad (5.6)$$

Applying steady states approximation to $[MG//H_2BrO_3^{2+}]$ in equation 5.2, we have

$$k_3 [MG^+] [H_2BrO_3^+] = k_4 [MG//H_2BrO_3^{2+}] [MG^+] \qquad (5.7)$$

And from equation 5.1,

$$[H_2BrO_3^+] = K [BrO_3^-] [H^+]^2 \qquad (5.8)$$

Substituting equations 5.7 and 5.8 in 5.6 gives

$$\text{Rate} = K k_3 [H^+]^2 [MG^+] [BrO_3^-] \qquad (5.9)$$

Equation 5.9 can be written as:

$$\text{Rate} = k^{I} [MG^{+}] [BrO_3^{-}] \qquad (5.10)$$

where $k^{I} = K k_3 [H^{+}]^2$

This is analogous to equation 4.6 where $k^{I} = k_2 = (30.81 \pm 0.36) \times 10^{-3}$ dm^3 mol^{-1} s^{-1}.

The outer-sphere mechanism is rationalized for the reaction given that:

1. Added ions had inhibitive effect on the rate of reaction which implied that the reaction centres were not linked by a bridging group.
2. Spectrum of partially initiated reaction did not show shift in wavelength maximum suggesting the absence of intermediate complex which is characteristic of inner-sphere mechanism.
3. Michaelis-Menten plot had zero intercept which is a further evidence supportive of lack of intermediate complex formation.

5.2 Malachite Green - Metabisulphite Ion System

The result of the stoichiometric investigations indicated that one mole of malachite green consumed one mole of metabisulphite ion. This agrees with the stoichiometries observed in the reactions of $S_2O_5^{2-}$ with crystal violet (Abdulsalam, 2015), rosaniline monochloride (Onu and Iyun, 2001) and basic fuchsin (Lawal, 1997). However, stoichiometry of 1:3 was established for the reduction of methylene blue with metabisulphite (Babatunde *et al*., 2013).

The order of the reaction was found to be one in both the oxidant and reductant respectively. Thus the reaction is second order overall and the second order rate constant was

determined to be (38.04 ± 0.30) $\times 10^{-2}$ dm^3 mol^{-1} s^{-1}. Similar order was obtained with respect to the reductant concentration by earlier researchers (Lawal, 1997, Onu and Iyun 2001 and Babatunde *et al*., 2013).

The study on the effect of hydrogen ion concentration, $[H^+]$, on the rate of the reaction showed that increase in hydrogen ion concentration decreased the rate of reaction with negative slope of 0.65 (Figure 4.14). Least square plot of k_2 versus $1/[H^+]$ had intercept (Figure 4.17) indicating that two parallel reaction pathways are available for the reaction: the acid independent and the inverse acid dependent pathways. The inverse acid pathway shows that there is a pre-equilibrium step involving a proton lost before the rate determining step. This means that the two rate-controlling steps are preceeded by a rapid equilibrium for which the equilibrium constant is small, and both forms (i.e the protonated and deprotonated forms) are reactive (Gupta and Gupta 1984). Similar acid dependence pathway has been reported on the oxidation of $S_2O_5^{2-}$ by basic fuchsin (Lawal, 1997, Onu and Iyun, 2001). This is in contradiction with the result of Babatunde *et al*., (2013) where enhancement in the rate was obtained by increase in hydrogen ion concentration in the reduction of methylene blue with $S_2O_5^{2-}$.

Investigation of the effect of ionic strength showed that increase in ionic strength of reaction medium increased the rate of reaction suggesting a positive salt effect. This is consistent with interaction between cation - cation or anion - anion in the rate determining step (Atkins and de Paula, 2002). Plot of log k_2 versus $\sqrt{I}$ (Fig. 4.20) gave a straight line with a slope of unity, implying that the product of the charges of these ions at the rate determining step is also unity. The positive ionic strength effect was supported by the observed increase in reaction rate with increase in dielectric constant of reaction medium (Table 4.6). A plot of k_2 versus 1/D is presented as Figure 4.23.

The inhibitive effect of added cations and anions suggests that the reaction might be operating via the outer-sphere mechanism (Myek *et al*., 2014). The formation of gel on addition of acrylamide to partially reacted mixture in the presence of excess methanol shows that the participation of free radicals in this reaction system is likely. Qualitative test for the oxidation product of $S_2O_5^{2-}$ confirmed sulphate ion by precipitation of $BaSO_4$ (Vogel, 1961).

On monitoring the spectra of the reaction mixture 2 minutes after the initiation of the reaction, there was neither a shift in the wavelength of maximum absorption of the malachite green ion nor enhanced absorbance, suggesting that there is no intermediate complex formed. Michaelis - Menten plot of $1/k_1$ versus $1/[S_2O_5^{2-}]$ gave a straight line which passed through the origin (Figure 4.35). This further suggests that no intermediate complex of significant stability was formed thereby supporting the proposition of the outer-sphere mechanism for this reaction.

Based on the above results, the following reaction scheme is therefore proposed for this outer-sphere reaction:

$$MG^+ + S_2O_5^{2-} + H_2O \overset{K_1}{\rightleftharpoons} MGO^- + HS_2O_5^- + H^+ \quad \text{(fast)} \quad (5.11)$$

$$MGO^- + HS_2O_5^- \xrightarrow{k_3} \text{Products} \quad \text{(slow)} \quad (5.12)$$

$$MG^+ + S_2O_5^{2-} \xrightarrow{k_4} \text{Products} \quad \text{(slow)} \quad (5.13)$$

Equation 5.12 and 5.13 are the rate determining steps. Therefore:

$$\text{Rate} = k_3 [MGO^-] [HS_2O_5^-] + k_4 [MG^+] [S_2O_5^{2-}] \quad (5.14)$$

From equation 5.11, $[MGO^{-}]\,[HS_2O_5^{-}] = K_1\,[MG^{+}]\,[S_2O_5^{2-}]\,[H^{+}]^{-1}$ (5.15)

Substituting equation 5.15 into 5.14, we have,

$$\text{Rate} = K_1k_3\,[MG^{+}]\,[S_2O_5^{2-}]\,[H^{+}]^{-1} + k_4\,[MG^{+}]\,[S_2O_5^{2-}] \quad (5.16)$$

$$= k^{II}\,[MG^{+}]\,[S_2O_5^{2-}] \quad (5.17)$$

where $k^{II} = k_4 + K_1k_3\,[H^{+}]^{-1}$

This is analogous to equation 4.6 where $k^{II} = k_2 = (38.04 \pm 0.30) \times 10^{-2}$ dm^3 mol^{-1} s^{-1}

The proposed outer-sphere mechanistic pathway was as due to the following reasons:

1. Added ions inhibition as observed in the reaction which is in favour of the outer-sphere mechanism. Such observation is an indication that coordination integrity of the reactant species remained intact during and prior to electron transfer process.
2. Spectroscopic evidence of stable reaction intermediates not formed during the course of the reaction and if formed, had a small formation constant.
3. The above assertion is further strengthened by the Michaelis-Menten plot which was linear without intercept. Lack of such kinetic evidence removes the chance of inner-sphere mechanism.

5.3 Malachite Green - Sulphite Ion System

The stoichiometric study showed that one mole of malachite green was consumed by one mole of SO_3^{2-}. Similar stoichiometry was reported for the oxidation of sulphite ion by indigo carmine (Edokpayi, *et al*., 2010), decolorization of methylene blue with sodium sulphite in aqueous media (Olajire and Olajide, 2014) and the reduction of toluidine blue with sulphite ion (Jonnalagada and Gollapalli, 2000). Under the stoichiometric condition for the reaction, SO_4^{2-} was obtained as an

inorganic reaction product. The presence of SO_4^{2-} was confirmed qualitatively by the addition of $BaCl_2$ followed by HCl which formed an insoluble white precipitate of $BaSO_4$ in excess HCl.

Kinetic study indicated first order dependence of the rate on $[MG^+]$ and $[SO_3^{2-}]$ respectively. Thus at $[H^+] = 5 \times 10^{-3}$ mol dm^{-3} and T = 27 ± 1°C, the rate equation is as shown by equation (4.6). Under experimental condition employed, k_2 was found to be $(24.56 \pm 0.37) \times 10^{-2}$ dm^3 mol^{-1} s^{-1}.

The effect of changes in hydrogen ion concentration on reaction rate is negligible suggesting that the reaction occur through an acid independent pathway. The non-dependence of this reaction on $[H^+]$ is in accord with the fact that neither the oxidant nor the reductant undergo significant protonation or deprotonation under the given reaction conditions. Similar result was reported by Edokpayi, *et al*., (2010).

The rate of reaction was found to increase with increase in the ionic strength (Table 4.3). The plot of log k_2 against $I^{½}$ gave a positive slope indicating that the reaction displayed a positive Bronsted – Debye salt effect (Figure 4.21), which therefore implies that at the activated complex, there is interaction between two liked-charged species and the product of the charges is +1.

Added anions increased the reaction rates (Table 4.10). This observation is typical of reactions occurring by the outer-sphere mechanism with the characteristic feature of the coordination integrity of the reactants maintained prior to and during the electron transfer process. Addition of acrylamide which serves as a radical scavenger to a partially reacted mixture in the presence of excess methanol gave a polymeric product in form of gel. This observation is in favour of probable participation of free radicals in this reaction.

Lack of spectroscopic evidence for the formation of intermediate complex as indicated in the Michaelis Menten plot (Figure 4.36) suggest that intermediate may be unimportant in the rate determining step.

Based on the above results, the following mechanistic scheme is hereby proposed for the outer-sphere reaction.

$$MG^{+} + SO_3^{2-} \xrightarrow{k_1} [MG^{+}//SO_3^{2-}] \quad \text{(fast)} \qquad (5.18)$$

$$[MG^{+}//SO_3^{2-}] \xrightarrow{k_3} \text{Products} \quad \text{(slow)} \qquad (5.19)$$

Equation 5.23 is the rate determining step. Therefore:

$$\text{Rate} = k_3 [MG^{+}//SO_3^{2-}] \qquad (5.20)$$

Applying steady state hypothesis to intermediate specie $[MG^{+}//SO_3^{2-}]$, we have

$$[MG^{+}//SO_3^{2-}] = k_1/k_3 [MG^{+}] [SO_3^{2-}] \qquad (5.21)$$

Substituting equation 5.21 into 5.20, we have

$$\text{Rate} = k_1 [MG^{+}] [SO_3^{2-}] \qquad (5.22)$$

$$\text{Therefore Rate} = k^{III} [MG^{+}] [SO_3^{2-}] \qquad (5.23)$$

where $k^{III} = k_1$

Equation 5.23 is analogous to equation 4.6 where $k^{III} = k_2 = (24.56 \pm 0.37) \times 10^{-2}$ dm^3 $mol^{-1}s^{-1}$

The choice of outer-sphere mechanism for this reaction is based on:

1. Catalysis of reaction rate by added ions which is characteristic of reaction that occurs through the outer-sphere mechanistic pathway.
2. Lack of spectroscopic evidence for the formation of intermediate complex as indicated in the Michaelis-Menten plot.

5.4 Malachite Green – Chlorite Ion System

The stoichiometric study showed that one mole of malachite green was consumed by one mole of ClO_2^-. Similar stoichiometry was reported for the redox reaction between pyrocatechol violet and chlorite ions (Adetoro *et al*., 2010) but Kudesia (2010), Bugaje (2006) and Nagaishi, *et al*., (1977) obtained a stoichiometry of 2:1 in the redox reaction of ClO_2^- with formaldehyde, $[Co(EDTA)]^{2-}$ and nitrite ion.

Kinetic study indicated that the reaction is first order with respect to malachite green and chlorite ion concentrations respectively. The order obtained is similar to that reported for the oxidation of formaldehyde by chlorite (Kudesia, 2010); oxidation of NO_2^- ion by chlorite (Nagaishi *et al*., 1977); oxidation of indigo carmine by chlorite (Falodun, 2015) and oxidation of pyrocatechol violet by chlorite (Adetoro *et al*., 2010).

The result of the acid dependence study showed that the rate constant increases with increase in $[H^+]$. Plot of log k_H^+ versus log $[H^+]$ gave a slope of 0.85, indicating that the reaction is first order with respect to $[H^+]$ (Figure 4.15). Plot of k_2 versus $[H^+]$ gave a straight line with an intercept. A graph of this nature indicates that the reaction occurs via acid dependent and acid independent pathways (Gupta and Gupta 1984). The acid dependent rate equation for the reaction can be represented by the equation below;

$$k_H^+ = a + b\ [H^+] \qquad (5.24)$$

Changes in ionic strength of reaction medium had no effect on reaction rate. The observed independence on the rate of reaction indicates that charged and neutral specie are present at the rate determining step.

Added anions and cations did not affect the rate of the reaction. An indication that the reaction might be operating via the inner-sphere mechanism (Ekdopayi *et al*., 2010). The absence of free radicals as observed from free radical test indicates that this species are not important in this reaction. Plot of $1/k_1$ versus $1/[ClO_2^-]$ displayed a zero intercept at the $1/k_1$ axis however spectra of the reaction mixture when compared with that of the dye alone indicated a shift from the absorption maximum of 620 to 600 nm. This observation is in support of reactions occurring via the inner-sphere mechanistic pathway (Bugaje, 2006).

On the basis of the above experimental observations, the following scheme is hereby proposed for this reaction.

$$ClO_2^- + H^+ \underset{}{\overset{K}{\rightleftharpoons}} HClO_2 \quad \text{(fast)} \qquad (5.25)$$

$$MG^+ + HClO_2 \xrightarrow{k_3} \text{Products} \quad \text{(slow)} \qquad (5.26)$$

$$MG^+ + ClO_2^- \xrightarrow{k_4} \text{Products} \quad \text{(slow)} \qquad (5.27)$$

Equations 5.26 and 5.27 are the rate determining steps, therefore;

$$\text{Rate} = k_3 [MG^+] [HClO_2] + k_4 [MG^+] [ClO_2^-] \qquad (5.28)$$

But from equation 5.25

$$[HClO_2] = K [ClO_2^-] [H^+] \qquad (5.29)$$

Substituting equation 5.29 into 5.28, we have

$$\text{Rate} = Kk_3 [MG^+] [ClO_2^-] [H^+] + k_4 [MG^+] [ClO_2^-] \qquad (5.30)$$

Therefore Rate = k^{IV} $[MG^+]$ $[ClO_2^-]$ (5.31)

where $k^{IV} = k_4 + Kk_3 [H^+]$

This is analogous to equation 4.6 where $k^{IV} = k_2 = (94.05 \pm 0.19) \times 10^{-2}$ dm^3 mol^{-1} s^{-1}.

The inner-sphere mechanism is proposed for this reaction given that:

1. Non-catalysis of reaction by the added ions is strongly suggestive of a reaction proceeding through the inner-sphere pathway.
2. Spectrum of partially initiated reaction showed a shift in wavelength maximum suggesting the formation of intermediate complex which is characteristic of inner-sphere reaction.

CHAPTER SIX

6.0 SUMMARY, CONCLUSION AND RECOMMENDATION

6.1 Summary and Conclusion

The kinetic study of the redox reactions of malachite green with these oxyanions BrO_3^-, $S_2O_5^{2-}$, SO_3^{2-} and ClO_2^- ions in aqueous acidic medium was carried out. The stoichiometry of 2:1 was observed for MG^+ - BrO_3^- system, 1:1 for MG^+ - $S_2O_5^{2-}$,

MG^+ - SO_3^{2-} and MG^+ - ClO_2^- systems respectively.

The reactions were second order overall at constant $[H^+]$ for all the systems. The rate of reaction is directly proportional to $[H^+]^2$ and $[H^+]$ for bromate and chlorite systems, inversely proportional to $[H^+]$ for metabisulphite system and had a negligible effect on the sulphite system.

The reactions are therefore in conformity with the following rate equations:

$$-\frac{d[MG^+]}{dt} = (a\,[H^+]^2)[MG^+][BrO_3^-] \qquad (6.1)$$

$$-\frac{d[MG^+]}{dt} = (b + c\,[H^+]^{-1})[MG^+][S_2O_5^{2-}] \qquad (6.2)$$

$$-\frac{d[MG^+]}{dt} = [H^+]^0\,[MG^+]\,[SO_3^{2-}] \qquad (6.3)$$

$$-\frac{d[MG^+]}{dt} = (d + e\,[H^+])[MG^+][ClO_2^-] \qquad (6.4)$$

where $a = 3.32 \times 10^{-1}$ dm^9 mol^{-3} s^{-1}, $b = 9.80 \times 10^{-2}$ dm^3 mol^{-1} s^{-1}, $c = 1.38 \times 10^{-3}$ s^{-1},

$d = 0.11$ dm^3 mol^{-1} s^{-1} and $e = 8.40 \times 10^{-2}$ s^{-1}.

The second order rate constant for the various systems were found to be:

$k_2 = (30.81 \pm 0.36) \times 10^{-3}$ dm^3 mol^{-1} s^{-1} for MG^+ - BrO_3^- system

$k_2 = (38.04 \pm 0.30) \times 10^{-2}$ dm^3 mol^{-1} s^{-1} for MG^+ - $S_2O_5^{2-}$ system

$k_2 = (24.56 \pm 0.37) \times 10^{-2}$ dm^3 mol^{-1} s^{-1} for MG^+ - SO_3^{2-} system

$k_2 = (94.05 \pm 0.19) \times 10^{-2}$ dm^3 mol^{-1} s^{-1} for MG^+ - ClO_2^- system

All reactions were sensitive to change in ionic strength except for the MG^+-ClO_2^- system which shows no dependent on ionic strength. Added ions inhibited the rate of reactions for bromate and metabisulphite systems and had no effect on the rate of reaction for the chlorite system. The rate of reaction of the sulphite system was catalysed by added anions.

Evidence of intermediate complex formation was suggested for the MG^+-ClO_2^- system by the shift in λ_{max} from 620-600 nm and no shift was observed for the other systems. Free radicals were observed for all the systems except for the chlorite system only. Thus the results obtained in this study shows that MG^+-BrO_3^-, MG^+-$S_2O_5^{2-}$ and MG^+-SO_3^{2-} reactions could be said to occur through the outer-sphere mechanism, while the MG^+-ClO_2^- reaction occur by the inner-sphere mechanism. Consequently the proposed plausible mechanisms are consistent with all the kinetic data obtained for all the systems investigated.

6.2 Recommendation

It is recommended that:

1. further studies should be carried out on the activated parameters of these reactions,
2. thorough analysis to identify the organic product should be made
3. more systems involving other oxidants and reductants should be studied for more information on the chemical characteristics of malachite green.
4. Data generated in kinetic and mechanistic studies in collaboration with data from toxicological studies and textile waste water assessment studies could be of great importance in improving the uses and handling of the dye in all areas of application.

REFERENCES

Abbas, A.E. and Nabeel, H.K. (2010). Kinetics of the reduction of hexacyanoferrate (III) 3,7-bis(dimethylamino)phenothionium chloride by metabisulphite ion in acidic medium. *Pelagia Research Library,* **4**(3): 69-78.

Abdulsalam, S. (2015). Kinetics and mechanisms of the redox reactions of crystal violet with some oxyanions in aqueous acidic medium. Unpublished M.Sc Thesis, Ahmadu Bello University, Zaria, Nigeria.

Adetoro, A., Iyun, J.F. and Idris, S.O. (2010). Kinetics and mechanism of bromate ion oxidation of pyrocatechol violet in aqueous hydrochloric acid. *Archives of Applied Science Res*earch, **2**(6): 177-184.

Adetoro, A., Iyun, J. F. and Idris, S.O. (2010). Kinetics and mechanism of oxidation of pyrocatechol violet by chlorite ion in aqueous hydrochloric acid. *Archives of Applied Science Research*, 2(5): 112-119.

Adetoro, A., Ladipo, M.K., Popoola, O.E. and Edokpayi, J.N. (2014). Electron transfer reaction and mechanism of crystal violet with bromate ion in aqueous hydrochloric acidic medium. *World Journal of Chemistry,* 9(2): 20-23.

Anwenting, B.I. (2012). Kinetics and mechanisms of the oxidation of nicotinic acid, l-cysteic acid, l-aspartic acid and l-tryptophan by permanganate ion in aqueous acidic medium. An unpublished M.Sc Thesis of Ahmadu Bello University, Zaria, Nigeria.

Arnaut, L., Formosinho, A. and Burrow, H. (2006). *Chemical kinetics from molecular structure to chemical reactivity*. Elsevier B.V; New York. pp. 1.

Asperger .S. (2003). *Chemical kinetics and inorganic reaction mechanisms*. 2nd Ed. Springer Science Business Media; New York. pp 1-3.

Atkins, P.W. and de Paula, J. (2002). *Physical Chemistry*. 7th Ed., Oxford University Press; Great Britain. pp 962.

Ayoko, G.A., Iyun, J.F. and El-Idris, I.F. (1991). Electro transfer at tetrahedral cobalt (II). Part I. kinetics of bromate ion reduction. *Transition Metal Chemistry,* **16**; 145.

Azhar, S.S., Liew, A.G., Suhardy, D., Hafiz, K.F.and Hatim, M.D.I., (2005). Dye removal from aqueous solution by using adsorption on treated sugarcane bagasse. *Journal of Applied Science,* 2(11); 1499.

Babatunde, O.A. (2005) Kinetics and mechanism of electron transfer reactions of mixed-valence di-μ-oxo tetrakis (1,10-phenanthroline) di manganese (iii,iv) ion and rosaniline hydrochloride with some reducing agents. An unpublished Ph.D Thesis of Ahmadu Bello University, Zaria, Nigeria.

Babatunde, O.A and Iyun, J.F. (2009). Kinetics and mechanism of the reaction of di-μ-oxo-tetrakis (1,10-phenanthroline)-dimaganese(III,IV) perchlorate by sulphite ion in acidic solution. *European Journal of Scientific Reseach,* 26; 406.

Babatunde, O.A., Faruruwa, M.D. and Umoru, P.E. (2013). Mechanism of the reduction of 3,7-bis(dimethylamino)phenothionium chloride by metabisulphite ion in acidic medium. *Pelagia Reseach Library,* **4**(3): 69-78.

Birk, J.P. (1978). Kinetics and mechanism of the reduction of bromate ion by hexachloroiridate(III). *Inorganic Chemistry,* **2**(17); 504-506.

Biswajit, P. (2014). Mechanism of the oxidative cleavage of diethylene glycol by bromated ion in acid medium. *Journal of Chemical and Pharmaceutical Research,* 6(7): 47-53.

Bugaje, B.M. (2006). Kinetics and mechanism of redox reaction of 3,7-bis (dimethylamino) phenazothionium chloride and ethylenediammine tetraacetatocobaltate(II) with some oxyanions in aqueous solution. An unpublished M. Sc. Thesis of ABU Zaria.

Candlin, J.P., Taylor, K.A. and Thompson, D.T. (1968). *Reactions of Transition-Metal Complexes.* Elservier Pub. Com. Amsterdam. Chap. 3, Pp 157 – 214.

Chaffe, E. and Edward, J.C. (1970). *Inorganic reaction mechanism.* Wiley, New York, Pp. 216.

Chowdhury, S. and Saha, P. (2010). Sea shell powder as a new adsorbent to remove basic green 4 (malachite green) from aqueous solutions: Equilibrium, kinetic and thermodynamic studies. *Chemical Engineering Journal,* 164: 168-177.

Cooke, D.O. (1979). *Inorganic Reaction Mechanism*. Allard and son Ltd. Dorking, pp. 1-38.

Crini, G., Peindy, H.N., Gimbert, F. and Robert, C. (2007). Basic green 4 (malachite green) from aqueous solution by adsorption using cyclodextrin-based adsorbent: kinetic and equilibrium studies. *Separation and Purification Technology,* 53: 97-110.

Dixon, J.M., Taniguchi, M. and Lindsey, J.S. (2005), "PhotochemCAD 2. A Refined Program with Accompanying Spectral Databases for Photochemical Calculations, Photochem. Photobiol., 81, 212-213.

Edokpayi, J.N. (2010). Kinetics and mechanisms of the redox reactions of indigo carmine with some oxyanions in aqueous acidic solution. An unpublished M.Sc Thesis submitted to Ahmadu Bello University, Zaria, Nigeria.

Ekdopayi, J.N., Iyun, J.F. and Idris, S.O. (2010). Kinetics and mechanism of the electron transfer reaction between sulphite ion and indigo carmine in aqueous acidic medium. *World Journal of Chemistry*, 5(1): 62-66

EUFIC, (2007). *Miniguide European Food information Council.* pp. 2.

Falodun, S.O. (2015). Kinetics and mechanisms of the redox reactions of indigo carmine with some oxyanions in aqueous acidic solution. An unpublished M.Sc Thesis submitted to Ahmadu Bello University, Zaria, Nigeria.

Finnegan, W.G., Pitter, .L and Hinsvark, B.A. (2002). Redox reaction in growing single crystals: a mechanistic interpretation of experimental result. *Journal of colloid and interface science,* 242(2): 373-381.

Garg, V.K., Kumar, R., Gupta, R., (2004). Removal of malachite green dye from aqueous solution by adsorption using agro-industry waste: a case study of Prosopis cineraria. *Dyes Pigment*, 62; 1-6.

Gupta, K.S. and Gupta, Y.K. (1984). Hydrogen-ion dependence of reaction rates and mechanism. *Journal of Chemistry Education,* **61**(11); 972-977.

Hamza, S.A. (2011). Kinetics and mechanisms of the redox reactions of toluidine blue with some oxyanions and ascorbic acid in aqueous acidic medium. An unpublished M.Sc Thesis, Ahmadu Bello University, Zaria, Nigeria.

House, J.E. (2008). *Inorganic Chemistry*, Academic press; Canada. Chapter 1, pp 3.

Idris, S.O., Bako, B., Iyun, J.F. and Myek, B. (2014). Kinetics and mechanism of the oxidation of bromopyrogallol red by bromate ion in aqueous hydrochloric acid medium. *International Journal of Modern Chemistry,* 6(2): 87-95.

Idris, S.O., Sunday, E., Ebitomi, M.O., Iyun, J.F. and Mohammed, Y. (2010). Mechanism of the redox reaction of hydroxylamine and bromate ion in aqueous hydrochloric acid medium. *Archives of Applied Science Research,* **2**(5): 316-324.

Idris, S.O., Tanimu, .A., Iyun, J. F. and Mohammed, Y. (2014). Kinetics and mechanism of the reaction of malachite green and dithionite ion. *International Research Journal of Pure & Applied Chemistry,* 5(2): 177-184.

Idris, S.O., Tanimu, A., Iyun, J.F. and Mohammed, Y. (2015). Kinetics and mechanism of malachite green oxidation by hypochlorite ion in aqueous acidic medium. *American Chemical Science Journal*, 5(2): 185-193. ISSN: 2249-0205.

Idris, S.O., Hassan, H., Iyun, J.F. and Mohammed, Y. (2014). Kinetics and mechanism of the periodate oxidation of malachite green in acidic medium. *Journal of Scientific Research and Reports,* 4(6).

Iyun, J.F. and Asala, M. (1994). Mechanism of the bromate oxidation of 3,7-bis (dimethyl)aminophenazothionium chloride. A paper presented at the 18th Annual Conference of the chemical society of Nigeria at Kano, 29th May to 2nd June, 1994.

Jonnalagadda, S.B. and Gollapali, N.R. (2000). Kinetics of reduction of toluidine blue with sulphite-kinetic salt effect in elucidation of mechanism. *Journal of chemistry Education*, 77: 4-12.

Knight, G.C. and Thompson, R.C. (1973). *Inorganic Chemistry.* Wiley; New York, 12;

63-66.

Kudesia, V.P. (2010). Mechanism of chlorite oxidation of formaldehyde by chlorite ion. *Bullettindes Chimiyues Belges,* 81(1): 623-628.

Lawal, H.M. (1997). The electron transfer reactions of pararosaniline chloride (Basic fuchsin) and trisoxalatocobaltate(III) iron in acidic medium. Ph.D Thesis, Abubakar Tafawa Balewa University, Bauchi, Nigeria.

Lohdip, Y.N. and Iyun, J.F. (1993). Kinetic studies of the oxidation of acetaldehyde with bromate ion in aqueous perchloric acid. *Journal of Chemical Society of Nigeria,* vol.18: pp 61-64.

Milne, G.W.A. (2005). *Gardner's commercially important chemicals: synonyms, trade names, and properties*. Wiley-Interscience: New York. pp 568. ISBN 0-471-73518-3.

McNaught A. D. and Wilkinson A. (1997). *Compendium of Chemical Terminology*, 2nd Ed. (the "Gold Book"). Blackwell Scientific Publications, Oxford. pp 465.

Mohammed, Y., Iyun, J.F. and Idris, S.O (2009). Kinetics approach to the mechanism of the redox reaction of malachite green by permanganate ion in aqueous acidic solution. *African Journal of pure and Applied Chemistry*, 3(12): 269-274.

Mohammed, Y., Iyun, J.F. and Idris, S.O (2010). Kinetics approach to the mechanism of the redox reaction of malachite green and nitrite ions in aqueous acidic medium. *Journal of Chemical Society of Nigeria,* vol. 35, pp 111-116.

Myek, B., Idris, S.O. and Iyun, J.F. (2014). Kinetics and mechanism of the oxidation of naphthol green b by peroxydisulphate ion in aqueous acidic medium. *International Journal of Inorganic Chemistry*, pp 1-4.

Nagaishi, T. (1979). Kinetics of oxidation of nitrate ion by hypochlorite ion or chorite ion in aqueous solution. *Kyuschi sangyo diagaku Kogakubu kekyu hohuku*, 14, 4-11.

Olajire, A.A and Olajide, A.J (2014). Kinetic study of decolorization of methylene blue with sodium sulphite in aqueous media: Influence of transition metal ions. *Journal of Physical Chemistry and Biophysics;* 4(2): 136-143.

Onu, A.D. and Iyun, J.F. (2001). Kinetics and mechanism of the oxidation of rosaniline monochloride with sodium metabisulphite in aqueous acid medium. *Journal of Chemical Society of Nigeria,* **28**: 156-159.

OSHA, (2008). *OSHA'S Hazard Communication Standard.* US Department of Labour pp. 1.

Osunlaja, A.A., Idris, S.O. and Iyun, J.F. (2012). Kinetics and mechanism of methylene blue with permanganate ion in aqueous acidic medium. *Archives of Applied ScienceResearch,* 4(2):772-780.

Qwabe, L., Brijesh, P. and Jonnalagadda, S.B. (2005). Mechanism of oxidation of brilliant cresyl blue with acidic chlorite and hypochlorous acid. A kinetic approach; *South Afrrican Journal Chemistry,* 58: 86-92.

Reuben, H.S., Irving, R.E. and Kenneth, K. (1994). Kinetics and mechanism of the oxidation of thiourea by bromate in acidic solution. *Journal of Physical Chemistry*, 98(2): 551-557.

Sharpe, A.G. (1982). *Inorganic Chemistry.* First edition Longman, London. Pp 518-534.

Shallangwa, G.A. (2005). Kinetics studies of the redox reactions of rosaniline hydrochloride wiyh some oxyanions in aqueous acid medium. M.Sc. Thesis of Ahmadu Bello University, Zaria, Nigeria.

Saha, P., Chowdhury, S., Gupta, S., Kumar, I. and Kumar, R. (2010). Assessment on the removal of malachite green using tamarind fruit shell as biosorbent. *Clean: soil Air Water*, 38(5-6): 437-445.

Sutin, N. (1968). Free energies, barriers and reactivity patterns in electron transfer reactions. *Account of Chemical Research,* 1: 225-231.

Tanimu, A., Idris, S.O. and Iyun, J.F. (2012). Kinetics of redox reaction between malachite green and hydroxyl ion. *International Journal of Science and Technology,* 2(3): 112-115.

Taube, R. (1968). Mechanisms of oxidation reduction reactions. *Journal of Chemistry Education,* **45**: 452-457.

Taube, H., Meyer, H. and Rich, R.L. (1953). Observation on the mechanism of electron transfer in solution. *Journal of American Chemical Society,* **75**: 4118.

Tsai, W.T. and Chen, H.R. (2010). Removal of malachite green from aqueous solution using low-cost chlorella-based biomass. *Journal of Hazardous Materials*, 175: 844-849.

Vogel, A.I. (1961). *Qualitative Inorganic Analysis;* including instrumental analysis: 3rd Edition, Longman Green, London, Pp. 272-277.

Zhang, J., Li, Y., Zhang, C. and Jing, Y. (2008). Adsorption of malachite green from aqueous solution onto carbon prepared from Arundo donax root. *Journal of Hazardous Materials,* 50; 774-780.